How does the powder mixture of ibuprofen and caffeine attenuate the solubility of ibuprofen? Comparative study for the xanthine derivatives to recognize their intermolecular interactions using Fourier-transform infrared (FTIR) spectra, differential scanning calorimetry (DSC), and X-ray powder diffractometry (XRPD).

Shoya Suenaga¶, Hikaru Kataoka¶, Kanji Hasegawa, Ryotaro Koga, Chihiro Tsunoda, Wataru Kuwashima, Tomohiro Tsuchida, and Satoru Goto*

Supplemental Materials

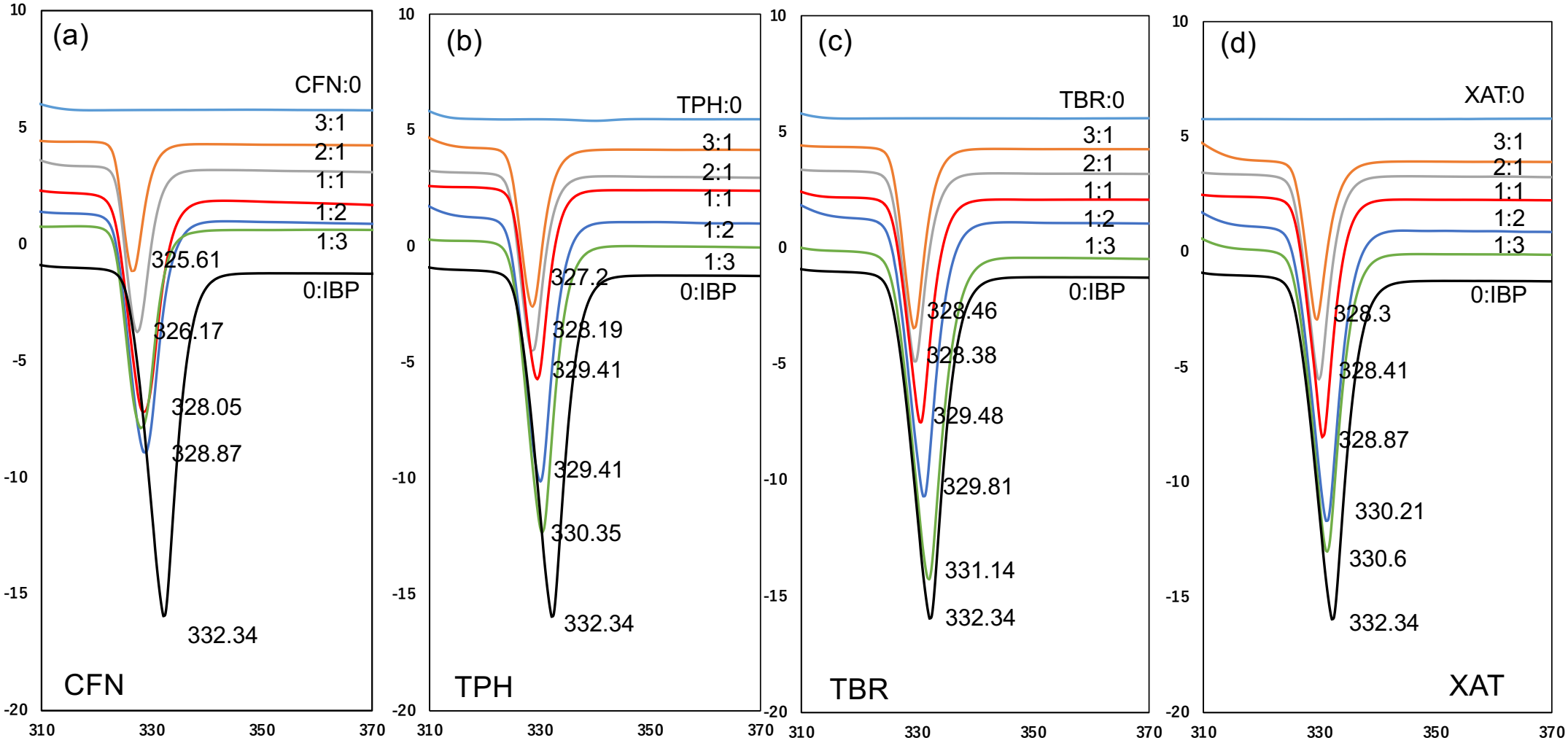

Figure S1. The endothermic signal of IBP melting in the DSC thermograms of the IBP mixtures with CFN (a), TPH (b), TBR (c), and XAT (d), which were expanded from the thermograms in Figure 4. Numbers expressed the temperatures of the peak tops. The intersections of the left-side tangent lines of peaks on the baseline extensions shifted in the mixtures of CFN/IBP and TPH/IBP. However, those in the mixtures of TBR/IBP and XAT/IBP were invariable, indicating no intermolecular interactions.

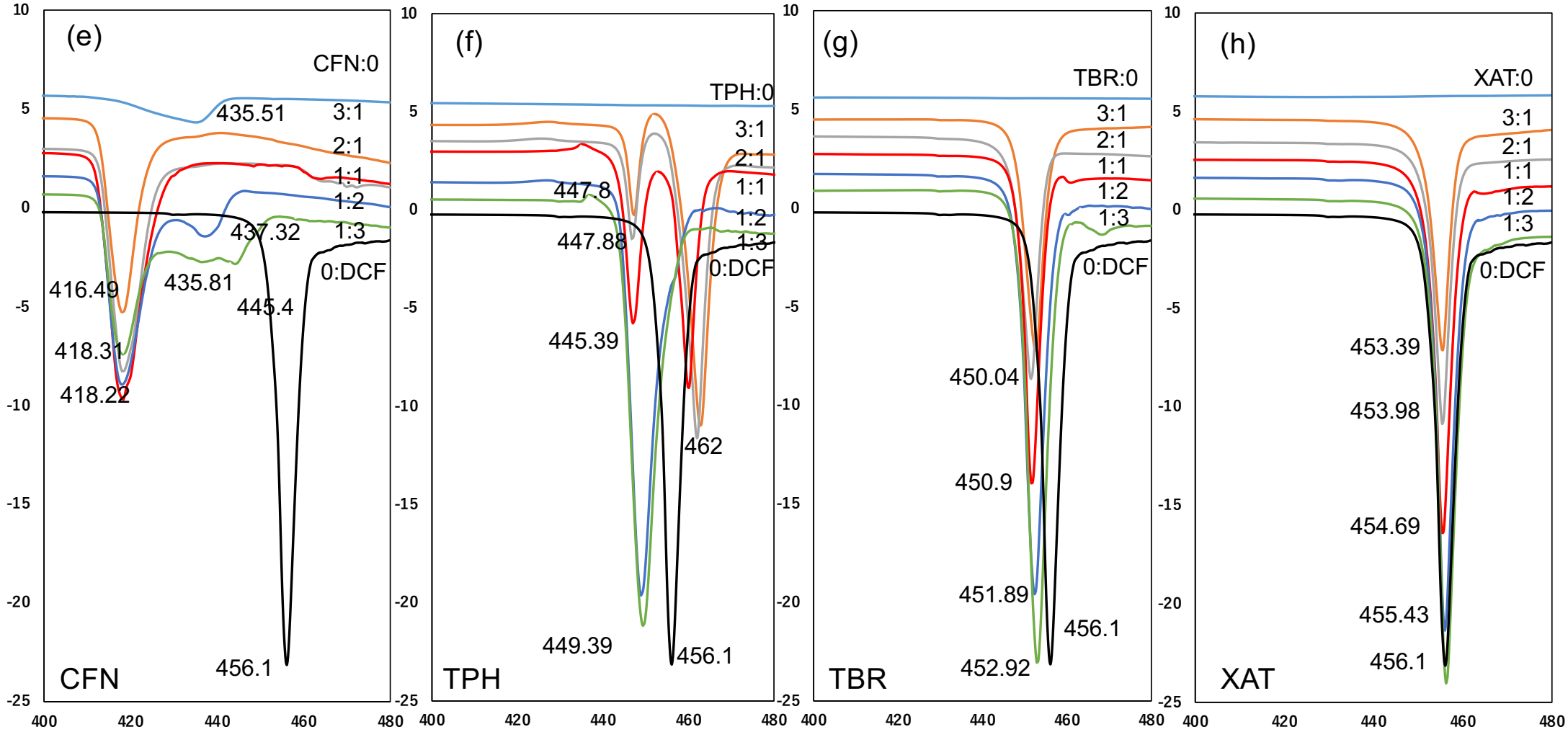

Figure S1. The endothermic signal of DCF melting in the DSC thermograms of the DCF mixtures with CFN (e), TPH (f), TBR (g), and XAT (h), which were expanded from the thermograms in Figure 4. Numbers expressed the temperatures of the peak tops. The intersections of the left-side tangent lines of peaks on the baseline extensions shifted in the mixtures of CFN/DCF, TPH/DCF, and TBR/DCF. However, those in the mixtures of XAT/DCF were invariable, indicating no intermolecular interactions.

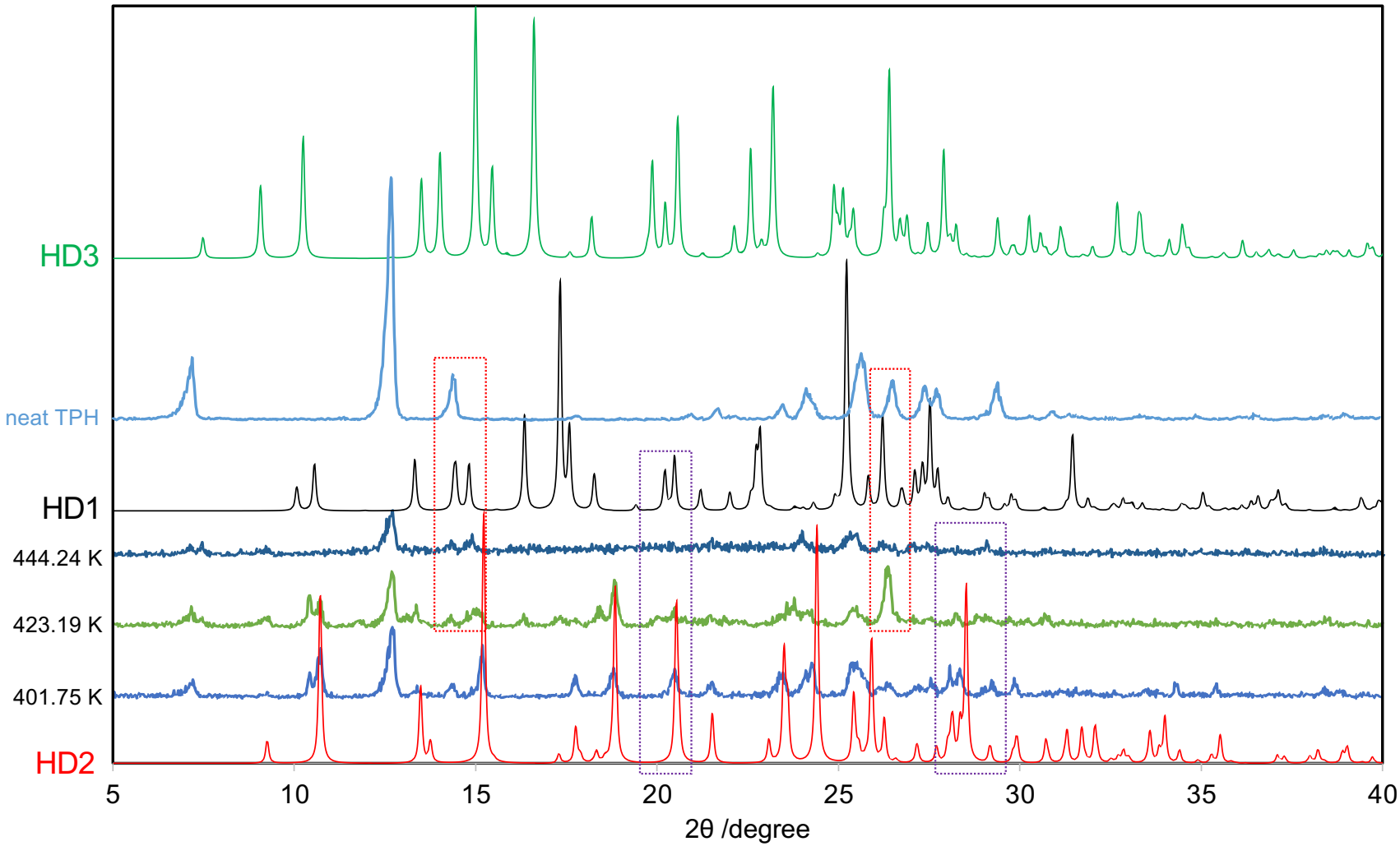

Figure S2. DSC-XRPD diffractograms of the neat TPH (sky blue), the TPH/DCF equimolar mixture at 401.75 K (cyan), 423.19 K (moss green), and 444.24 K (indigo) from Figure 5(h), and the simulated diffractograms of DCF with its polymorphs of HD1 (black), HD2 (red), and HD3 (green).

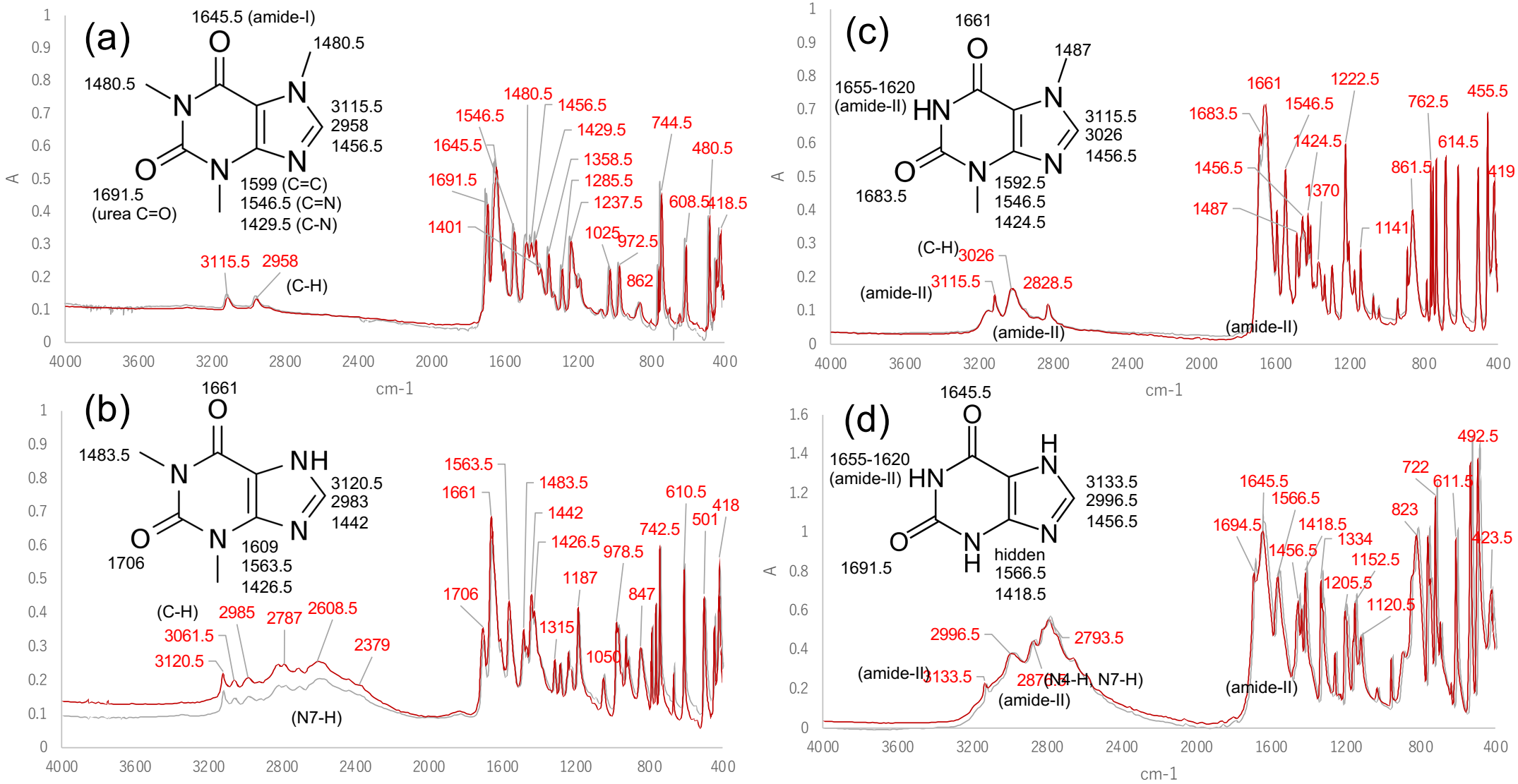

Figure S3. The ATR-FTIR spectra of CFN (a), TPH (b), TBR (c), and XAT (d). Bordeaux lines show spectra of neat crystals, and gray lines show their solids standing for 7 days. Numbers adjacent to noticeable peaks express the corresponding wave numbers. It was considered no particular changes in the significant peaks.

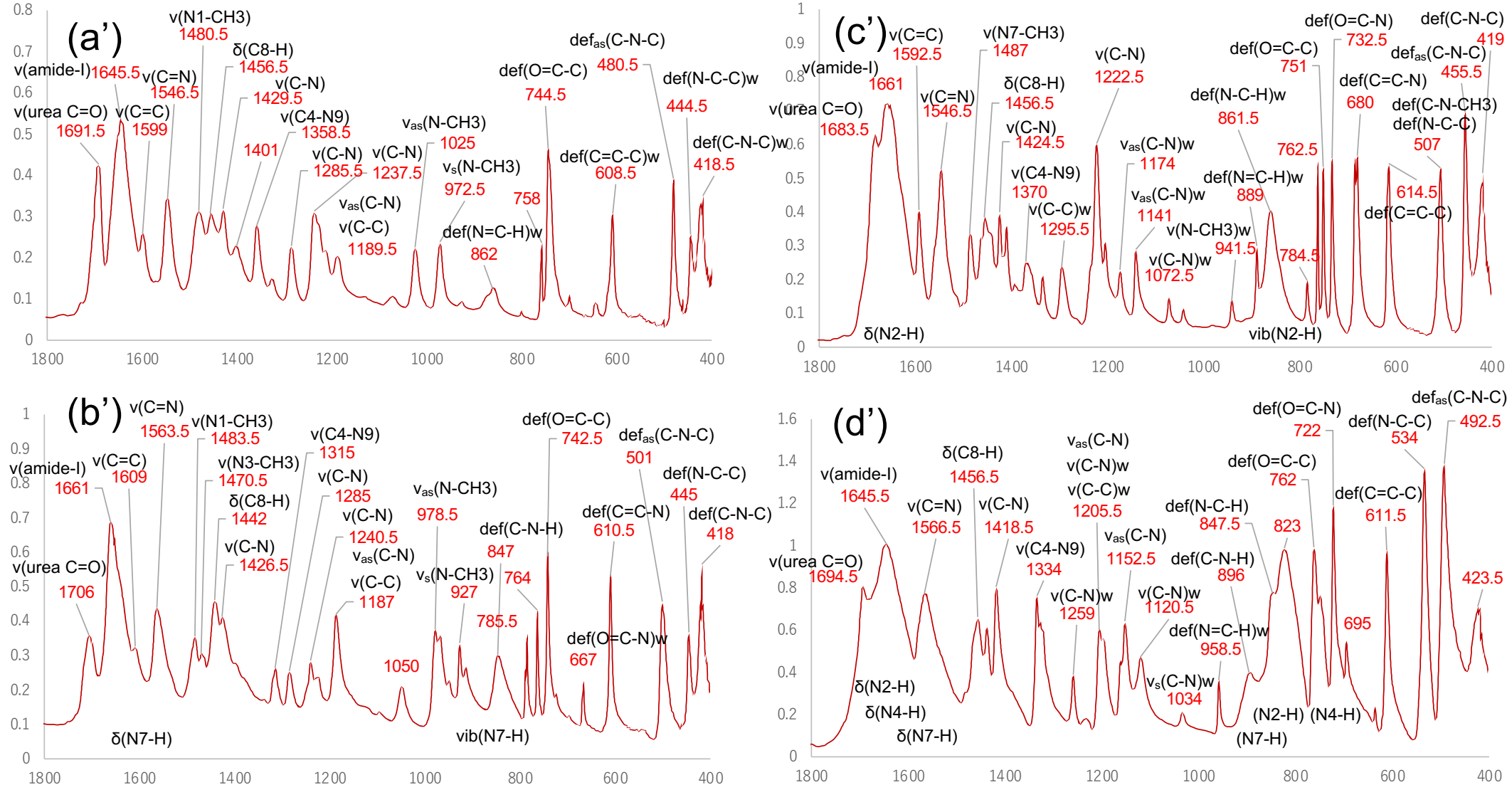

Figure S3. Expansions of the FTIR spectra of CFN (a'), TPH (b'), TBR (c'), and XAT (d') into the wavenumber range of 1800-400 cm^{-1}. Numbers adjacent to noticeable peaks express the corresponding wave numbers. Their assignments to the moieties were appended.

Table S1. The signal assignments for the normal modes of the structural vibrations in the ATR-FTIR spectra of the neat XAT derivatives.

	CFN	TPH	TBR	XAT
Purine C8-H stretching	3112, 2958	3121, 2985	3116, 3026	3134, 2997
Amide-II (N2-H stretching)	-	-	2829	2877
N3-H, N7-H stretching	-	2787, 2609	-	2794, …
Urea C2=O stretching: Falk 1989	1692	1706	1684	1695
Amide-I C6=O stretching: Falk 1989	1646	1661	1661	1646
Amide-II N1-H bending (scissoring)	-	-	1655-1620	1655-1620
Purine C4=C5 stretching: Cohen 1975	1599	1609	1592	n.d.
Purine C8=N9 stretching: Cohen 1975	1547	1564	1547	1567
substitution CH3 bending (1453)	1480	1484	1487	-
Purine C8-H bending: Cohen 1975	1457	1442	1457	1457
Purine C5-N7 stretching: Silverstein	1430	1427	1425	1419
Purine C4-N9 stretching	1359	1315	1370	1334
Purine C-N, C-O vibration: Cohen 1975	1289,1238, 1190	1285,1241, 1187	1295,1223, 1174	1259,1206, 1153

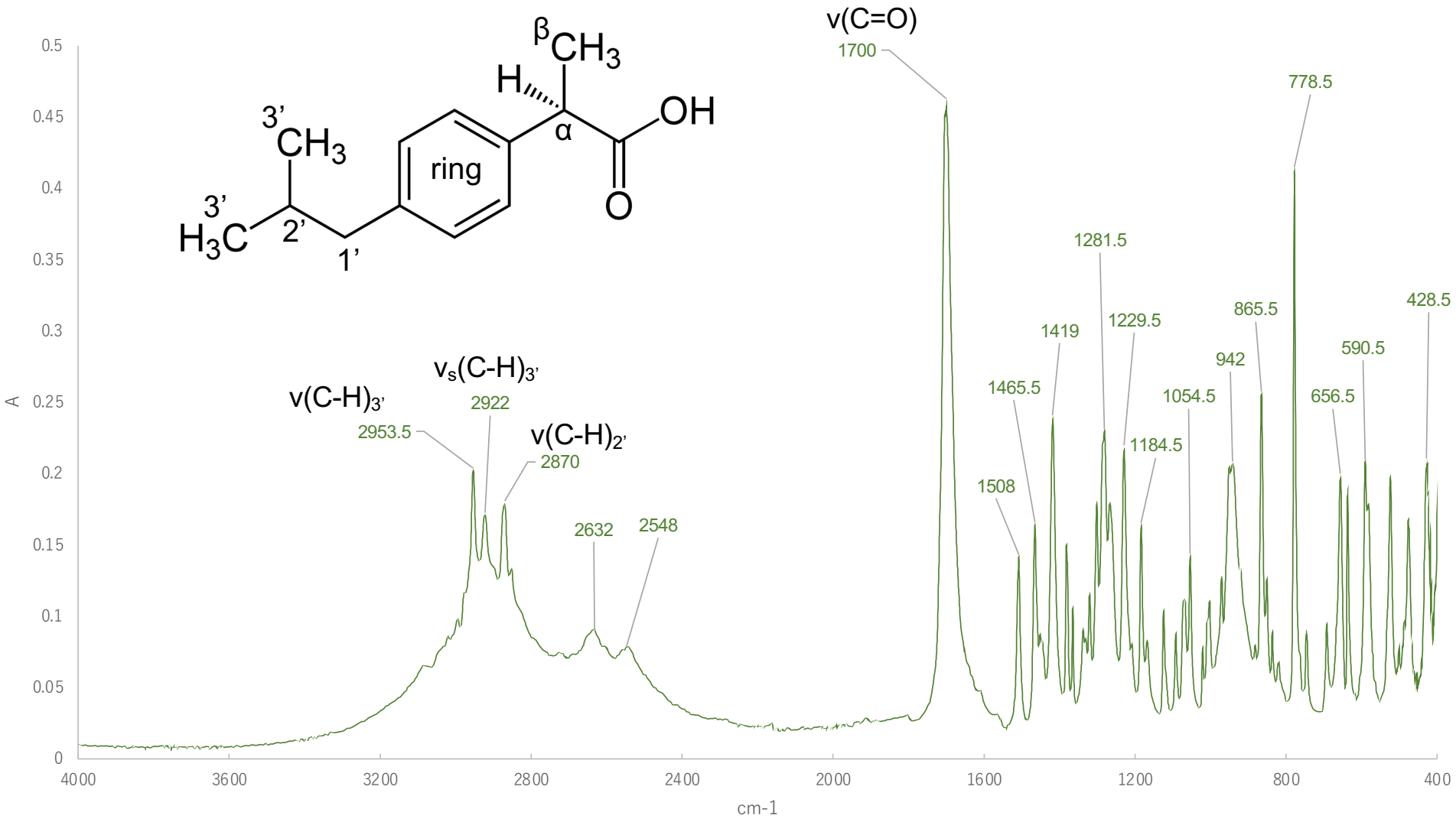

Figure S4. The ATR-FTIR spectra of IBP.

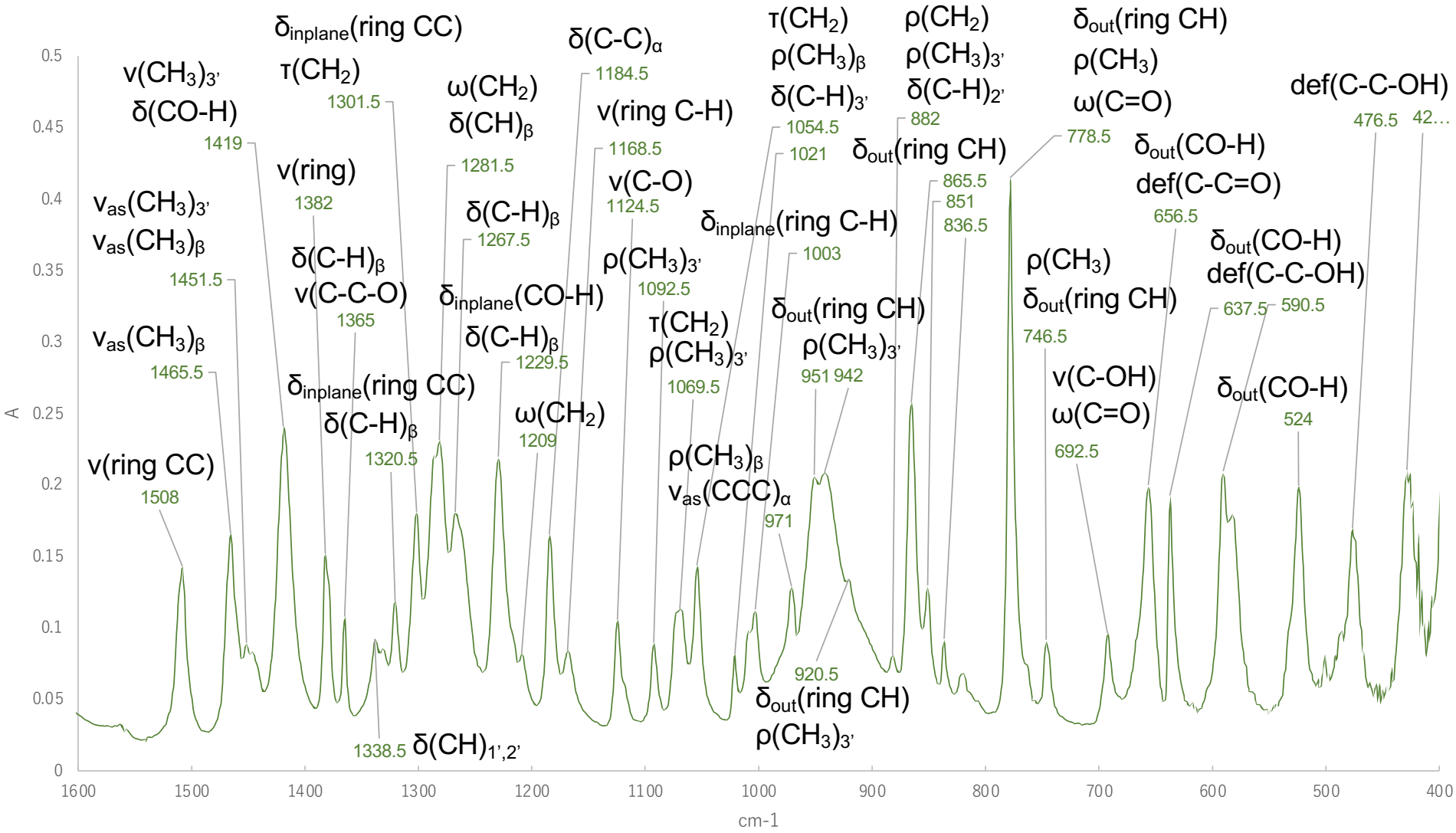

Figure S4. The ATR-FTIR spectra of IBP. Vibration modes were represented as v: stretching, δ: bending, ω: wagging, ρ: rocking, and τ: twisting.

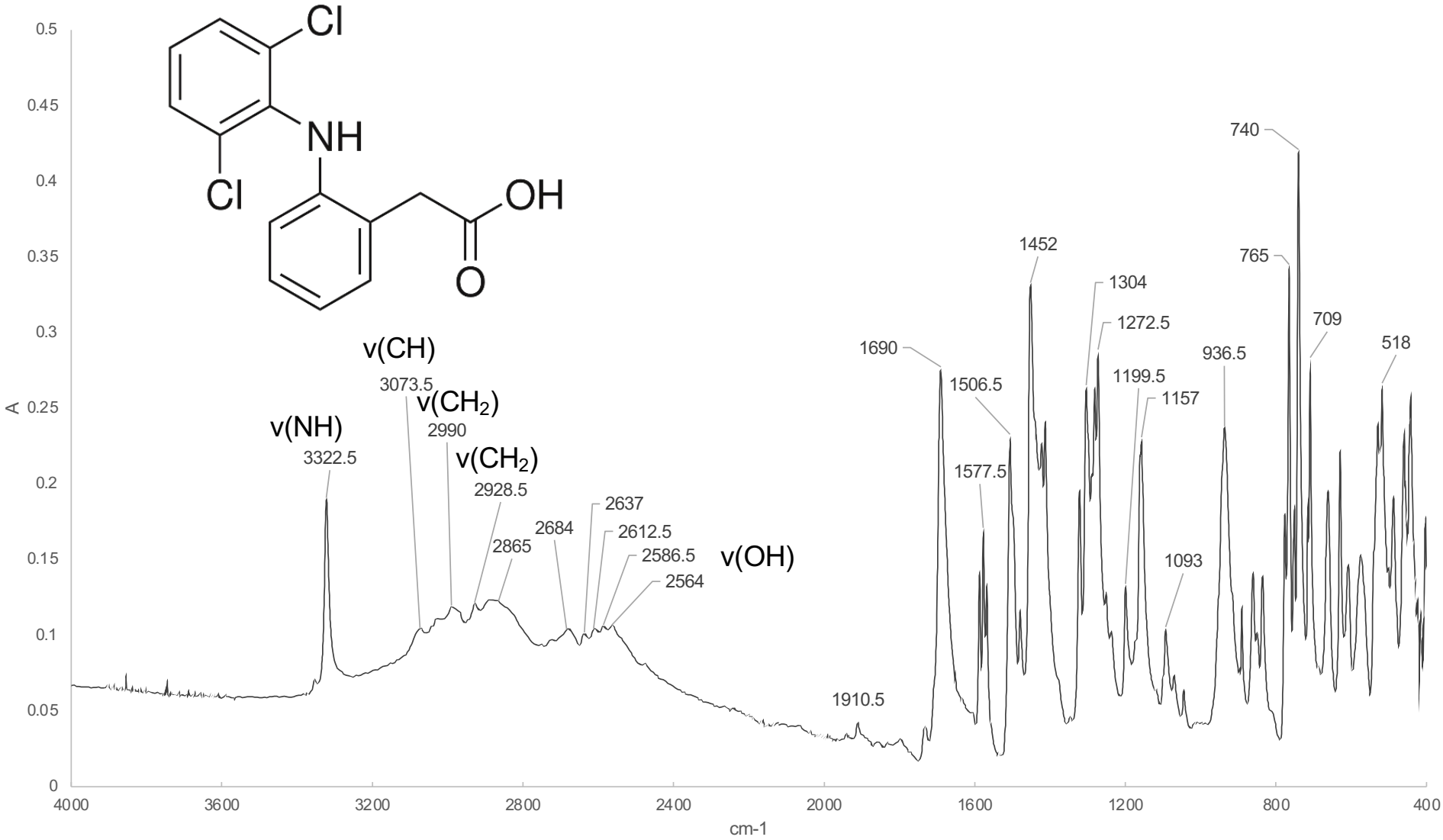

Figure S4. The ATR-FTIR spectra of DCF.

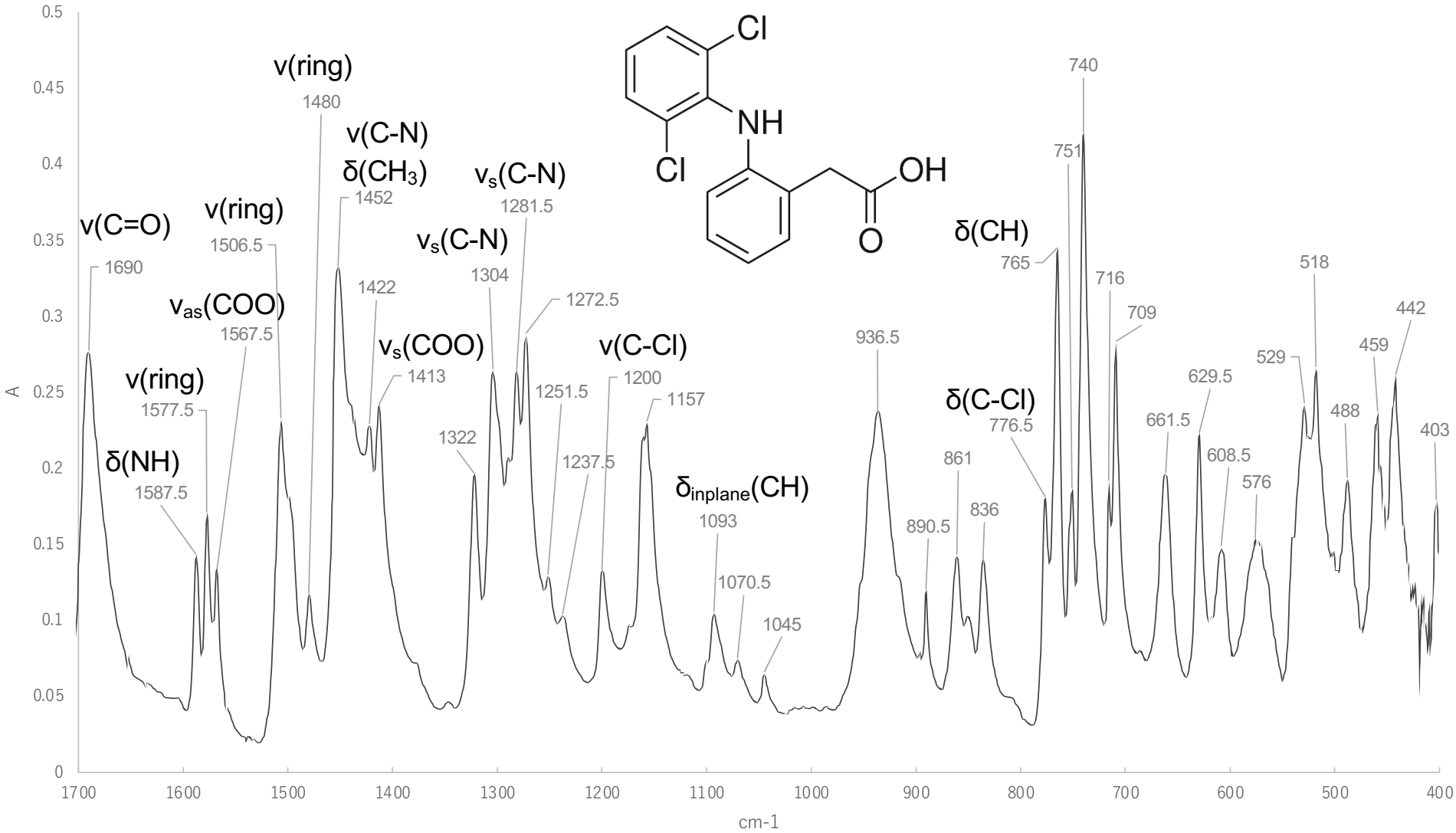

Figure S4. The ATR-FTIR spectra of DCF. Vibration modes were represented as ν: stretching, δ: bending, ω: wagging, ρ: rocking, and τ: twisting.

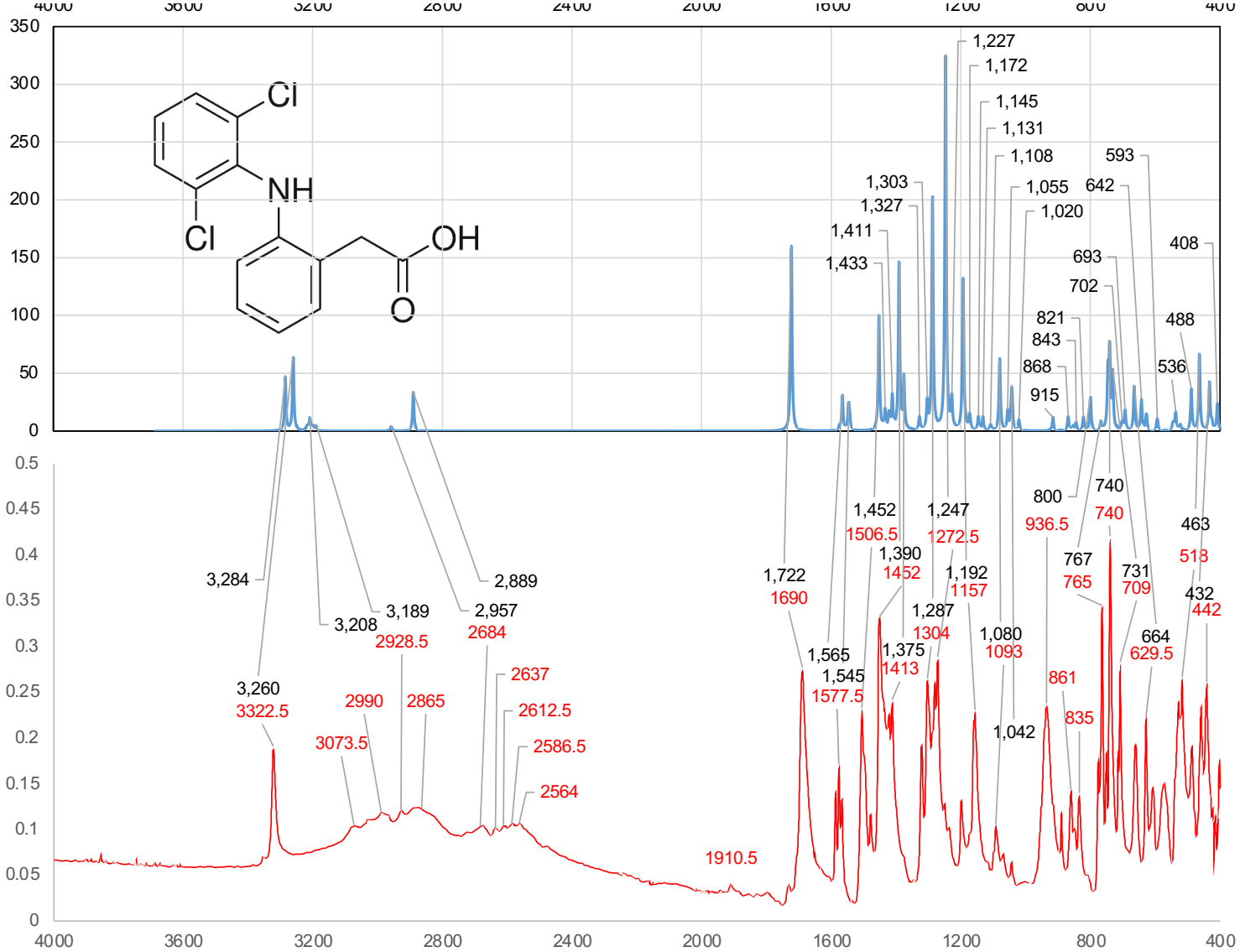

Figure S4. The ATR-FTIR spectra of DCF. Assignment the FTIR signals onto the simulated peaks in the normal mode analysis.

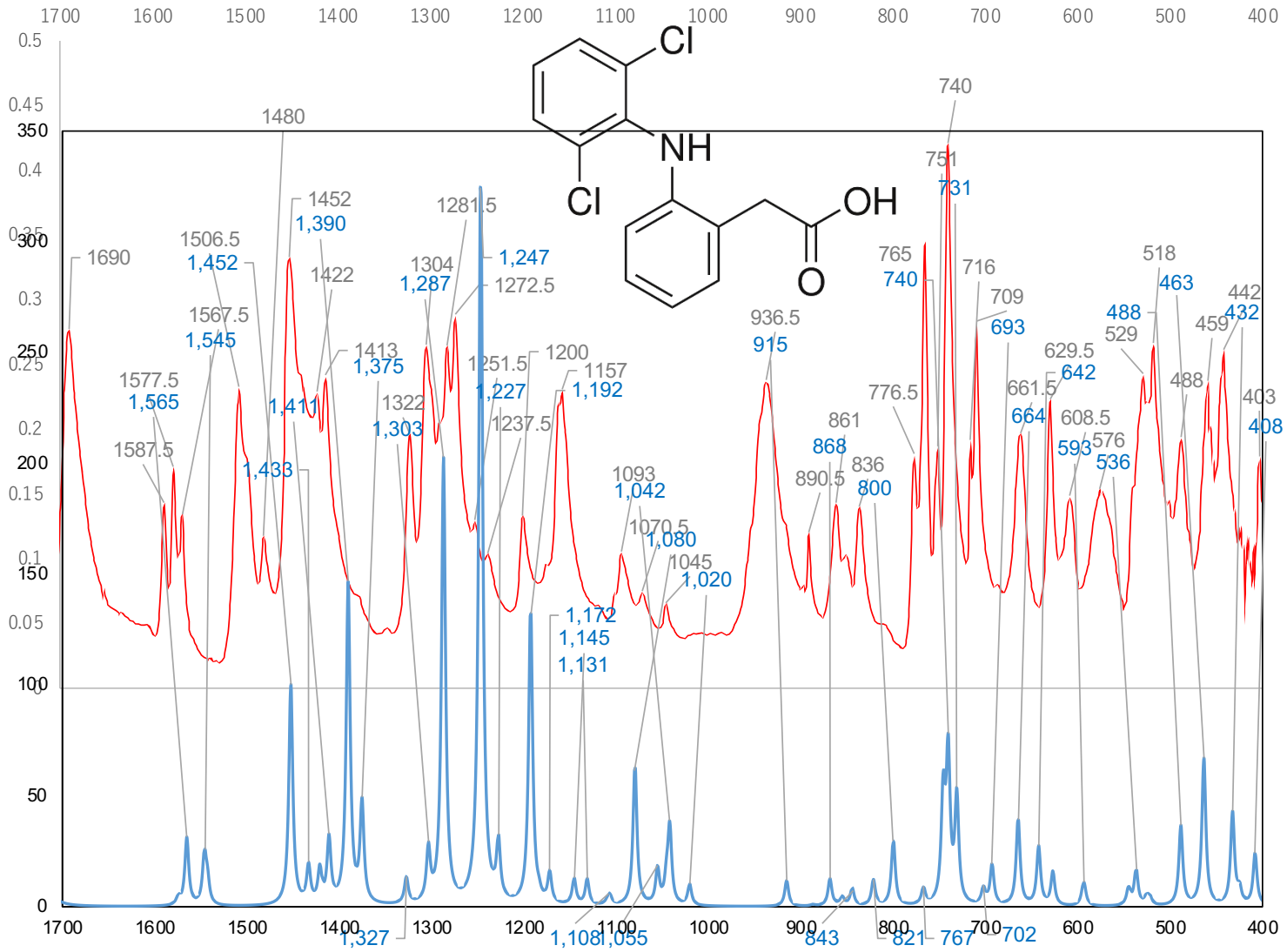

Figure S4. The ATR-FTIR spectra of DCF. Assignment the FTIR signals onto the simulated peaks in the normal mode analysis.

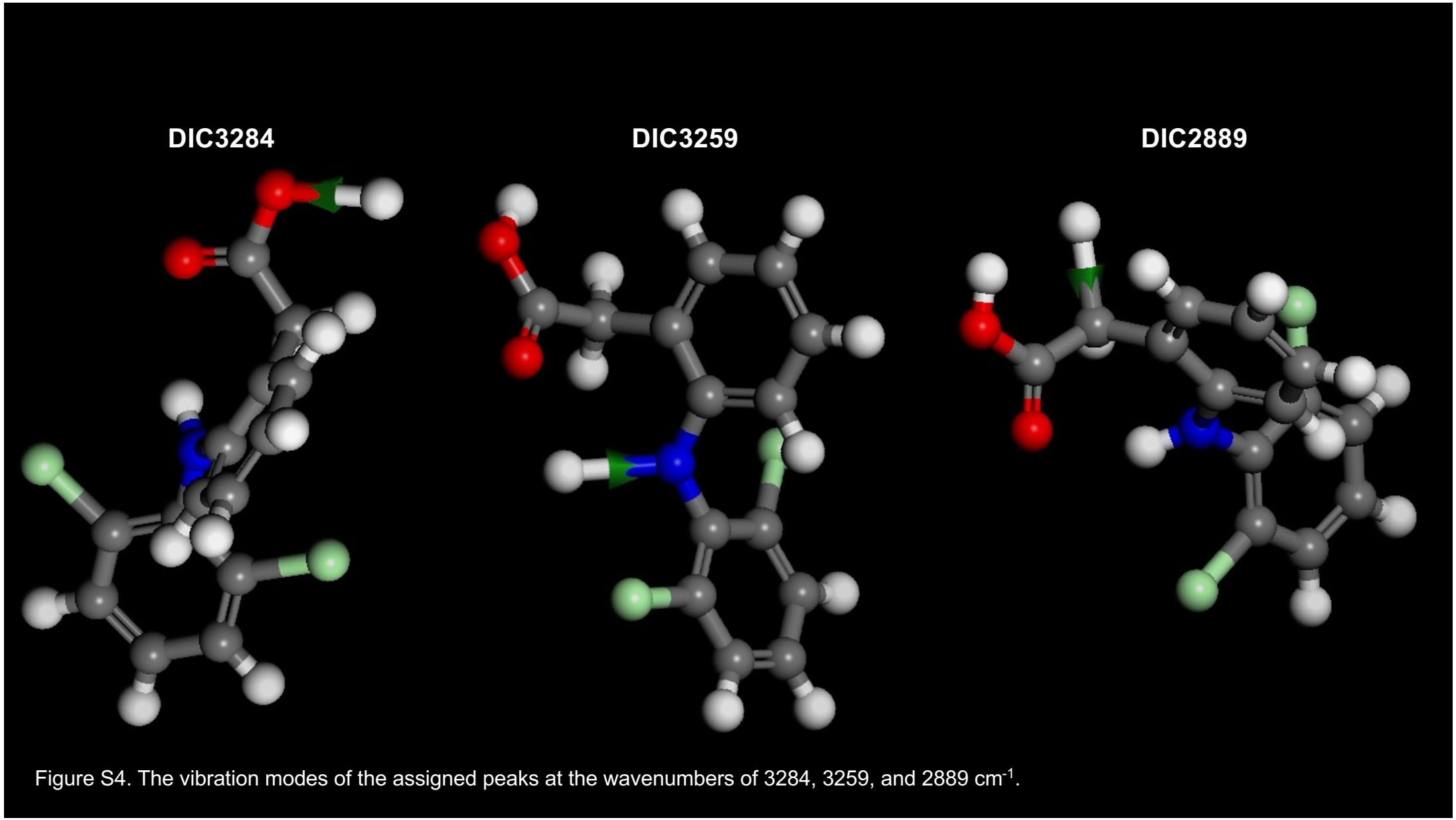

Figure S4. The vibration modes of the assigned peaks at the wavenumbers of 3284, 3259, and 2889 cm^{-1}.

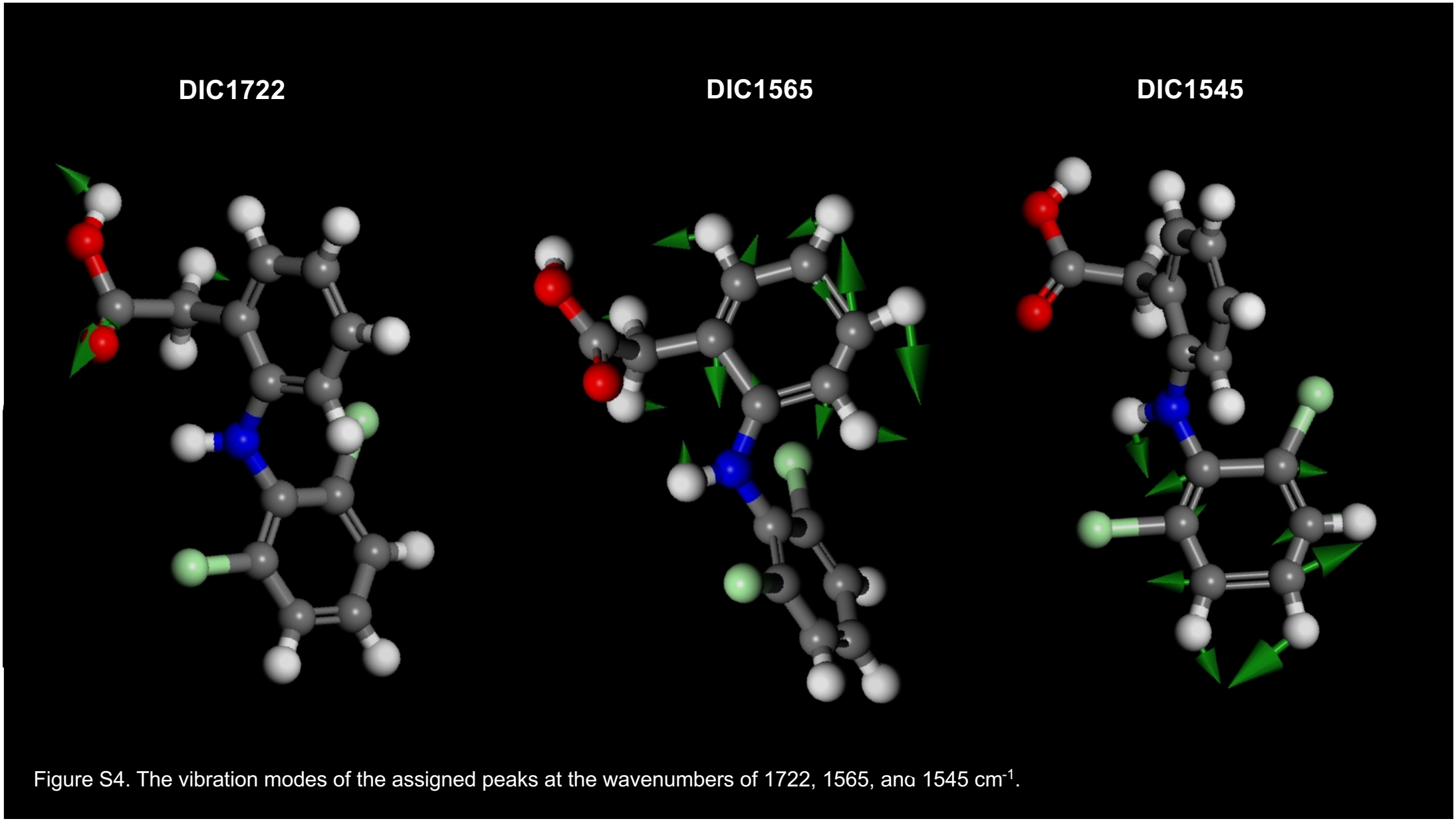

Figure S4. The vibration modes of the assigned peaks at the wavenumbers of 1722, 1565, and 1545 cm^{-1}.

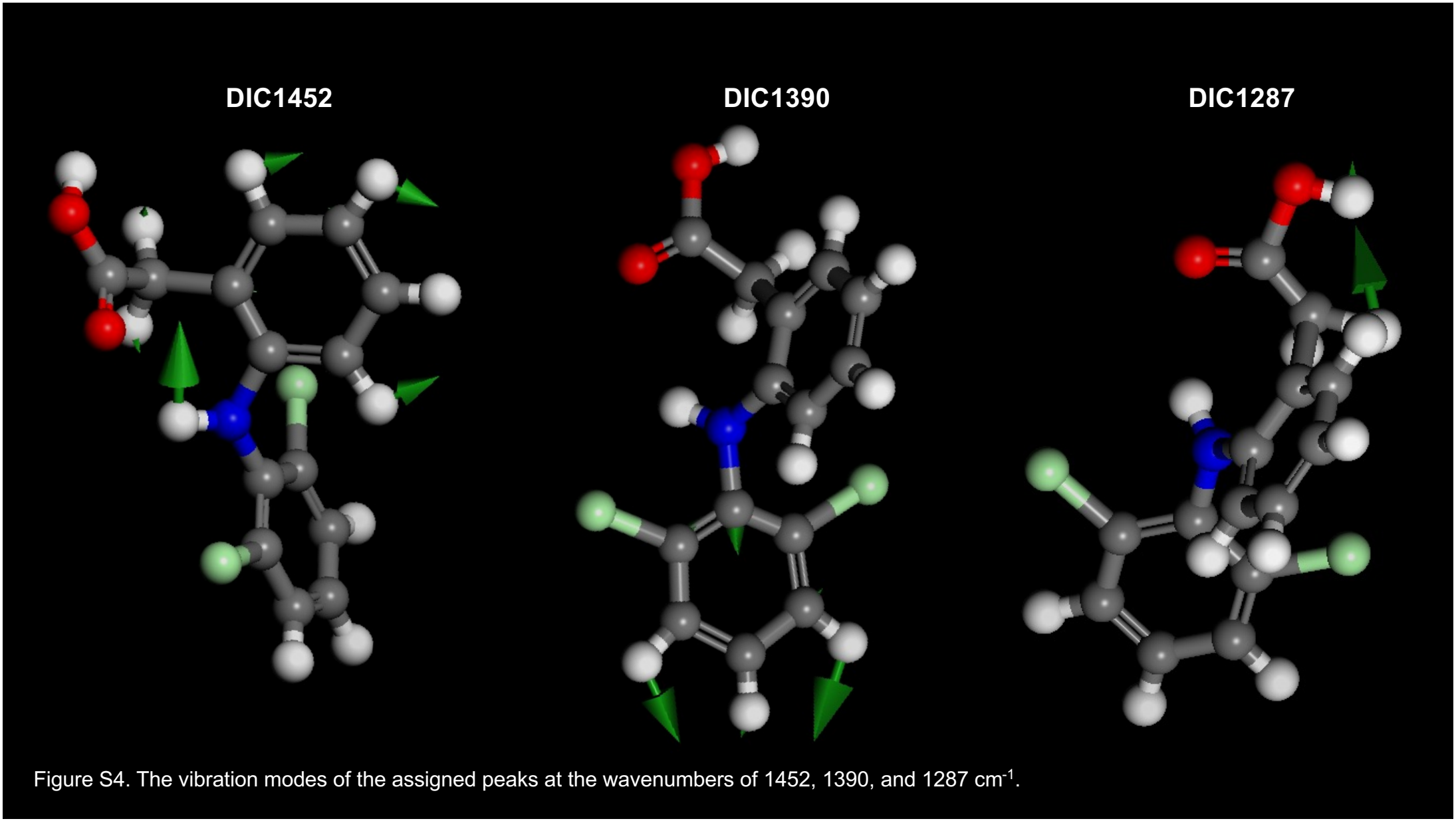

Figure S4. The vibration modes of the assigned peaks at the wavenumbers of 1452, 1390, and 1287 cm^{-1}.

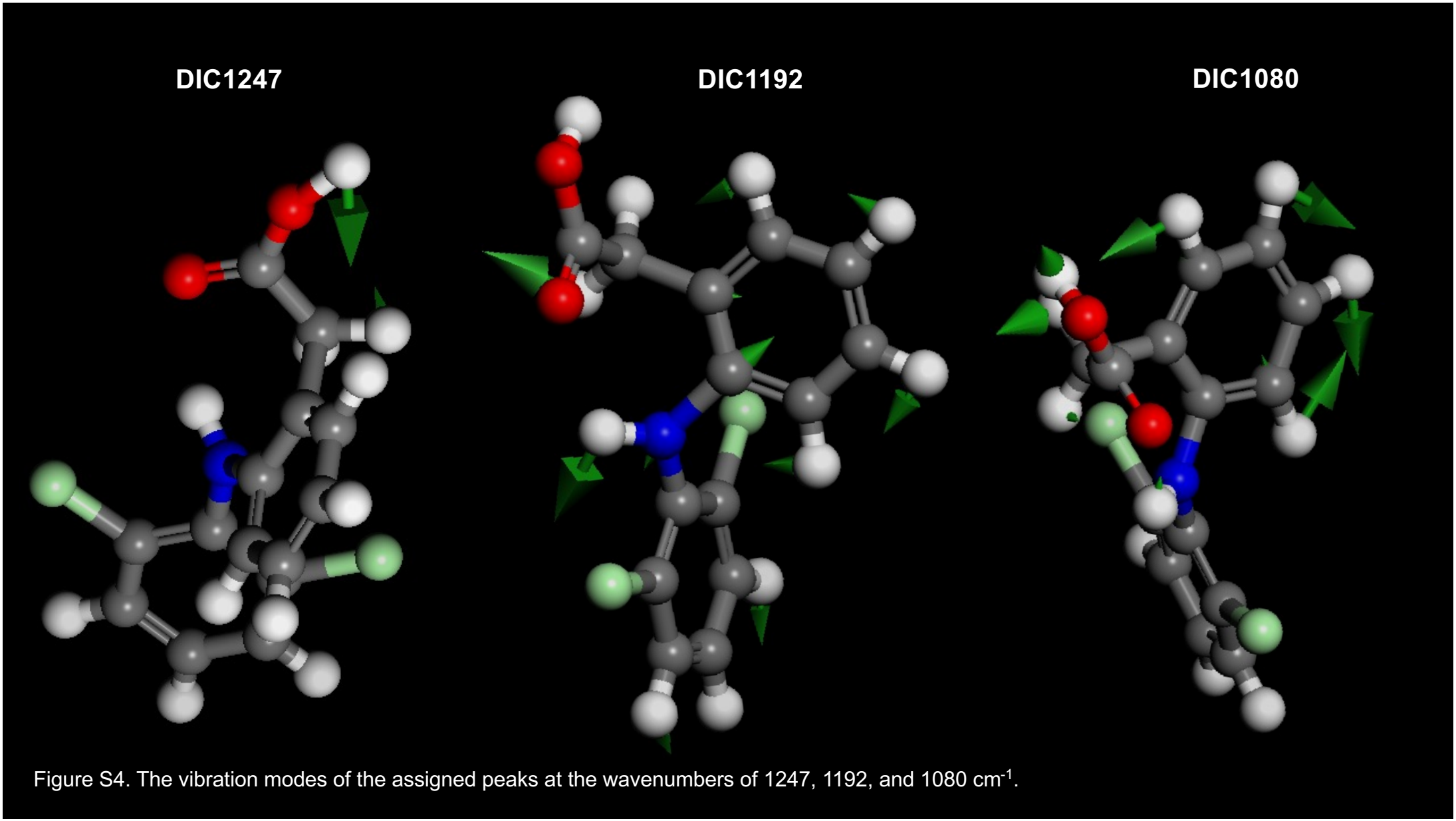

Figure S4. The vibration modes of the assigned peaks at the wavenumbers of 1247, 1192, and 1080 cm^{-1}.

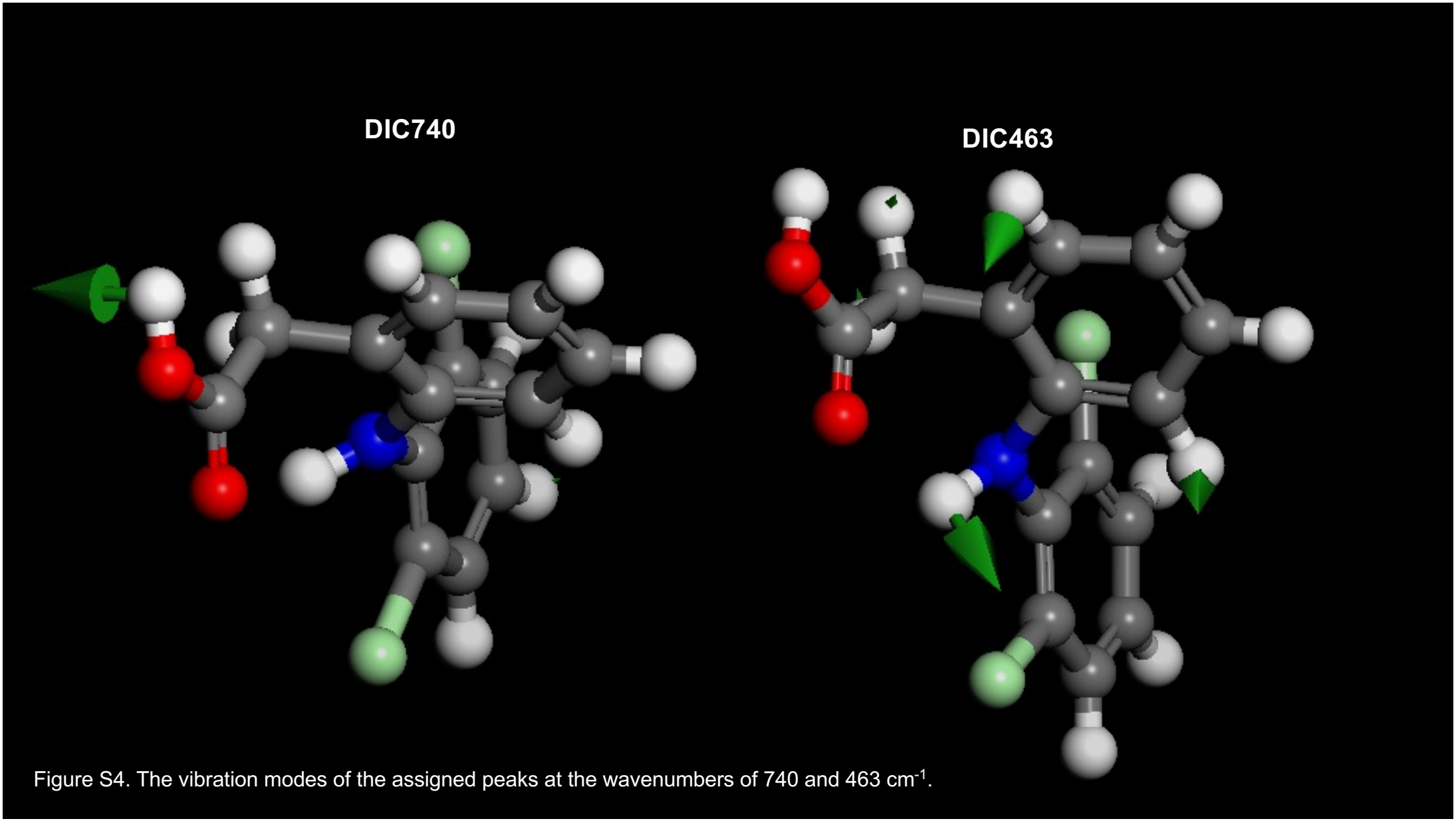

Figure S4. The vibration modes of the assigned peaks at the wavenumbers of 740 and 463 cm^{-1}.

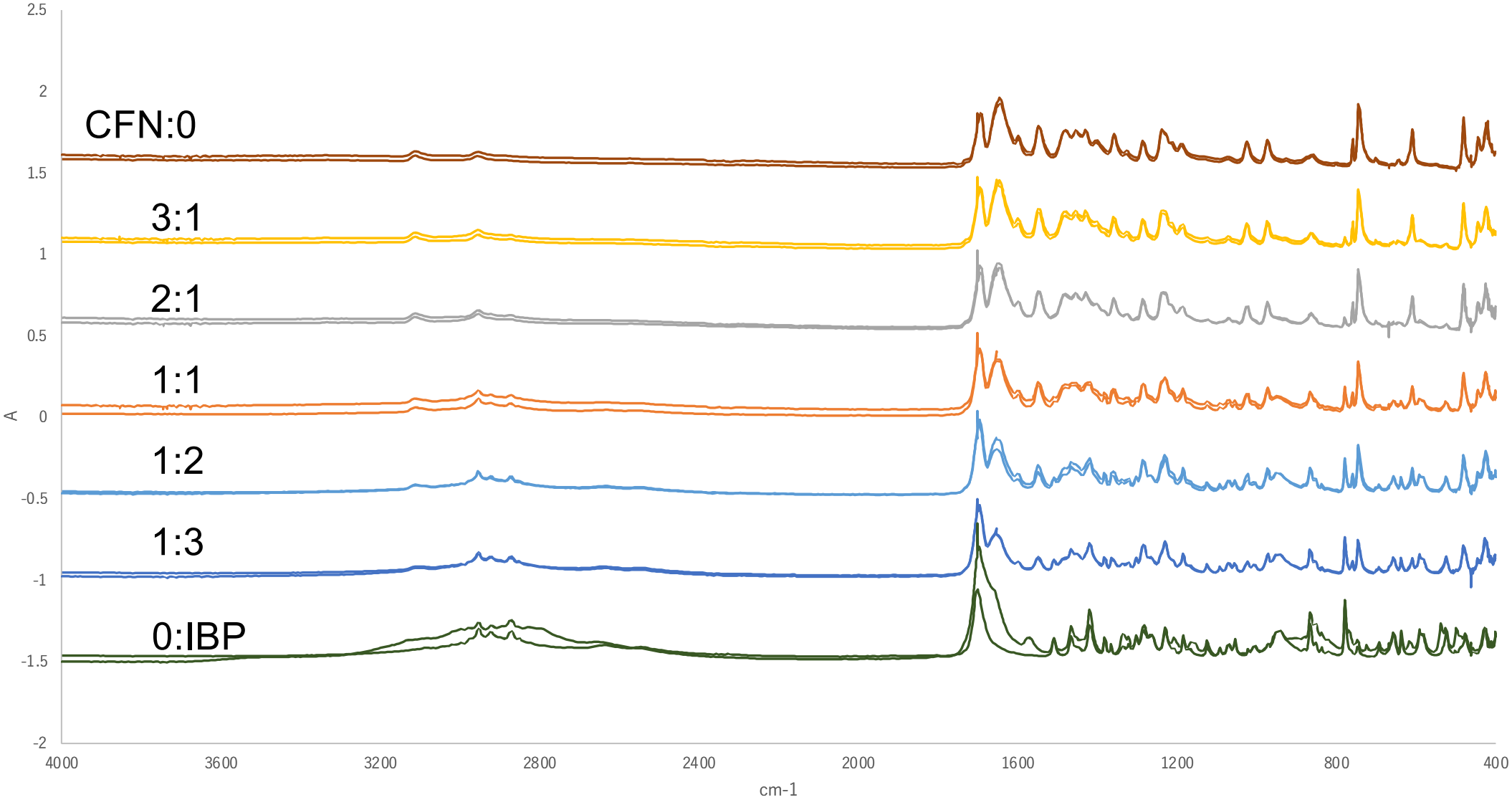

Figure S5. (a) Crystalline FTIR spectra of mixtures of IBP with CFN at various molar ratios. Neat CFN (brown), neat IBP (black), and their mixtures at the ratios of 3:1 (yellow), 2:1 (gray), 1:1 (orange), 1:2 (sky blue), and 1:3 (blue) were measured twice.

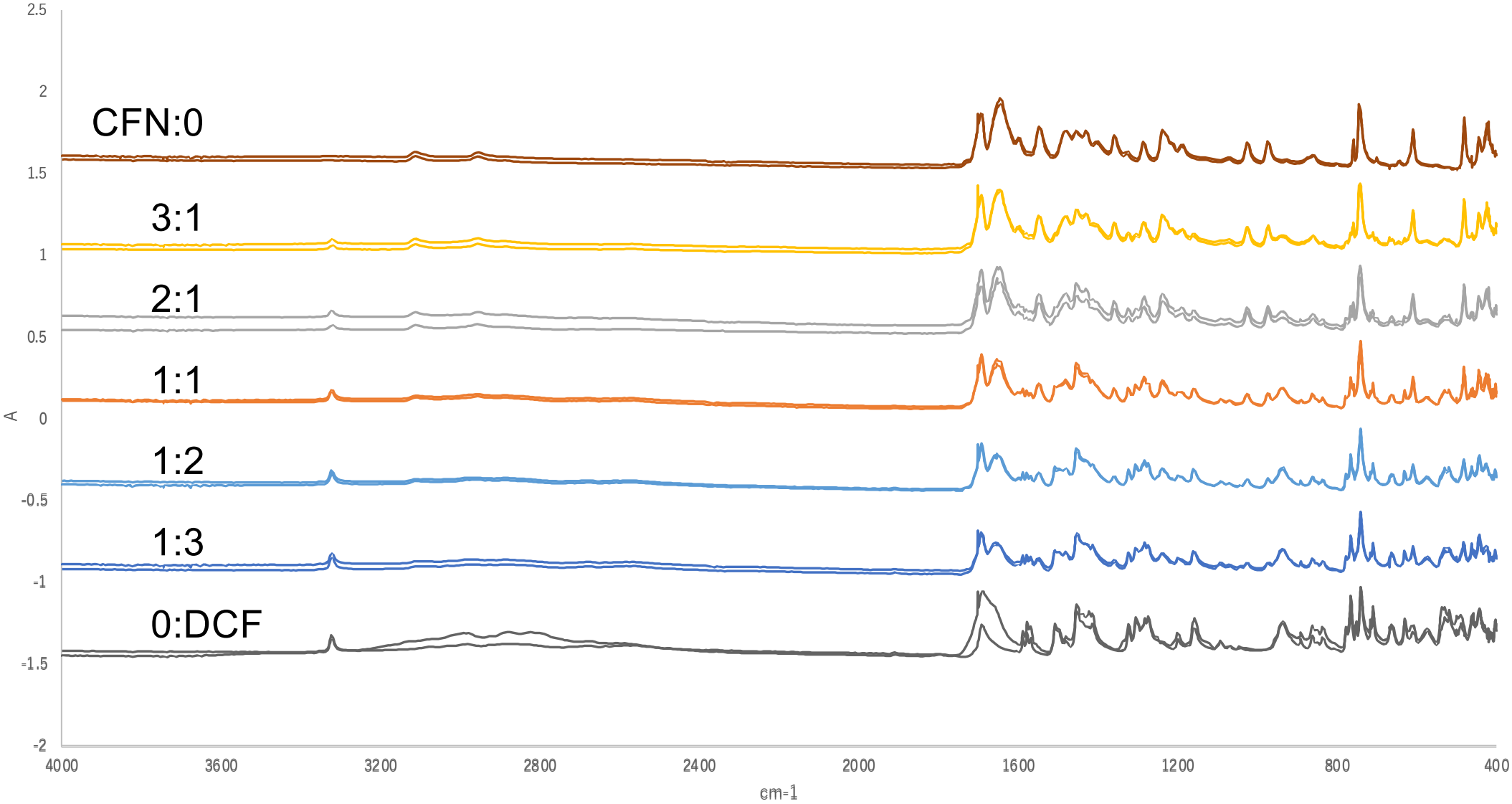

Figure S5. (b) Crystalline FTIR spectra of mixtures of DCF with CFN at various molar ratios. Neat CFN (brown), neat DCF (black), and their mixtures at the ratios of 3:1 (yellow), 2:1 (gray), 1:1 (orange), 1:2 (sky blue), and 1:3 (blue) were measured twice.

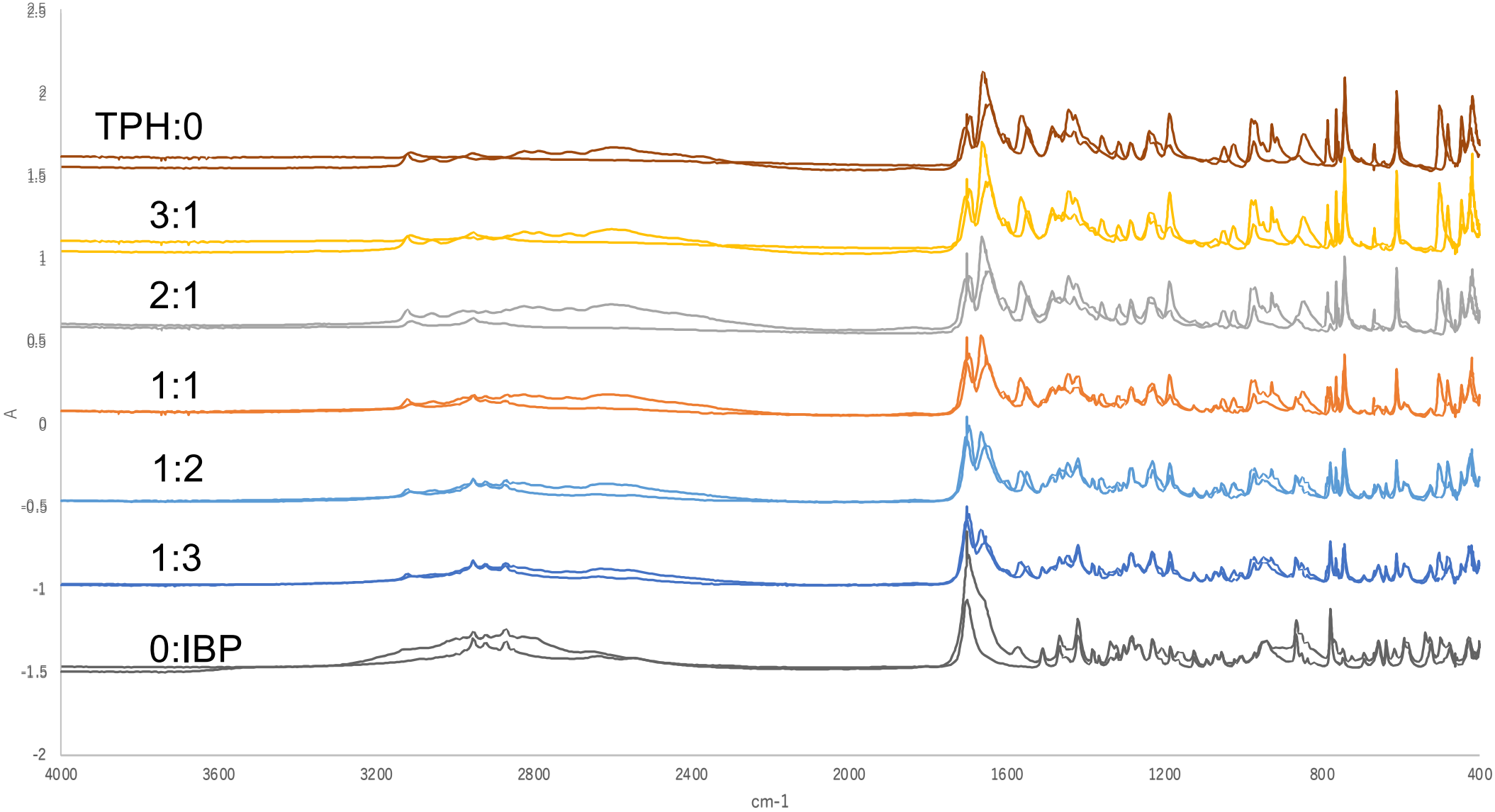

Figure S5. (c) Crystalline FTIR spectra of mixtures of IBP with TPH at various molar ratios. Neat TPH (brown), neat IBP (black), and their mixtures at the ratios of 3:1 (yellow), 2:1 (gray), 1:1 (orange), 1:2 (sky blue), and 1:3 (blue) were measured twice.

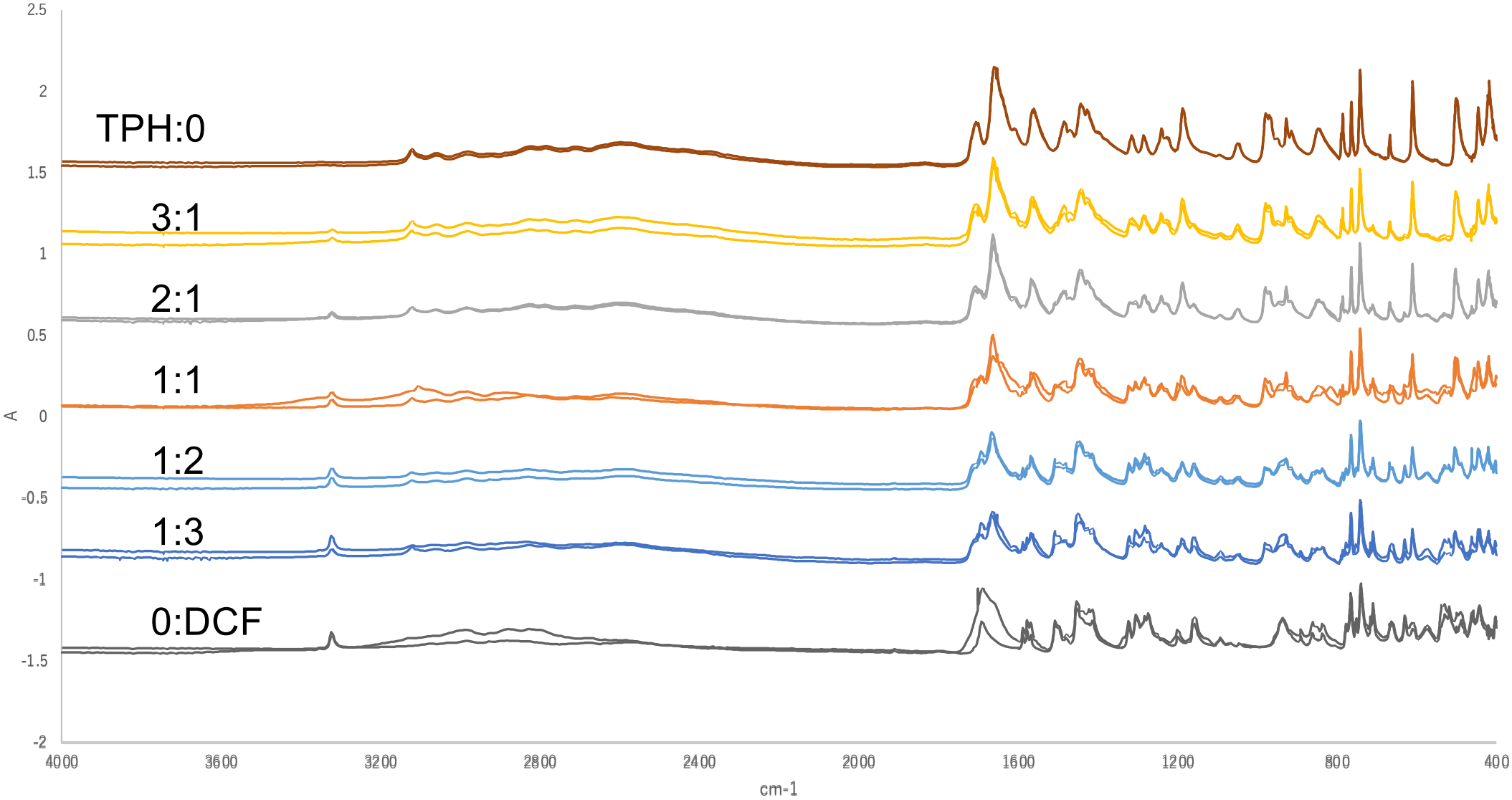

Figure S5. (d) Crystalline FTIR spectra of mixtures of DCF with TPH at various molar ratios. Neat TPH (brown), neat DCF (black), and their mixtures at the ratios of 3:1 (yellow), 2:1 (gray), 1:1 (orange), 1:2 (sky blue), and 1:3 (blue) were measured twice.

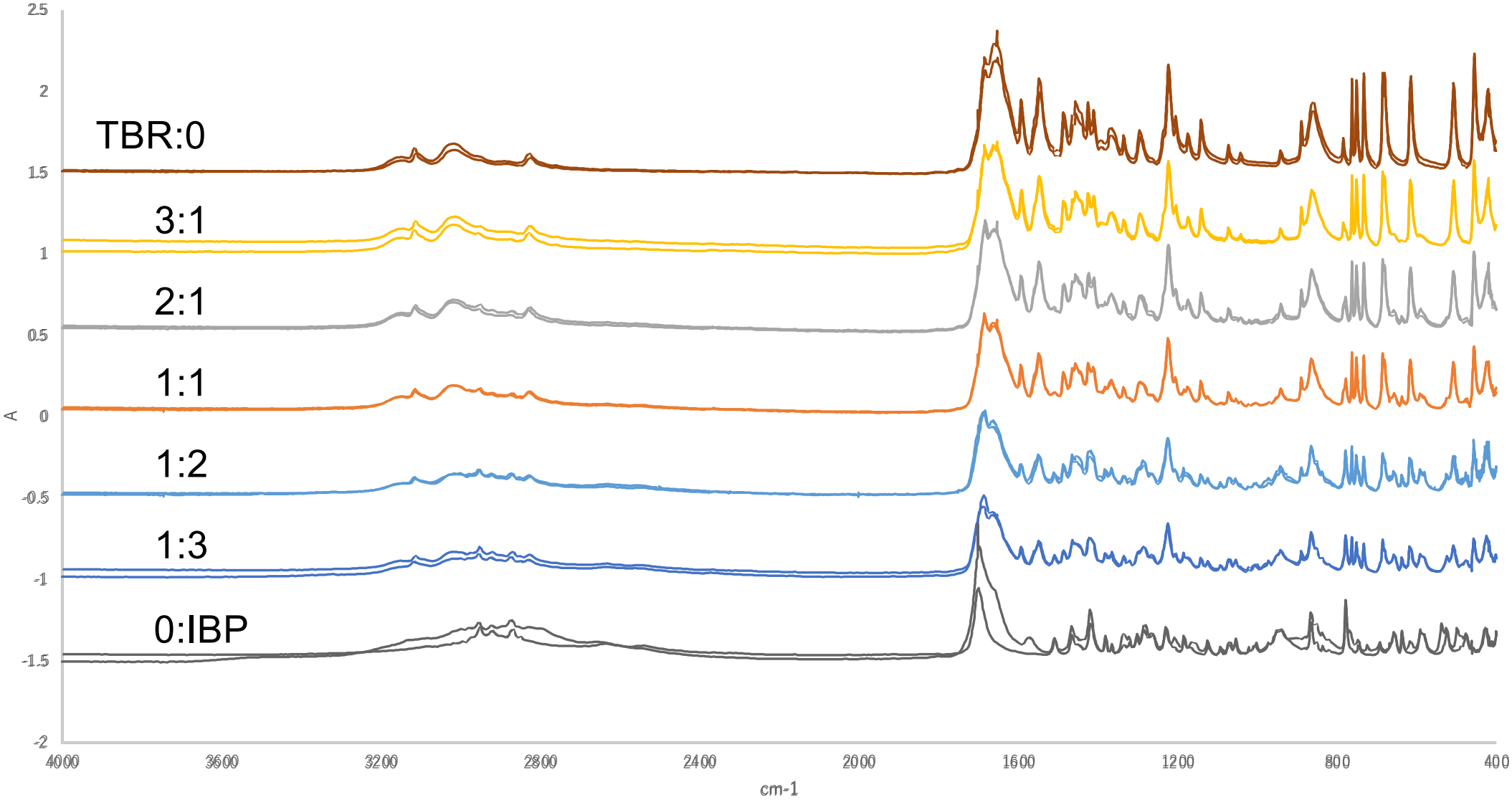

Figure S5. (e) Crystalline FTIR spectra of mixtures of IBP with TBR at various molar ratios. Neat TBR (brown), neat IBP (black), and their mixtures at the ratios of 3:1 (yellow), 2:1 (gray), 1:1 (orange), 1:2 (sky blue), and 1:3 (blue) were measured twice.

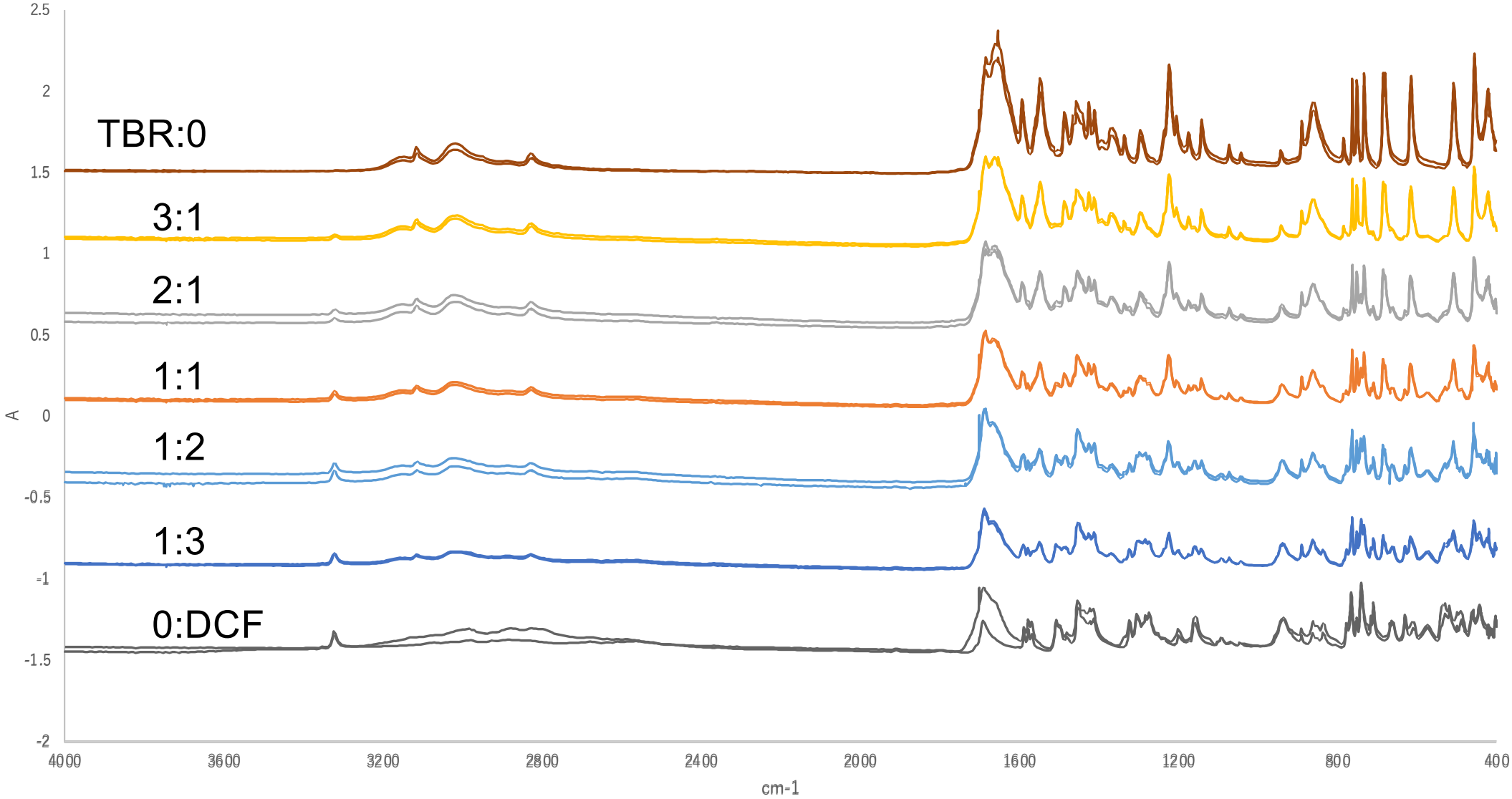

Figure S5. (f) Crystalline FTIR spectra of mixtures of DCF with TBR at various molar ratios. Neat TBR (brown), neat DCF (black), and their mixtures at the ratios of 3:1 (yellow), 2:1 (gray), 1:1 (orange), 1:2 (sky blue), and 1:3 (blue) were measured twice.

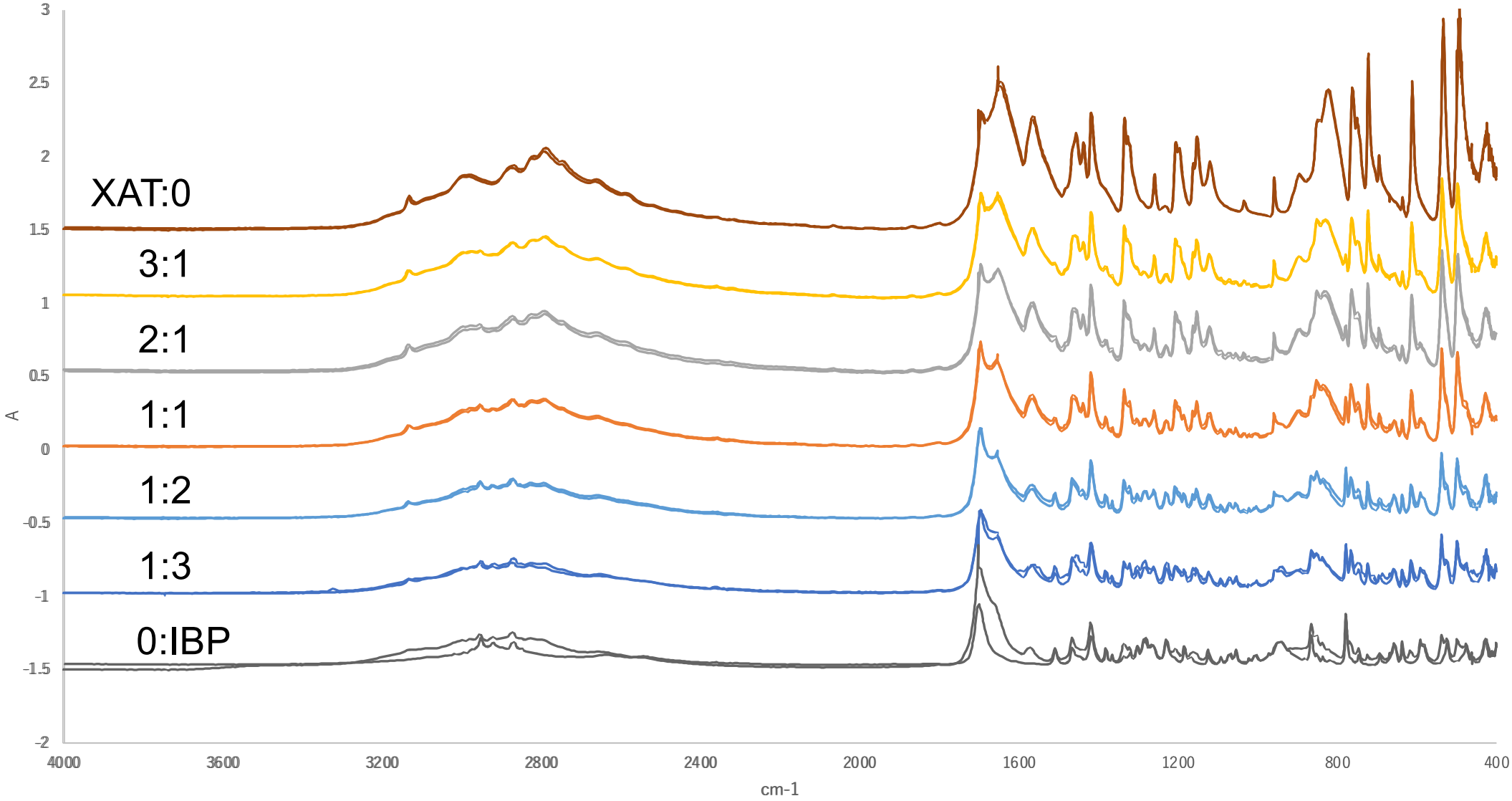

Figure S5. (g) Crystalline FTIR spectra of mixtures of IBP with XAT at various molar ratios. Neat XAT (brown), neat IBP (black), and their mixtures at the ratios of 3:1 (yellow), 2:1 (gray), 1:1 (orange), 1:2 (sky blue), and 1:3 (blue) were measured twice.

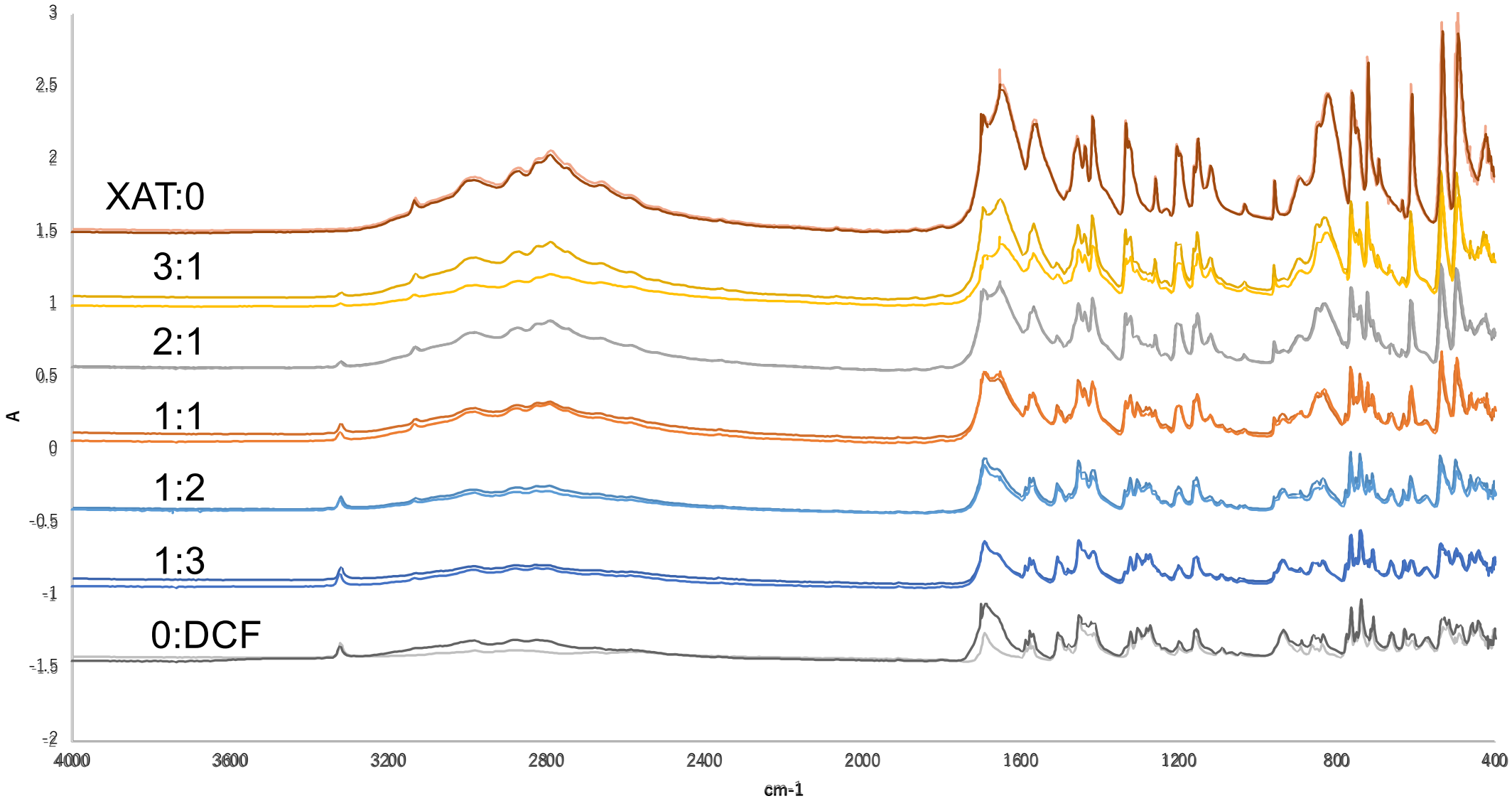

Figure S5. (h) Crystalline FTIR spectra of mixtures of DCF with XAT at various molar ratios. Neat XAT (brown), neat DCF (black), and their mixtures at the ratios of 3:1 (yellow), 2:1 (gray), 1:1 (orange), 1:2 (sky blue), and 1:3 (blue) were measured twice.

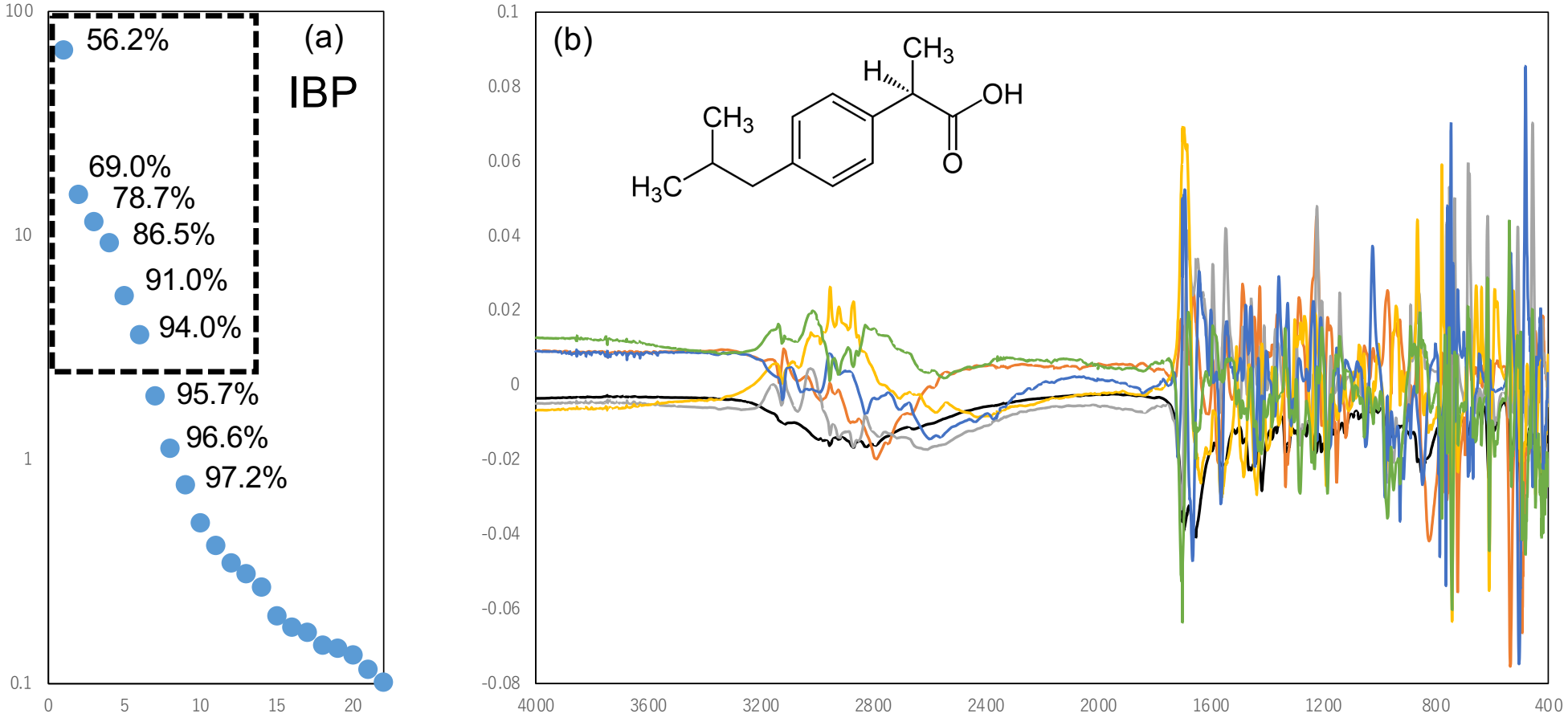

Figure S6. Summarized results of SVD computation for the IBP mixtures with the XAT derivatives: (a) the singular values and their corresponding cumulative sum of variances and (b) the first to sixth basis functions (94%). Curves in descending order were represented by colors of black, orange, gray, yellow, blue, and green.

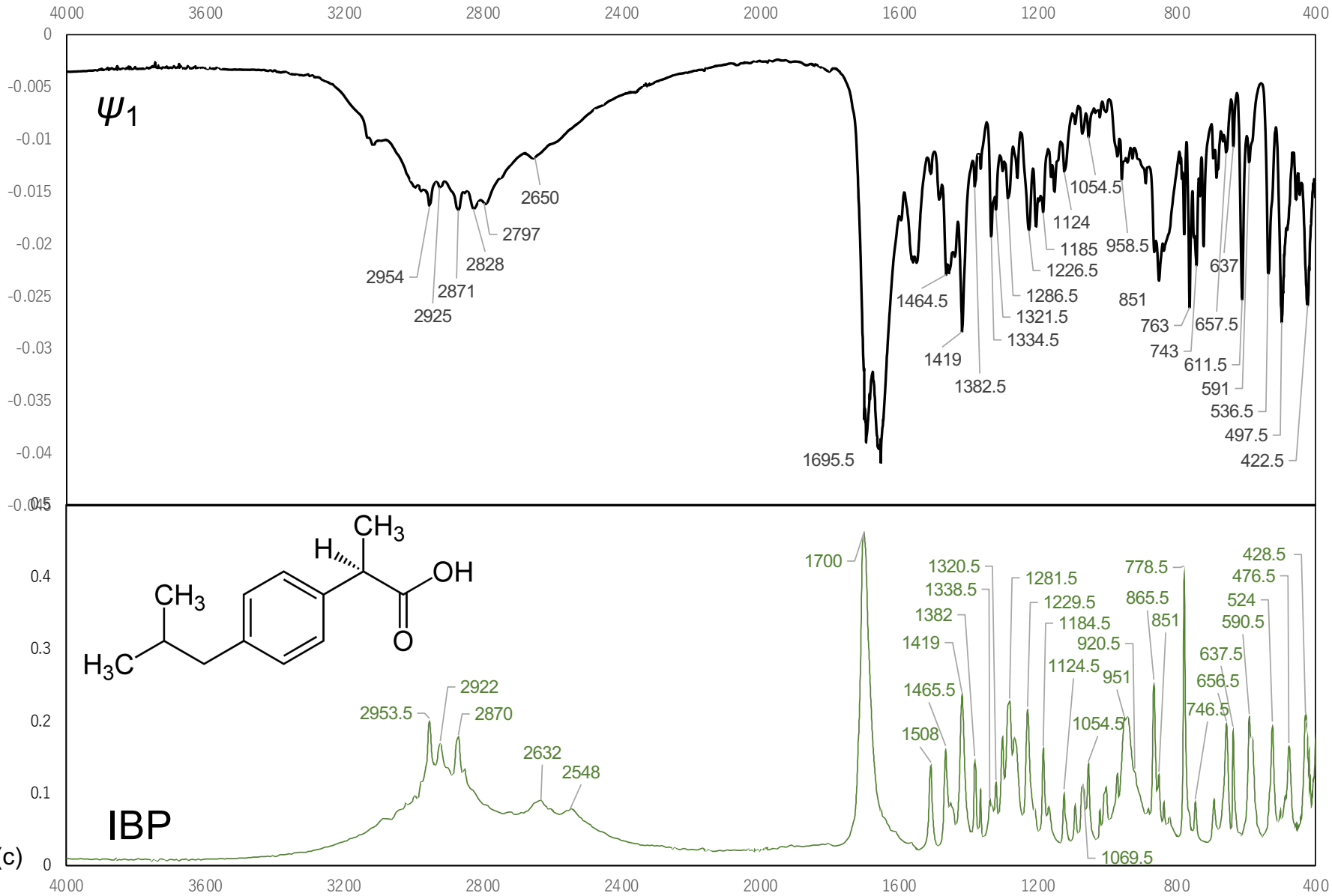
ψ1
2954
2925
2871
2828
2797
2650
1695.5
1464.5
1419
1382.5
1334.5
1321.5
1286.5
1226.5
1185
1124
1054.5
958.5
851
763
743
637
657.5
611.5
591
536.5
497.5
422.5
IBP
CH3
H
OH
O
CH3
H3C
2953.5
2922
2870
2632
2548
1700
1508
1465.5
1419
1382
1338.5
1320.5
1281.5
1229.5
1184.5
1124.5
1069.5
1054.5
951
920.5
865.5
851
778.5
746.5
656.5
637.5
590.5
524
476.5
428.5
4000
3600
3200
2800
2400
2000
1600
1200
800
400
0
-0.005
-0.01
-0.015
-0.02
-0.025
-0.03
-0.035
-0.04
0.4
0.3
0.2
0.1

Figure S6(c)

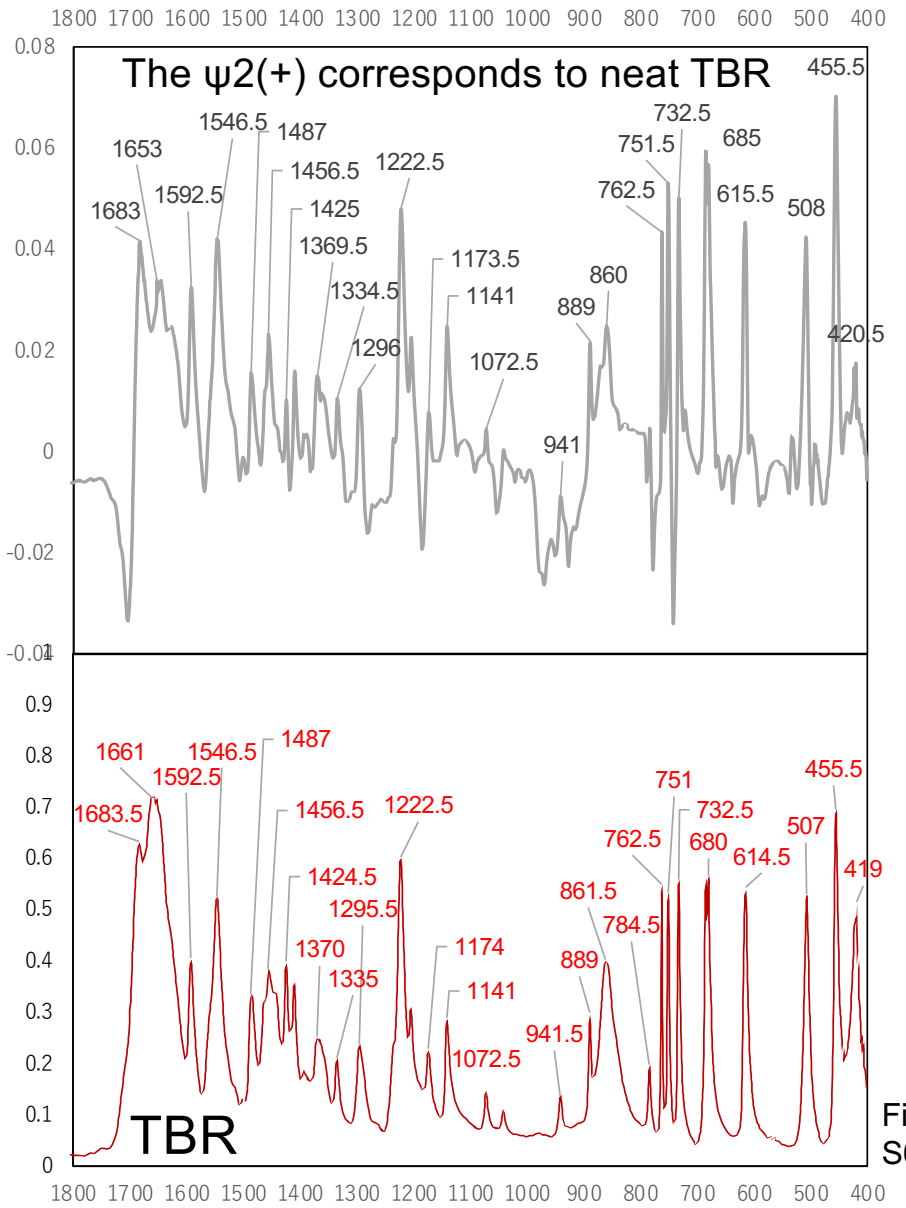

Figure S6(d)

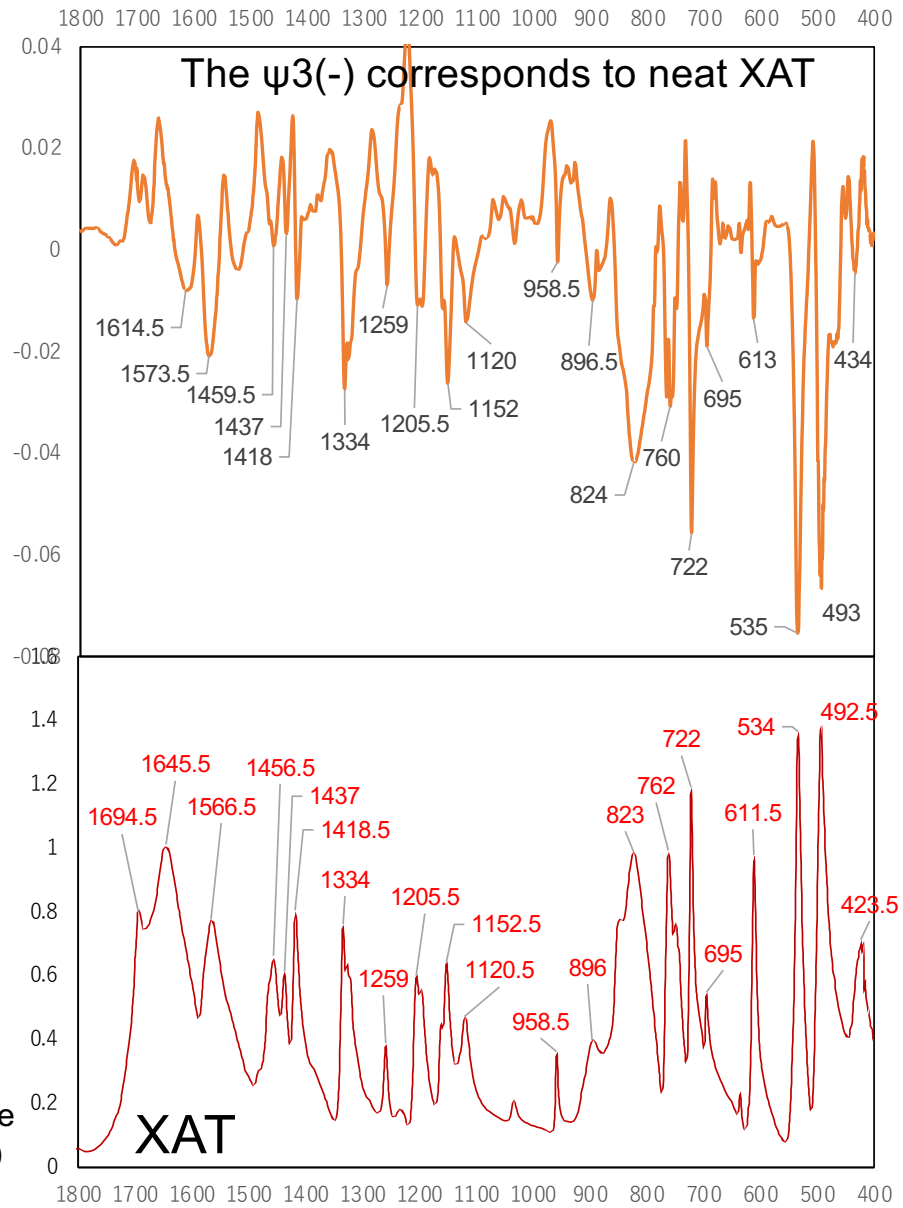

Figure S6(e)

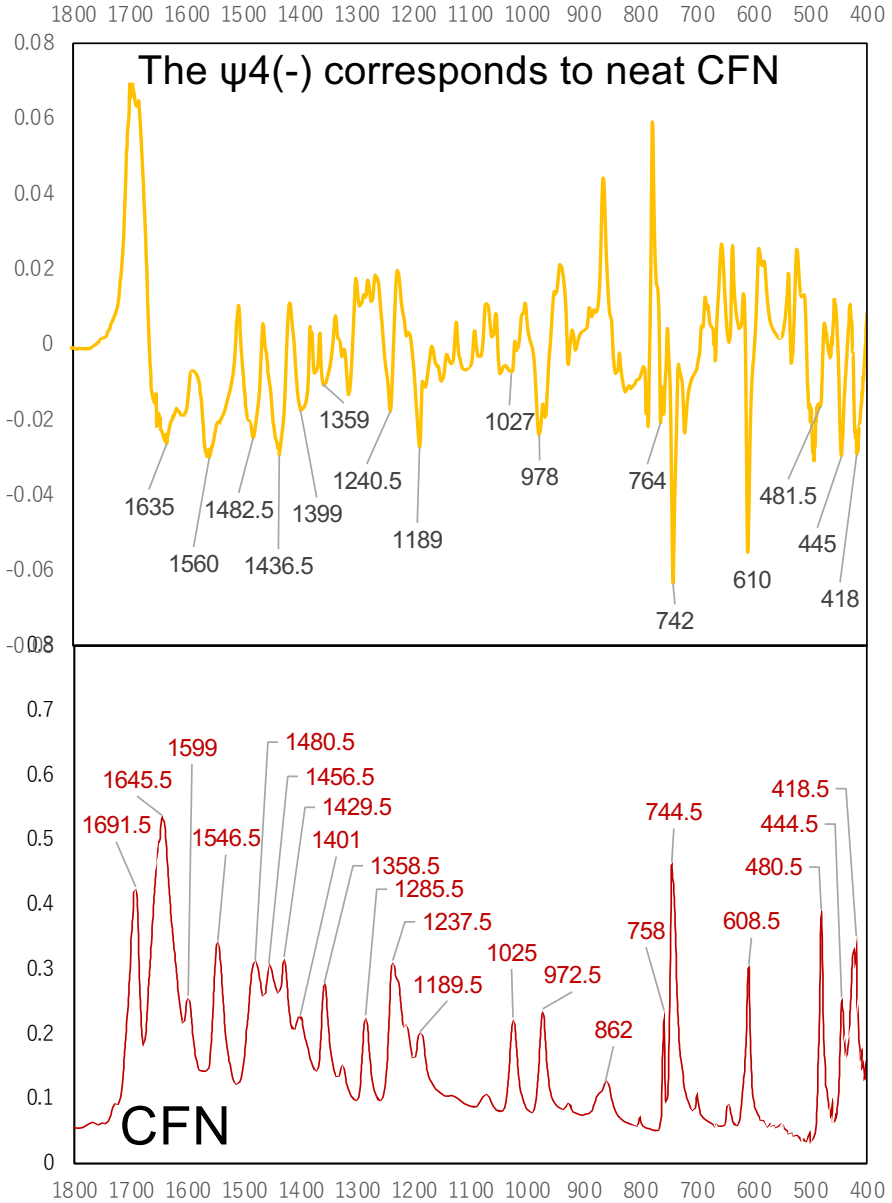

Figure S6(f)

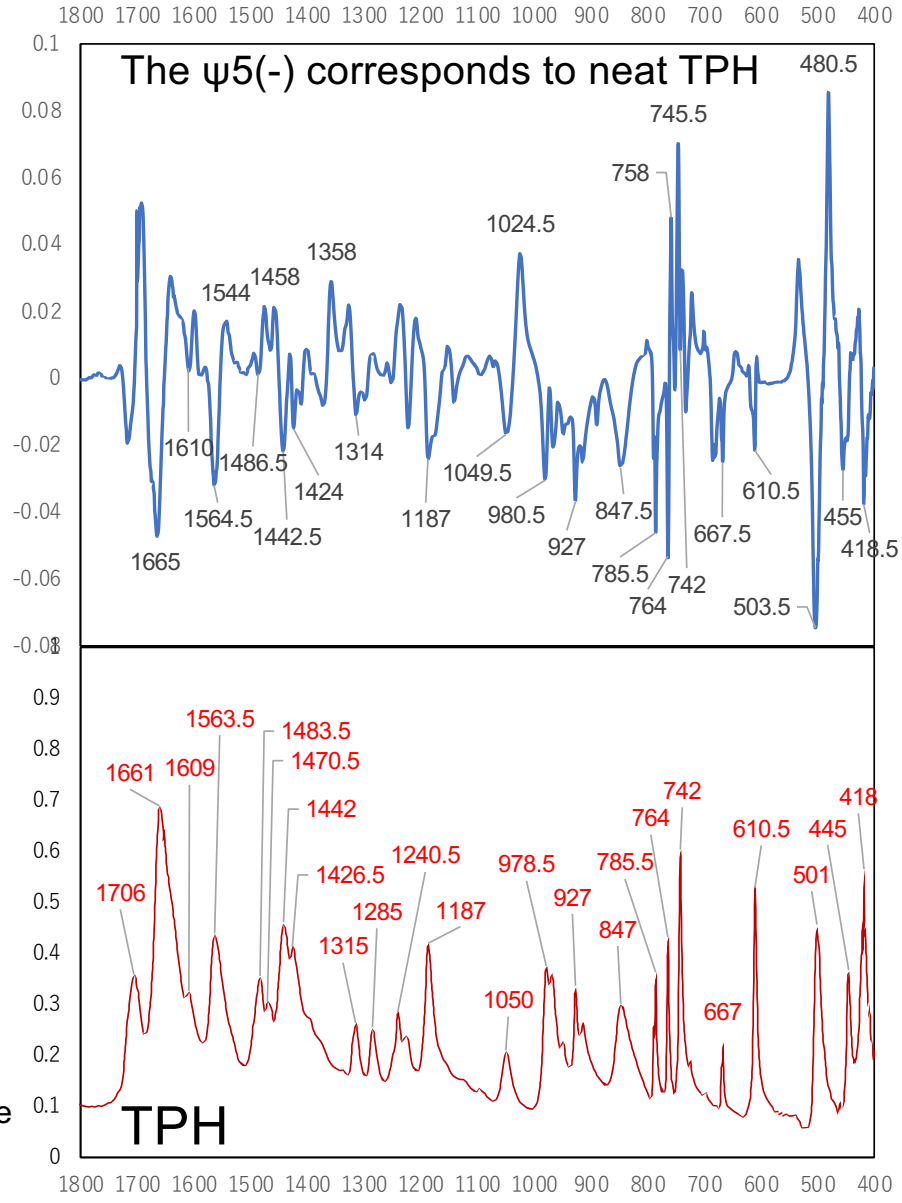

Figure S6(g)

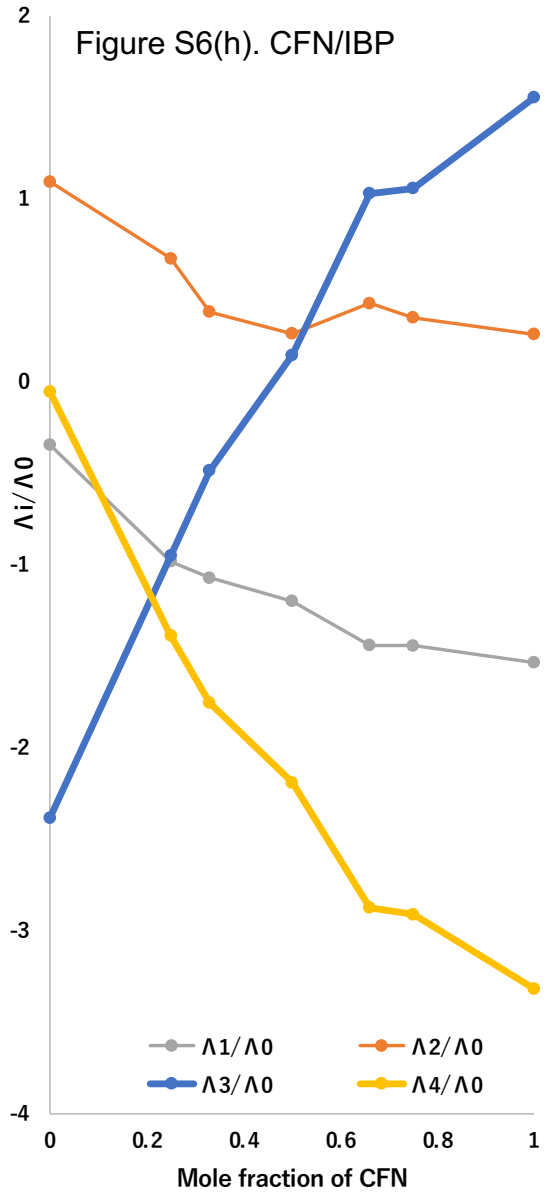
Figure S6(h). CFN/IBP
Λi/Λ0
Mole fraction of CFN
Λ1/Λ0
Λ2/Λ0
Λ3/Λ0
Λ4/Λ0

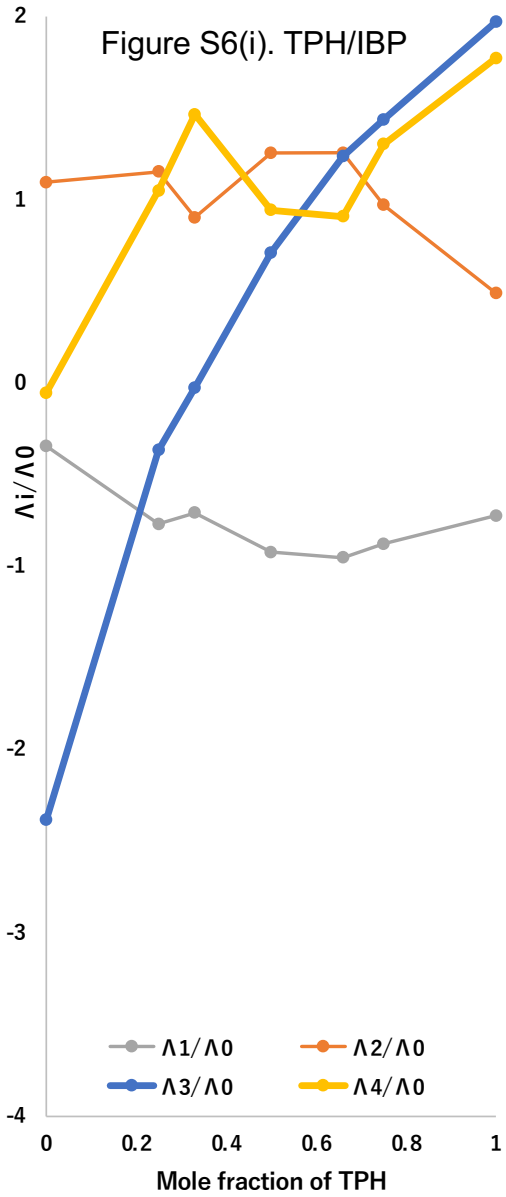
Figure S6(i). TPH/IBP
Λi/Λ0
Mole fraction of TPH
Λ1/Λ0
Λ2/Λ0
Λ3/Λ0
Λ4/Λ0

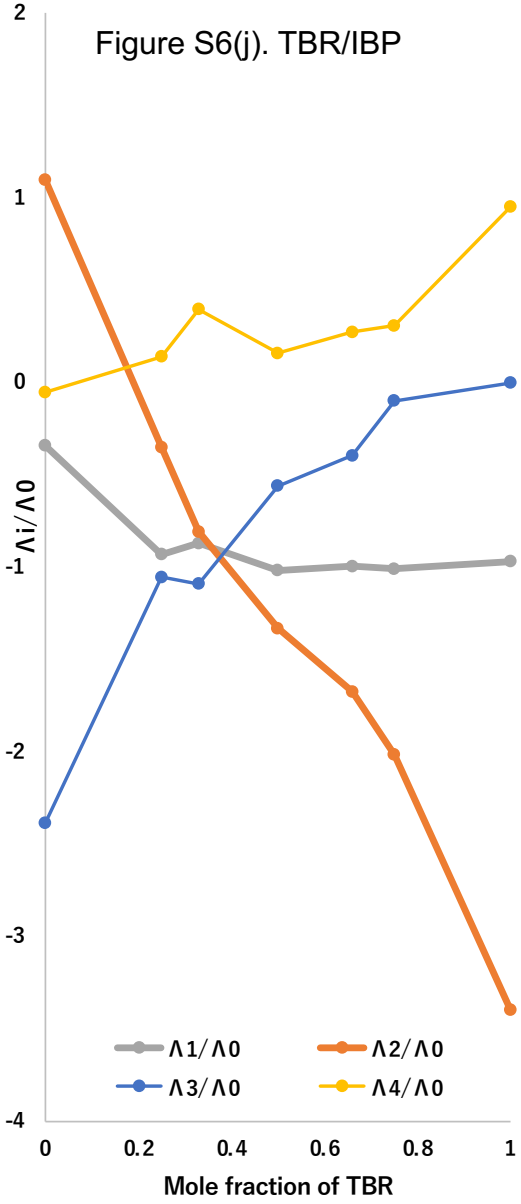
Figure S6(j). TBR/IBP
Λi/Λ0
Mole fraction of TBR
Λ1/Λ0
Λ2/Λ0
Λ3/Λ0
Λ4/Λ0

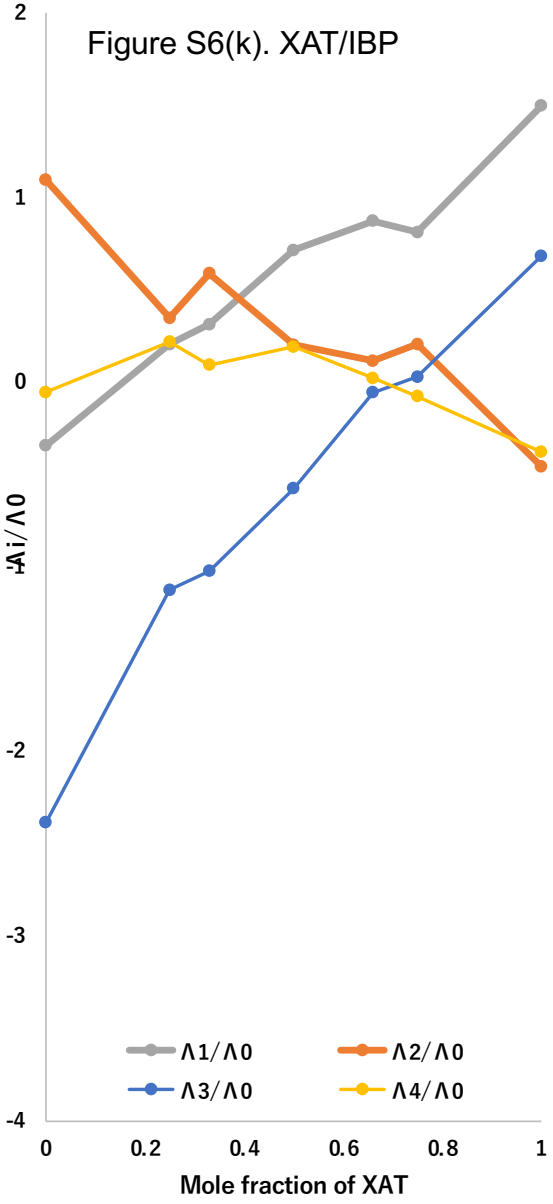
Figure S6(k). XAT/IBP
Λi/Λ0
Mole fraction of XAT
Λ1/Λ0
Λ2/Λ0
Λ3/Λ0
Λ4/Λ0

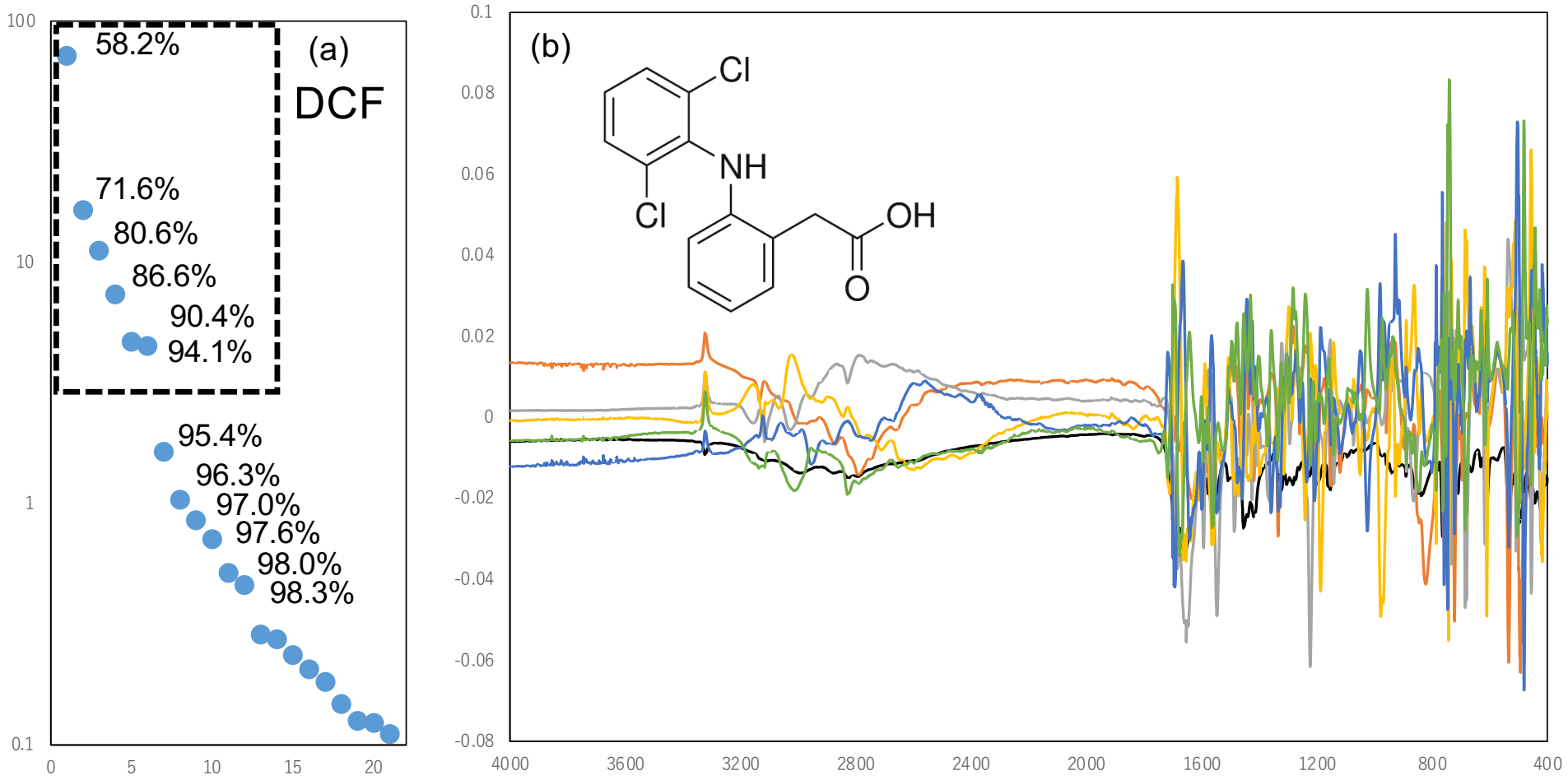

Figure S7. Summarized results of SVD computation for the DCF mixtures with the XAT derivatives: (a) the singular values and their corresponding cumulative sum of variances and (b) the first to sixth basis functions (94%). Curves in descending order were represented by colors of black, orange, gray, yellow, blue, and green.

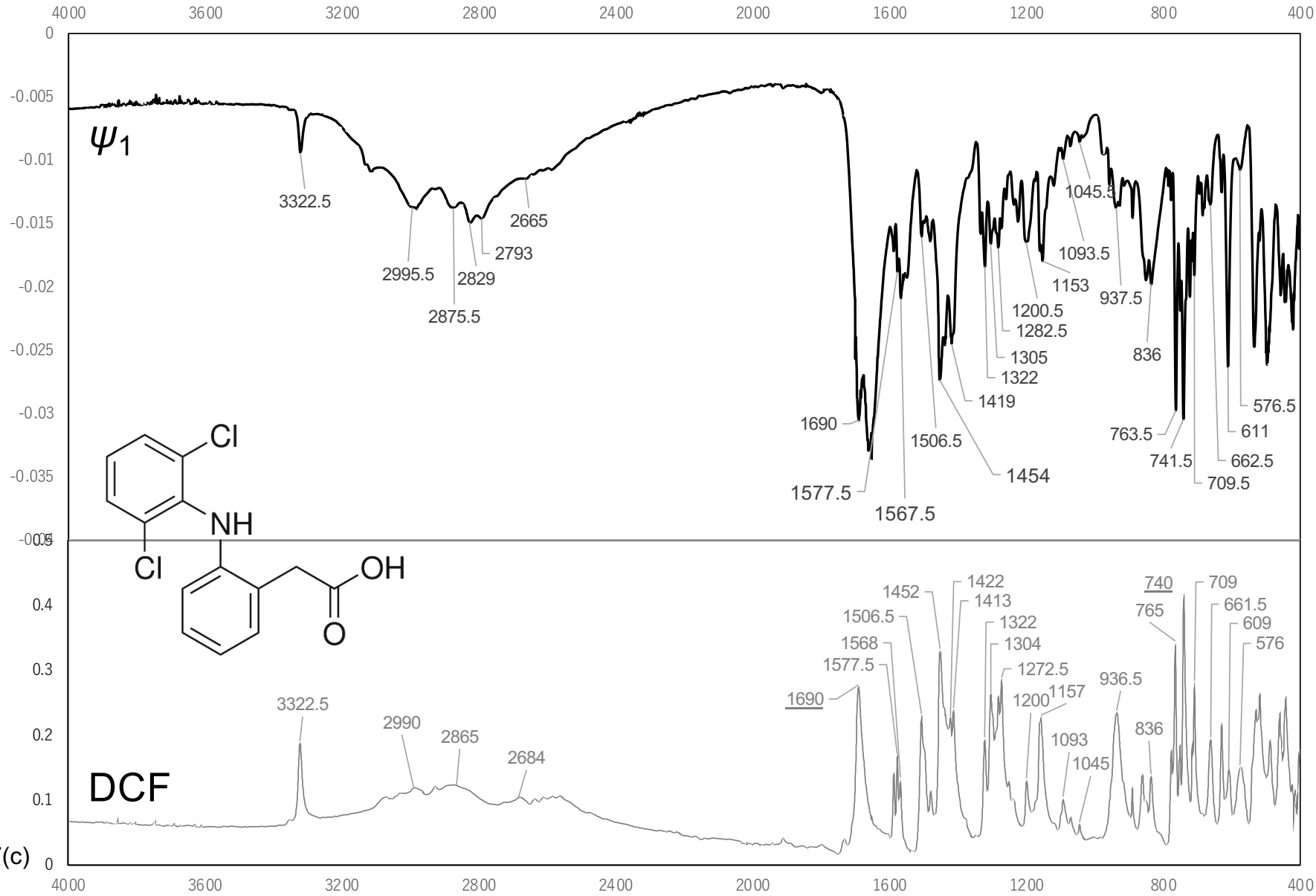
4000
3600
3200
2800
2400
2000
1600
1200
800
400
0
-0.005
-0.01
-0.015
-0.02
-0.025
-0.03
-0.035
-0.04
ψ1
3322.5
2995.5
2875.5
2829
2793
2665
1690
1577.5
1567.5
1506.5
1454
1419
1322
1305
1282.5
1200.5
1153
1093.5
1045.5
937.5
836
763.5
741.5
709.5
662.5
611
576.5
Cl
NH
Cl
OH
O
DCF
3322.5
2990
2865
2684
1690
1577.5
1568
1506.5
1452
1422
1413
1322
1304
1272.5
1200
1157
1093
1045
936.5
836
765
740
709
661.5
609
576
0.4
0.3
0.2
0.1
0

Figure S7(c)

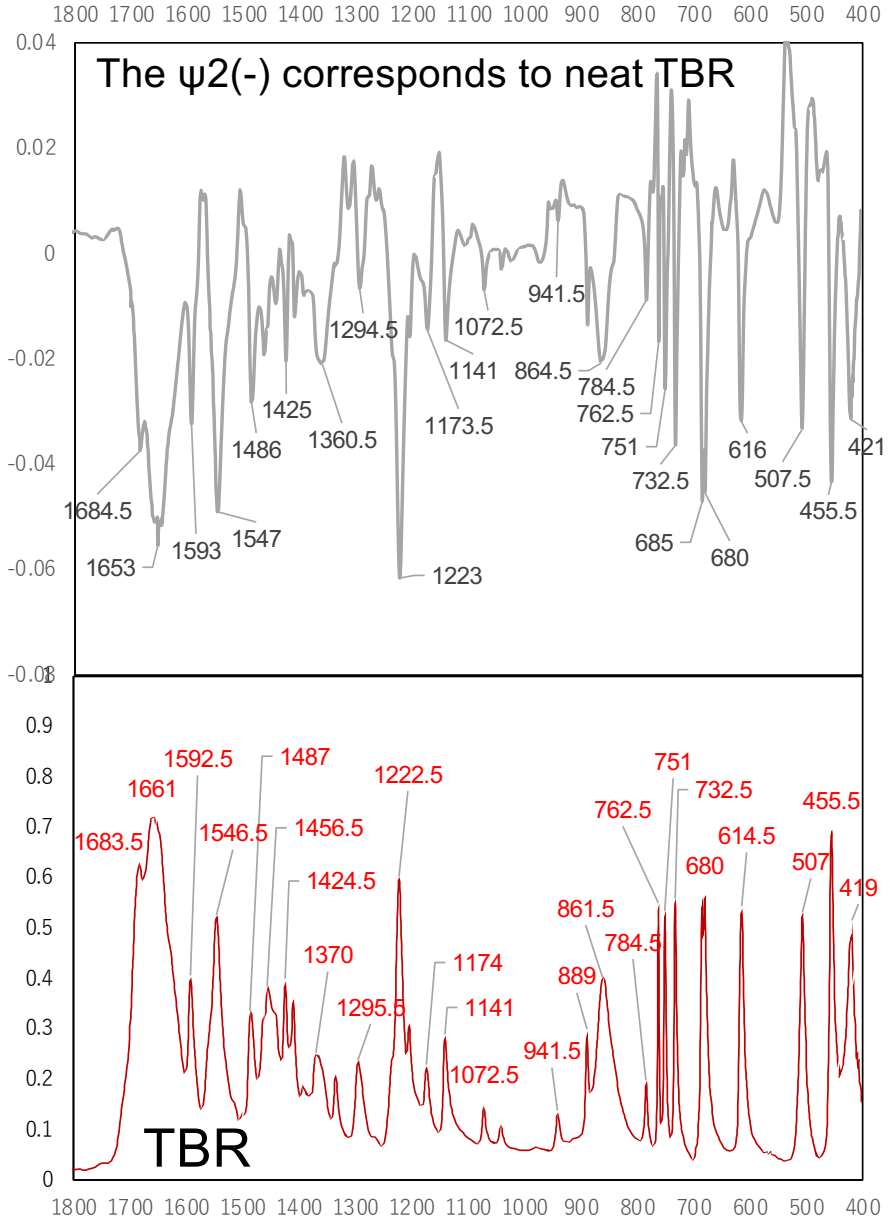

Figure S7(d)

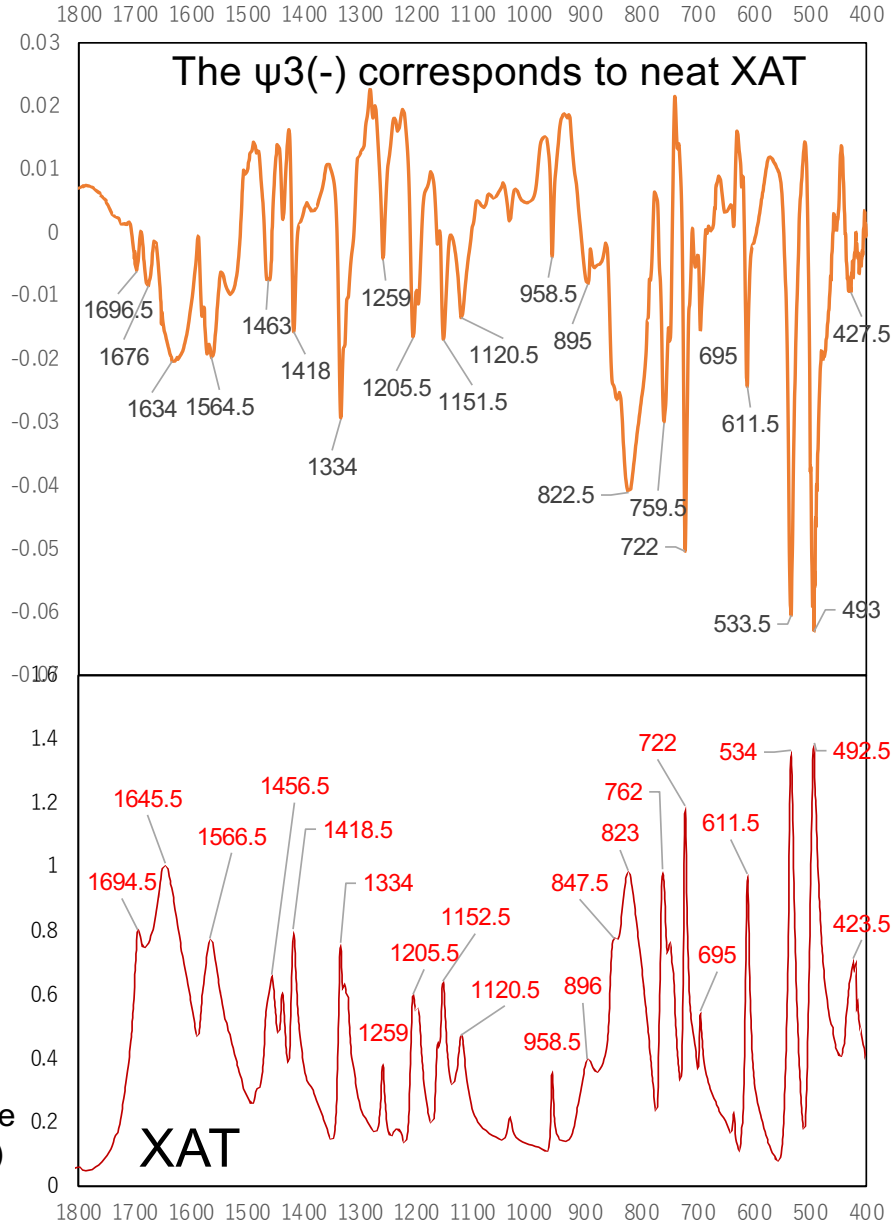

Figure S7(e)

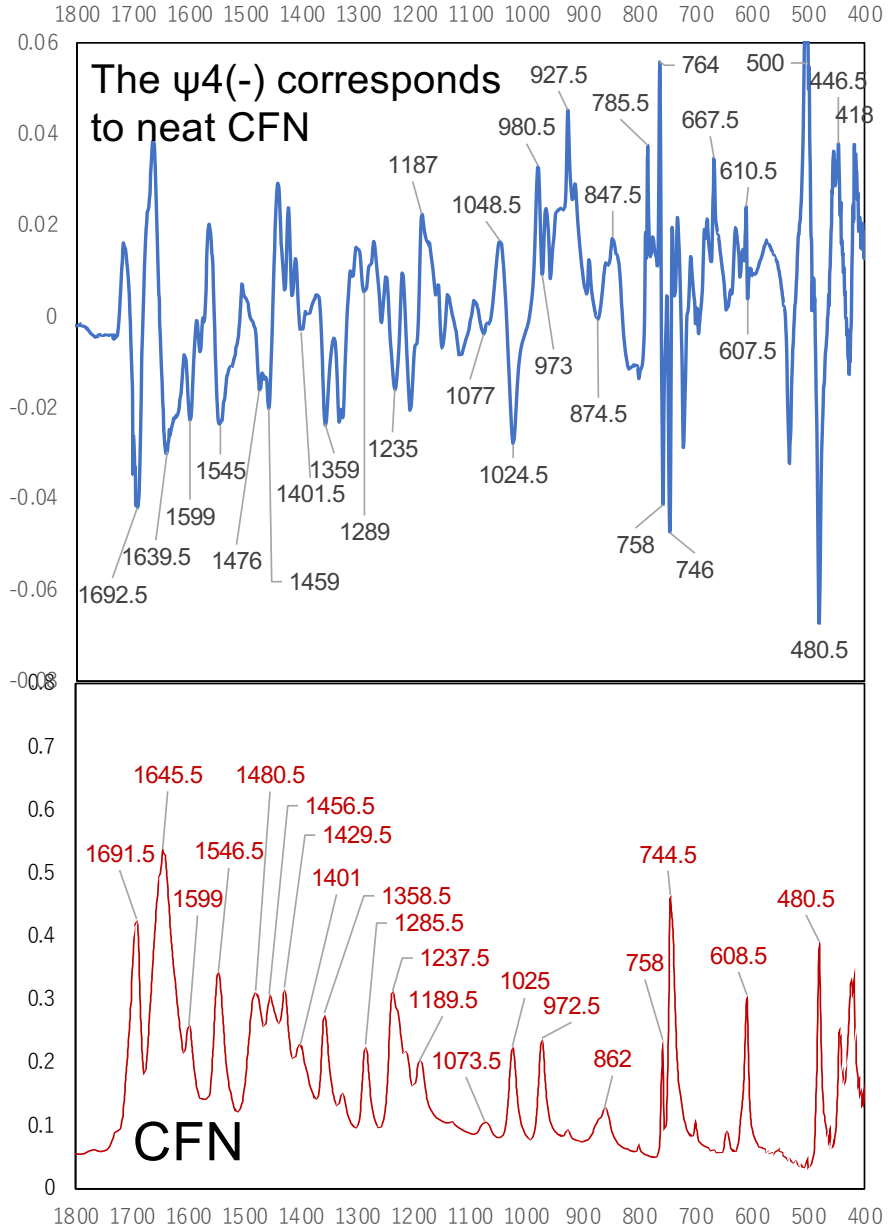

Figure S7(f)

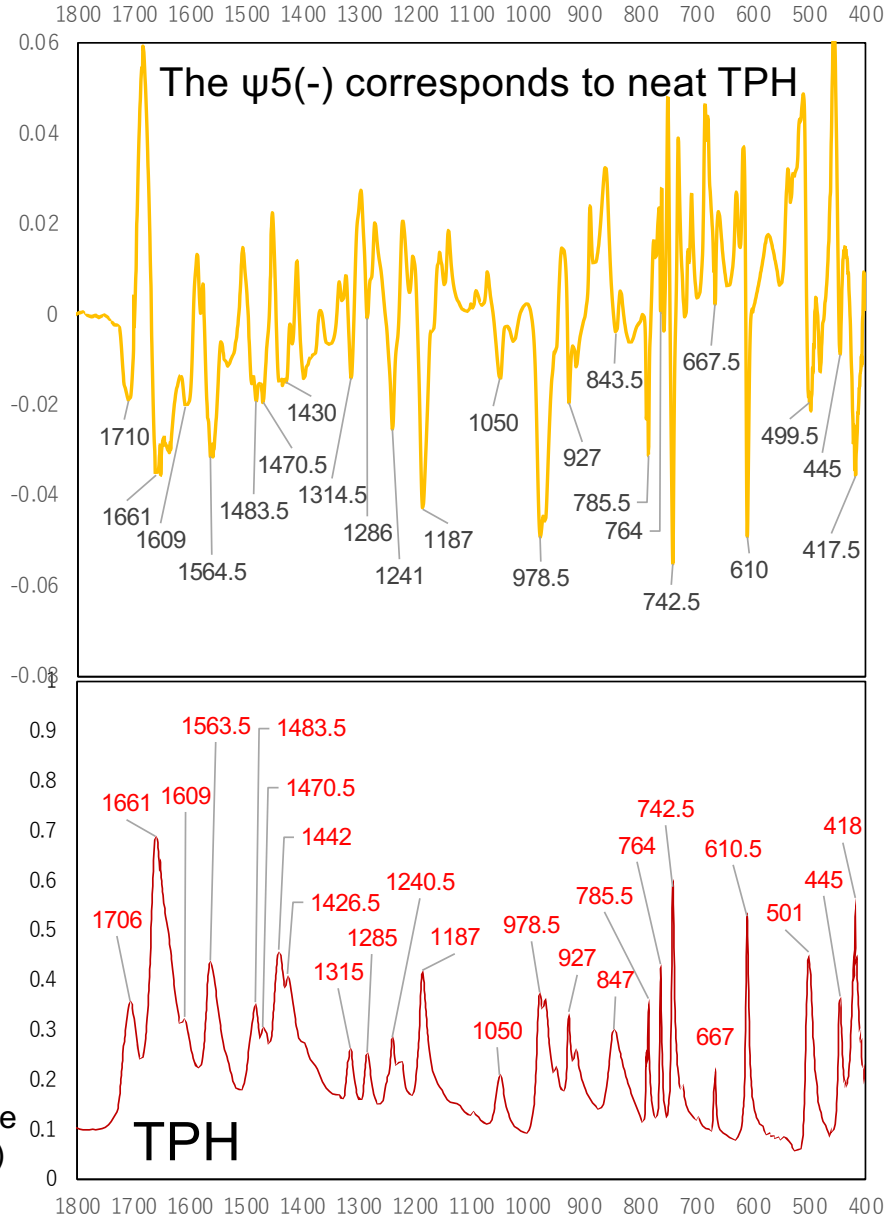

Figure S7(g)

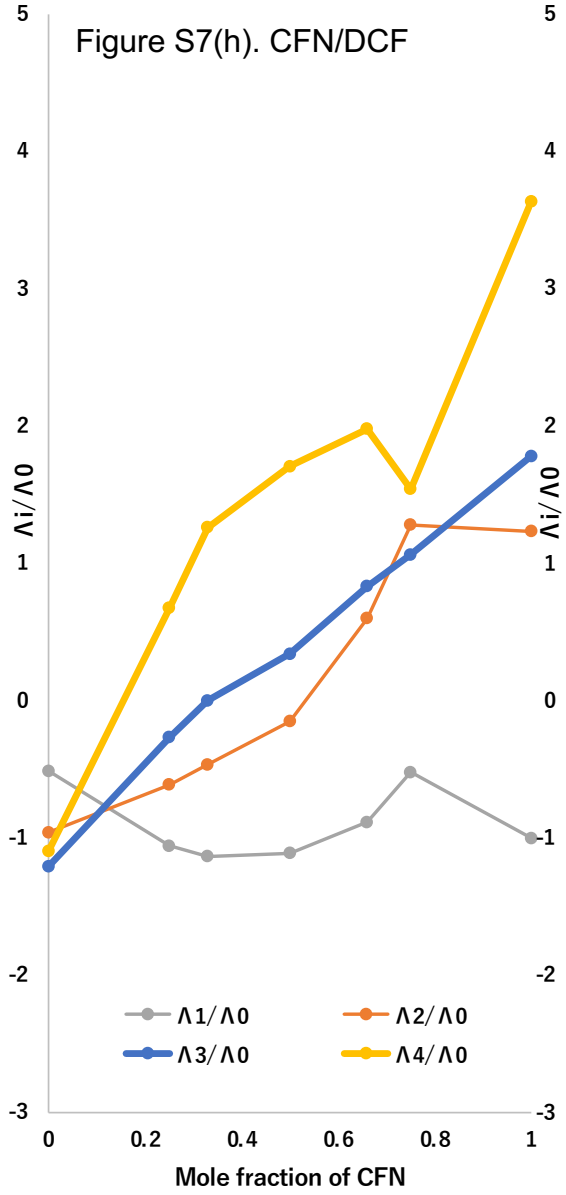
Figure S7(h). CFN/DCF
Λi/Λ0
Λ1/Λ0
Λ2/Λ0
Λ3/Λ0
Λ4/Λ0
Mole fraction of CFN

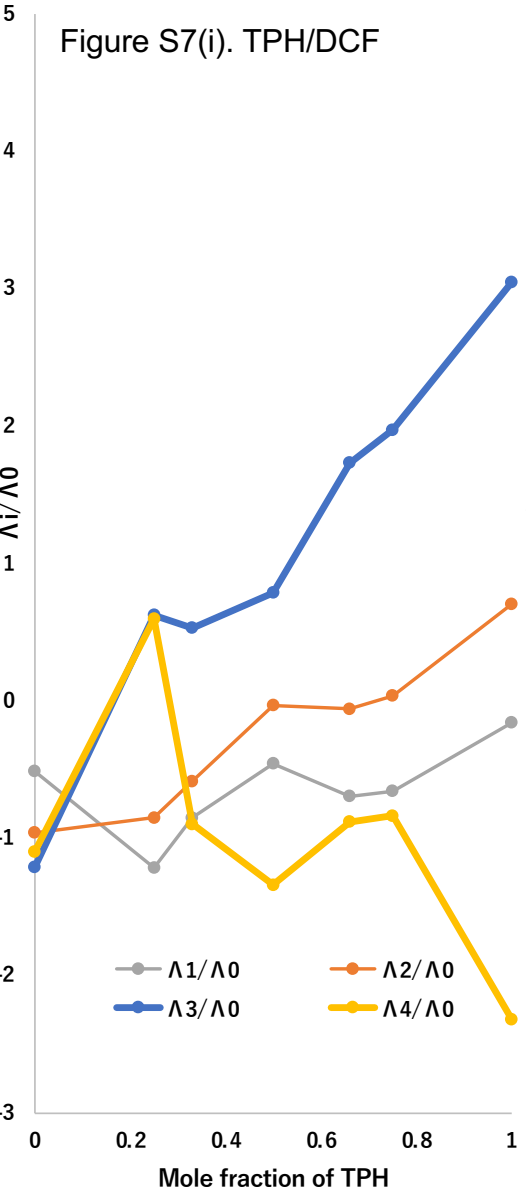
Figure S7(i). TPH/DCF
Λi/Λ0
Λ1/Λ0
Λ2/Λ0
Λ3/Λ0
Λ4/Λ0
Mole fraction of TPH

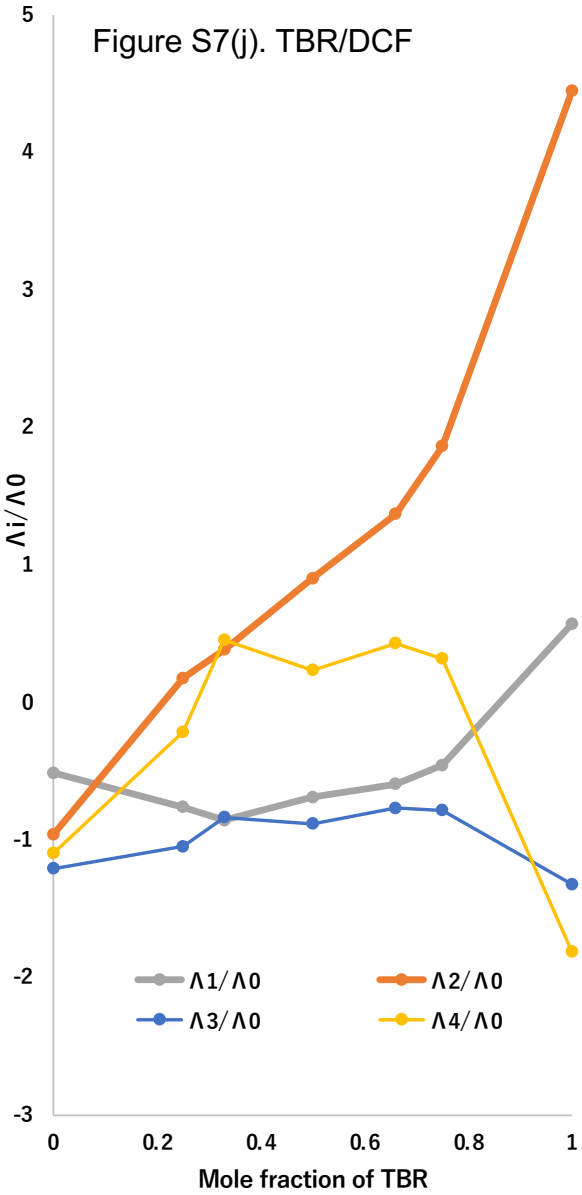
Figure S7(j). TBR/DCF
Λi/Λ0
Λ1/Λ0
Λ2/Λ0
Λ3/Λ0
Λ4/Λ0
Mole fraction of TBR

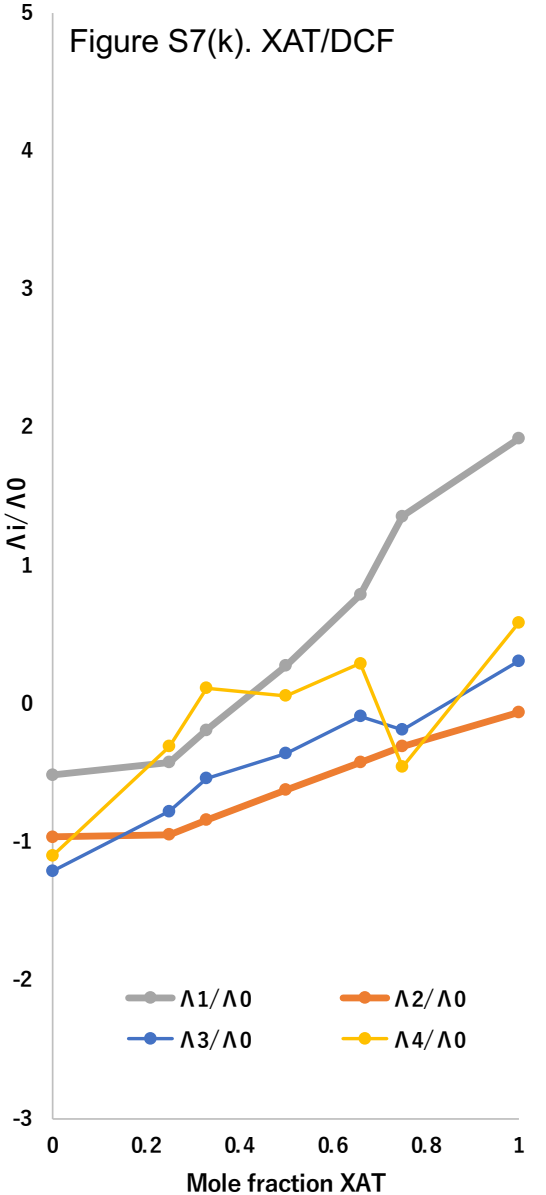
Figure S7(k). XAT/DCF
Λi/Λ0
Λ1/Λ0
Λ2/Λ0
Λ3/Λ0
Λ4/Λ0
Mole fraction XAT

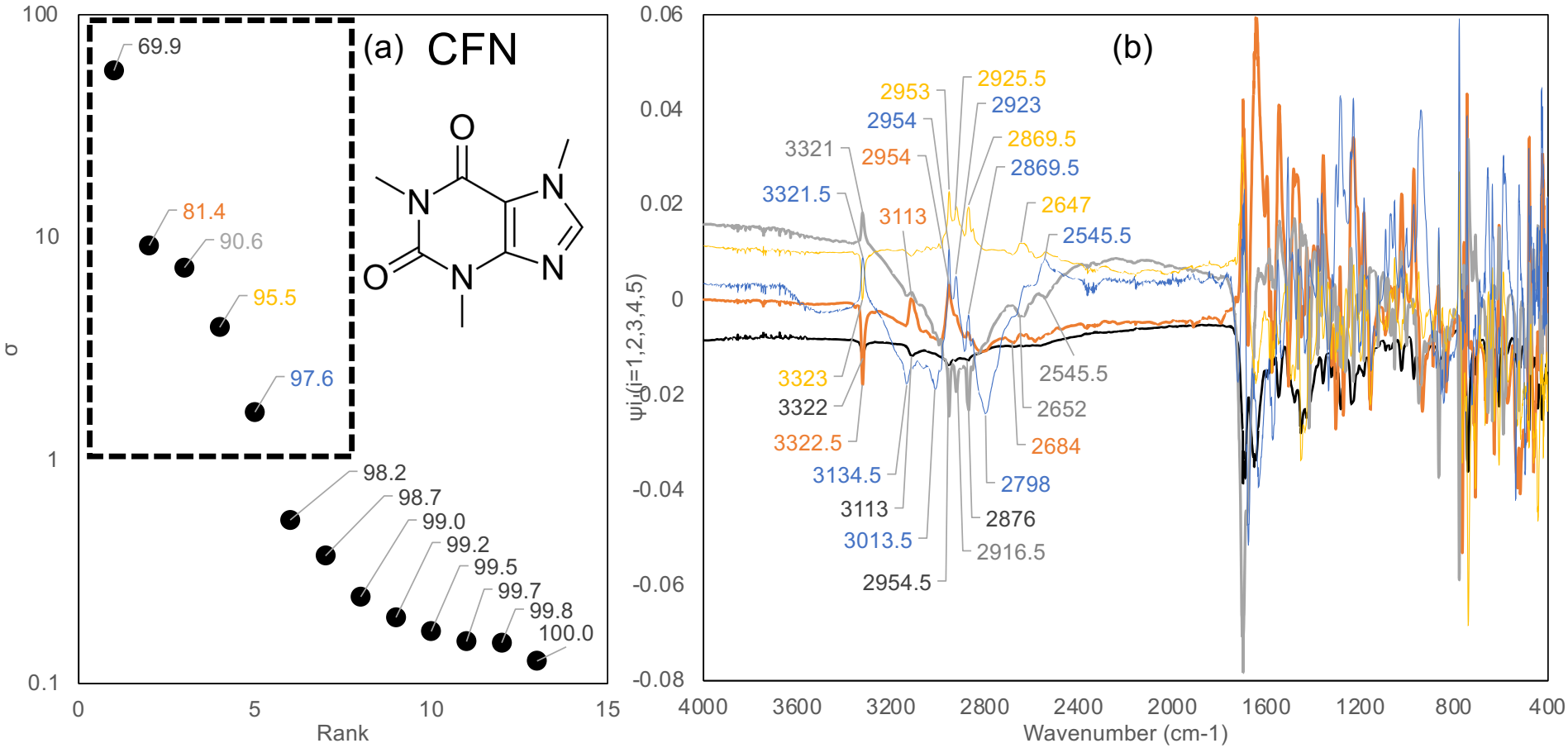

Figure S8. SVD computation for FTIR spectra of CFN/IBP and CFN/DCF mixtures provided singular values σi (a) and Basis spectra ψi(b). Cumulative proportions of σi were appended beside the σ plots, indicating that higher five σ's satisfied 97.6 percent of the variance. The basis spectra decomposed by the SVD computation corresponded to the components ψ1 (black), ψ2 (orange), ψ3 (gray), ψ4 (yellow), and ψ5 (blue). Details of ψ's assignments to the observed spectra in the wavenumber range 1800-400 cm^{-1} are followed (e-o).

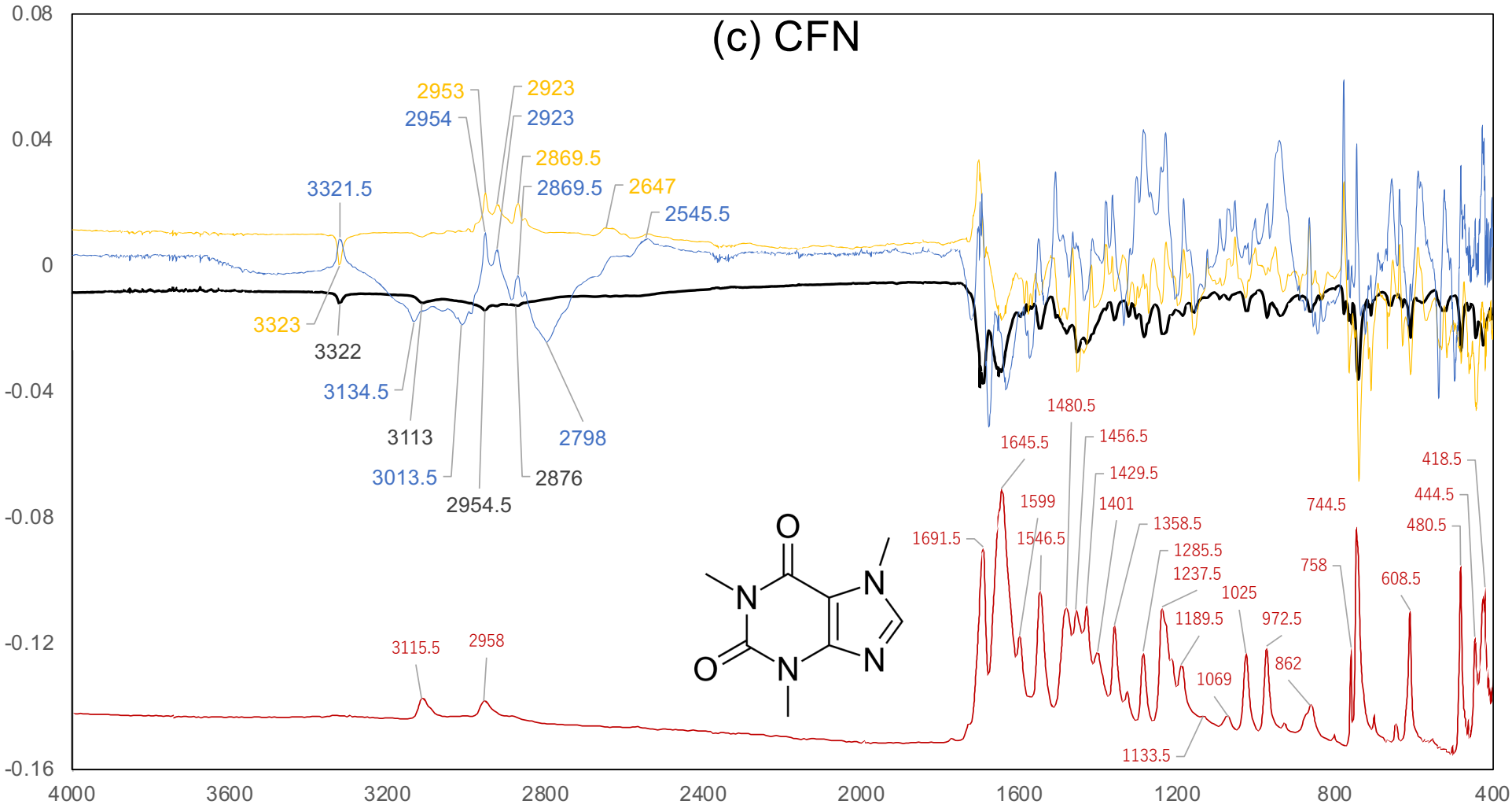

Figure S8. The basis spectra decomposed by the SVD computation corresponded to the components at the rank of 1 (black), 4 (yellow), and 5 (blue).

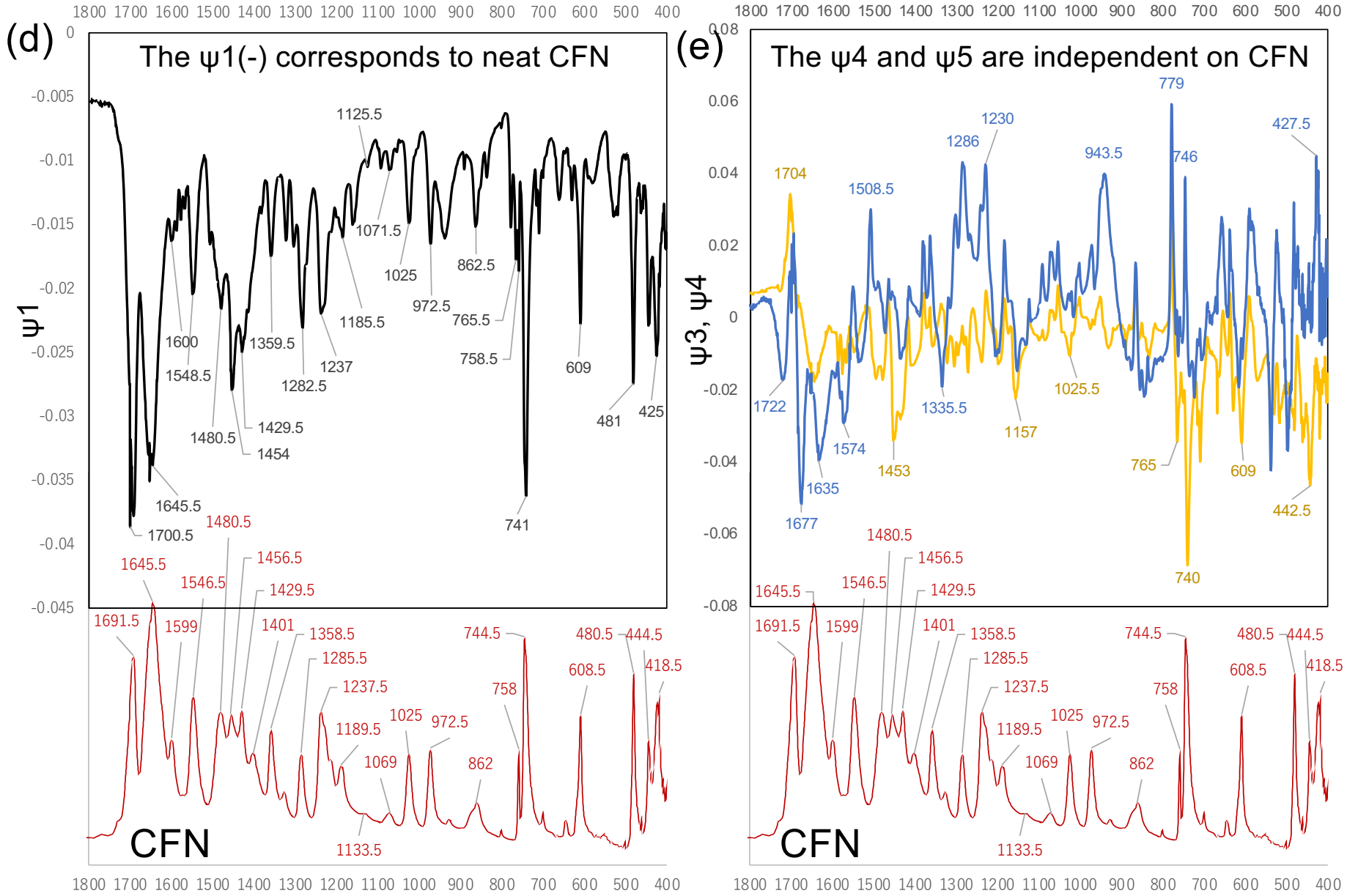
(d)
The ψ1(-) corresponds to neat CFN
ψ1
1125.5
1071.5
1025
862.5
972.5
765.5
1185.5
758.5
1600
1359.5
1237
1548.5
1282.5
609
481
425
1480.5
1429.5
1454
1645.5
1700.5
741
1691.5
1645.5
1599
1546.5
1480.5
1456.5
1429.5
1401
1358.5
1285.5
1237.5
1189.5
1025
972.5
1069
862
744.5
758
608.5
480.5
444.5
418.5
1133.5
CFN
(e)
The ψ4 and ψ5 are independent on CFN
ψ3, ψ4
779
1230
1286
427.5
943.5
746
1704
1508.5
1722
1335.5
1025.5
1157
1574
1453
765
609
1635
442.5
1677
740
1480.5
1456.5
1645.5
1546.5
1429.5
1691.5
1599
1401
1358.5
1285.5
1237.5
744.5
480.5
444.5
608.5
418.5
1189.5
1025
972.5
758
1069
862
1133.5
CFN

Figure S8

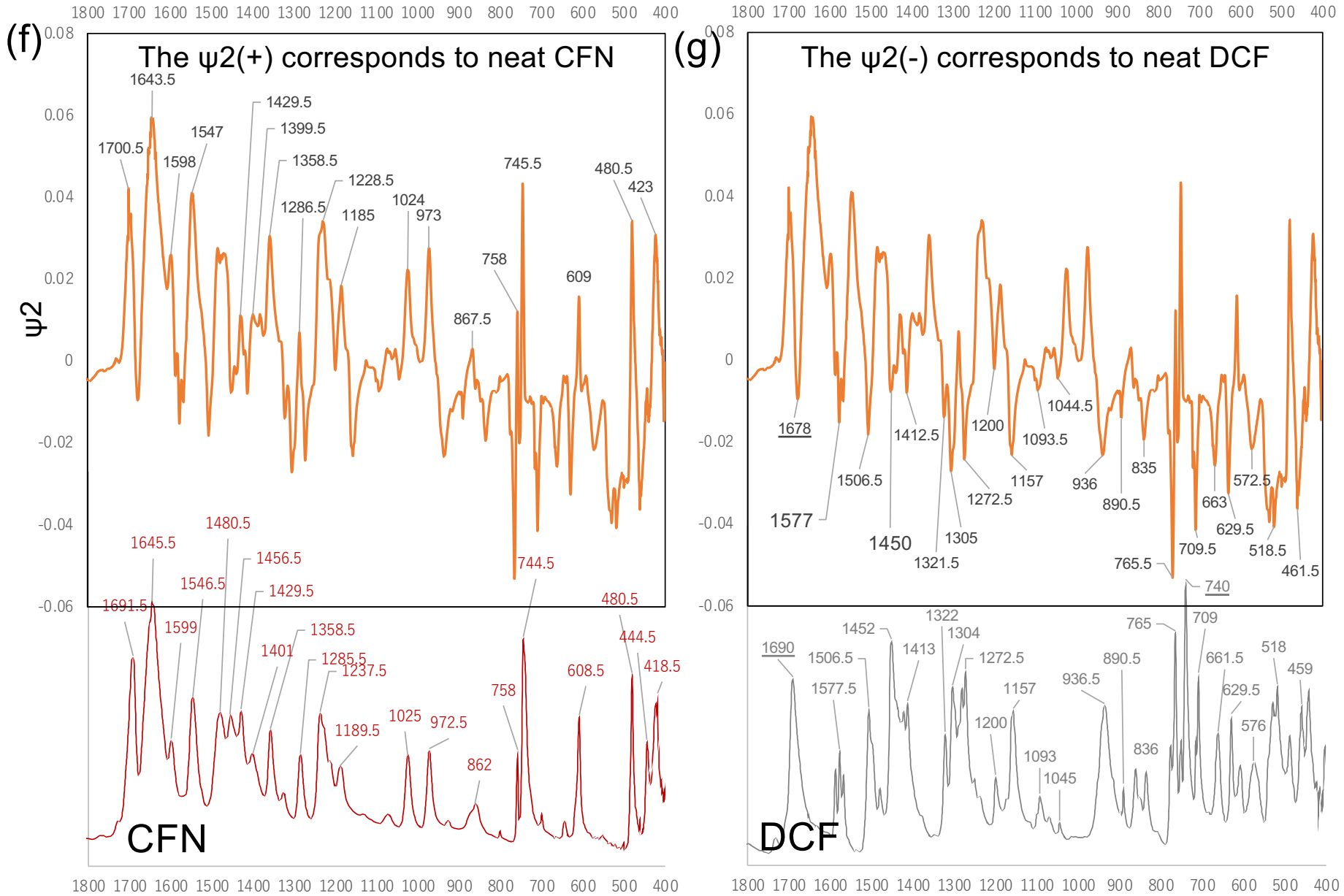
(f)
The ψ2(+) corresponds to neat CFN
ψ2
1643.5
1700.5
1598
1547
1429.5
1399.5
1358.5
1228.5
1286.5
1185
1024
973
745.5
480.5
423
758
609
867.5
1645.5
1480.5
1691.5
1599
1546.5
1456.5
1429.5
1401
1358.5
1285.5
1237.5
744.5
480.5
444.5
418.5
608.5
758
1189.5
1025
972.5
862
CFN
(g)
The ψ2(-) corresponds to neat DCF
1678
1577
1506.5
1450
1412.5
1321.5
1305
1200
1272.5
1157
1093.5
1044.5
936
890.5
835
765.5
709.5
663
629.5
572.5
518.5
461.5
740
1690
1577.5
1506.5
1452
1413
1322
1304
1272.5
1200
1157
1093
1045
936.5
890.5
836
765
709
661.5
629.5
576
518
459
DCF

Figure S8

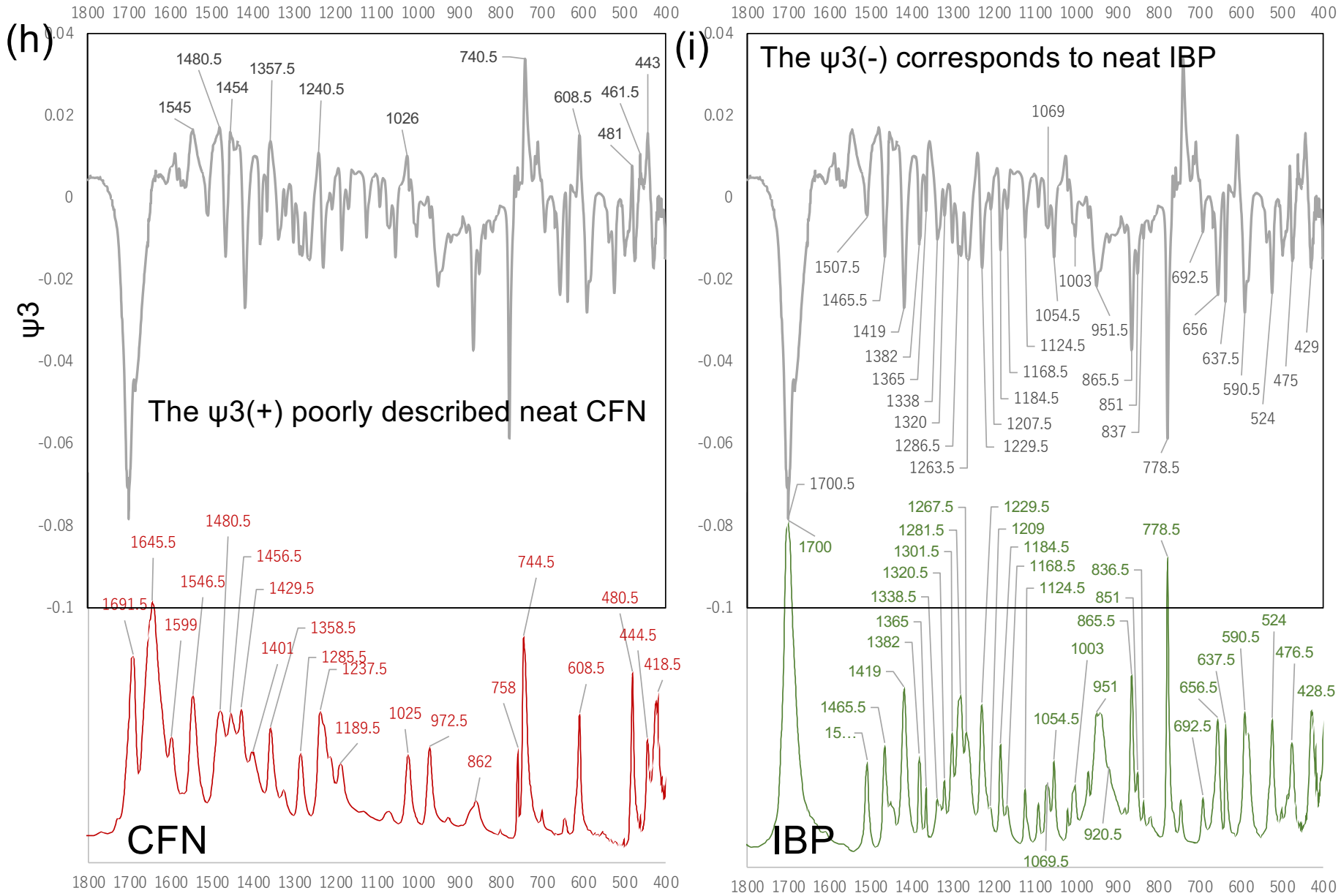
(h)
ψ3
The ψ3(+) poorly described neat CFN
CFN
1480.5
1357.5
1454
1545
1240.5
1026
740.5
608.5
461.5
443
481
1645.5
1480.5
1691.5
1599
1546.5
1456.5
1429.5
1401
1358.5
1285.5
1237.5
1189.5
1025
972.5
862
758
744.5
608.5
480.5
444.5
418.5
(i)
The ψ3(-) corresponds to neat IBP
IBP
1069
1507.5
1465.5
1419
1382
1365
1338
1320
1286.5
1263.5
1229.5
1207.5
1184.5
1168.5
1124.5
1054.5
1003
951.5
865.5
851
837
778.5
692.5
656
637.5
590.5
524
475
429
1700.5
1700
1267.5
1281.5
1301.5
1320.5
1338.5
1365
1382
1419
1465.5
1229.5
1209
1184.5
1168.5
1124.5
836.5
851
778.5
865.5
1003
951
1054.5
920.5
1069.5
524
590.5
637.5
656.5
692.5
476.5
428.5

Figure S8

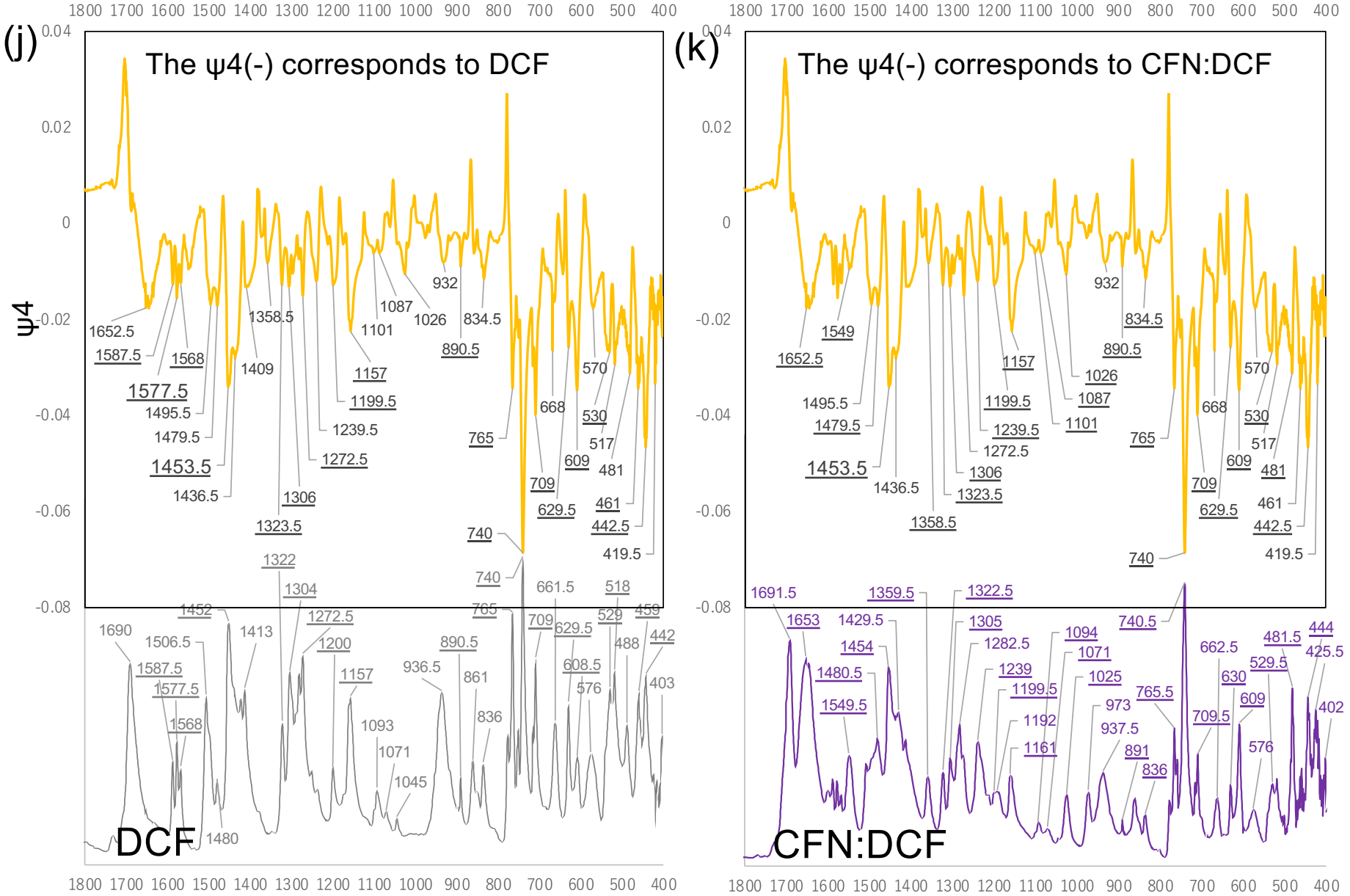
(j)
The ψ4(-) corresponds to DCF
ψ4
DCF
(k)
The ψ4(-) corresponds to CFN:DCF
CFN:DCF

Figure S8

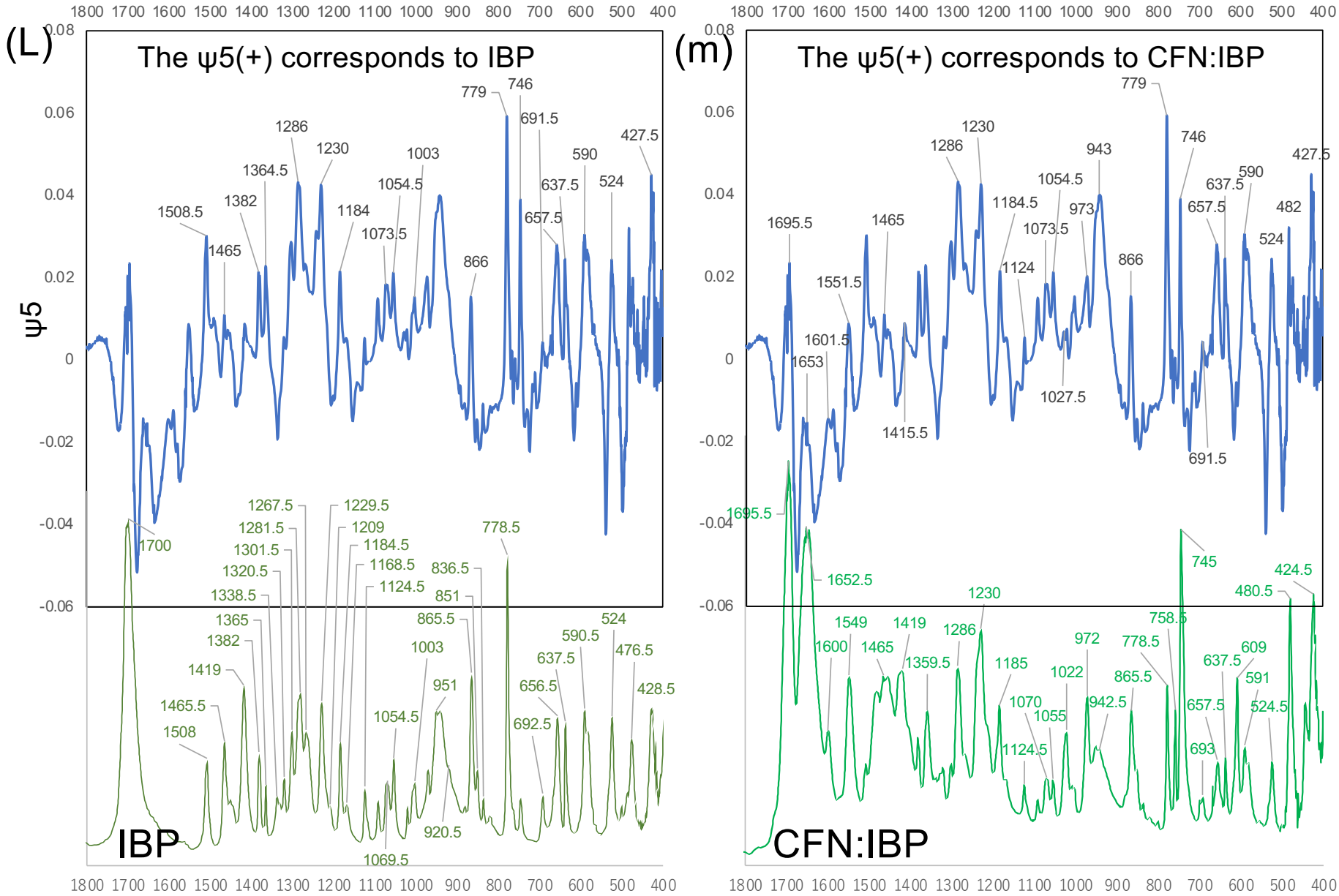
(L)
The ψ5(+) corresponds to IBP
ψ5
IBP
(m)
The ψ5(+) corresponds to CFN:IBP
CFN:IBP

Figure S8

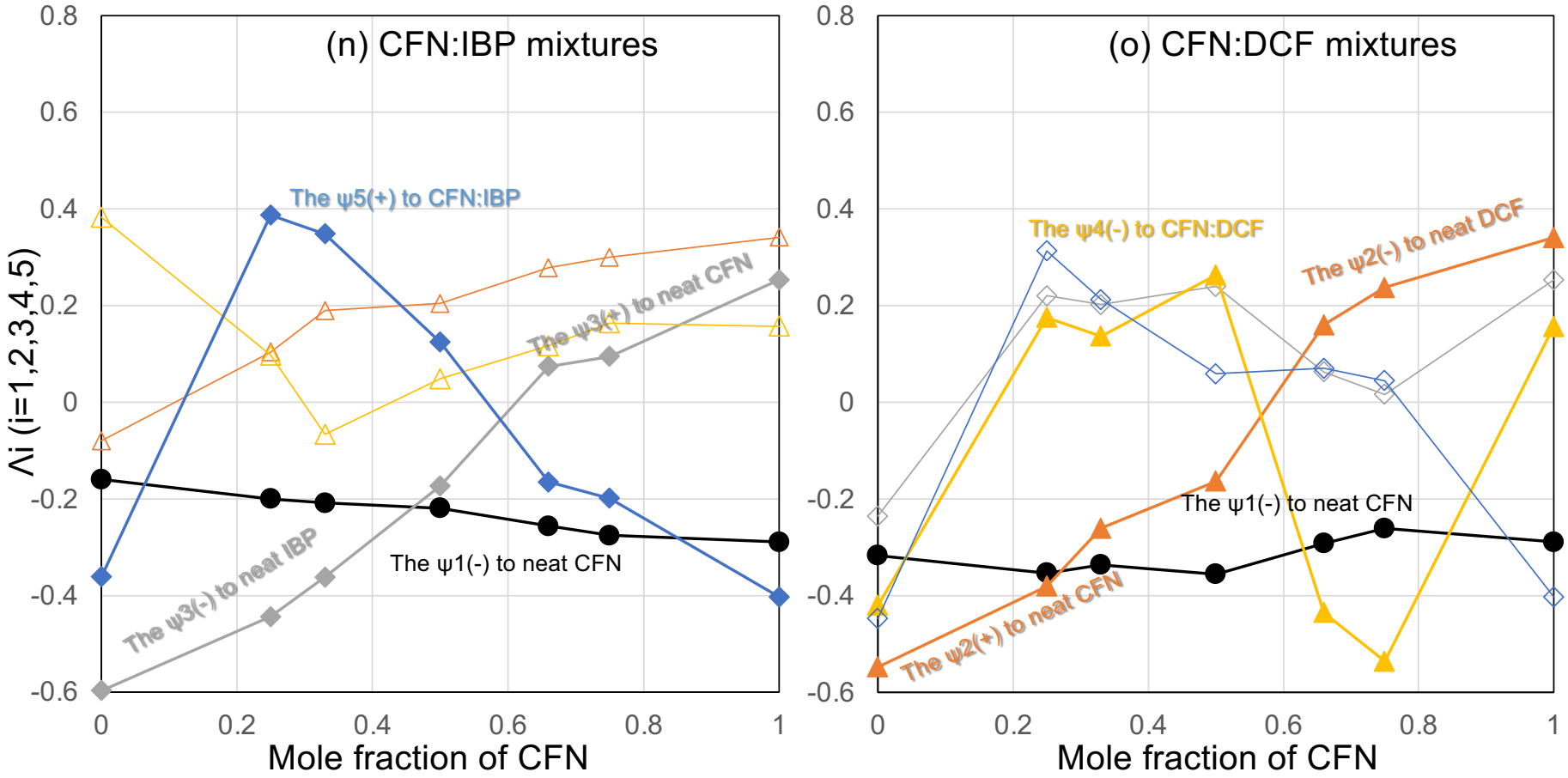

Figure S8 (n and o). The components of the first to fifth singular vectors as a function of mole fraction of CFN. The λ1, λ2, λ3, λ4, and λ5 were represented by closed black circles, orange triangles, gray diamonds, yellow triangles, and blue diamonds. For λ2, λ3, λ4, and λ5, closed and open symbols corresponded to the composition with the basis functions correlated to which the IBP or DCF mixtures, respectively.

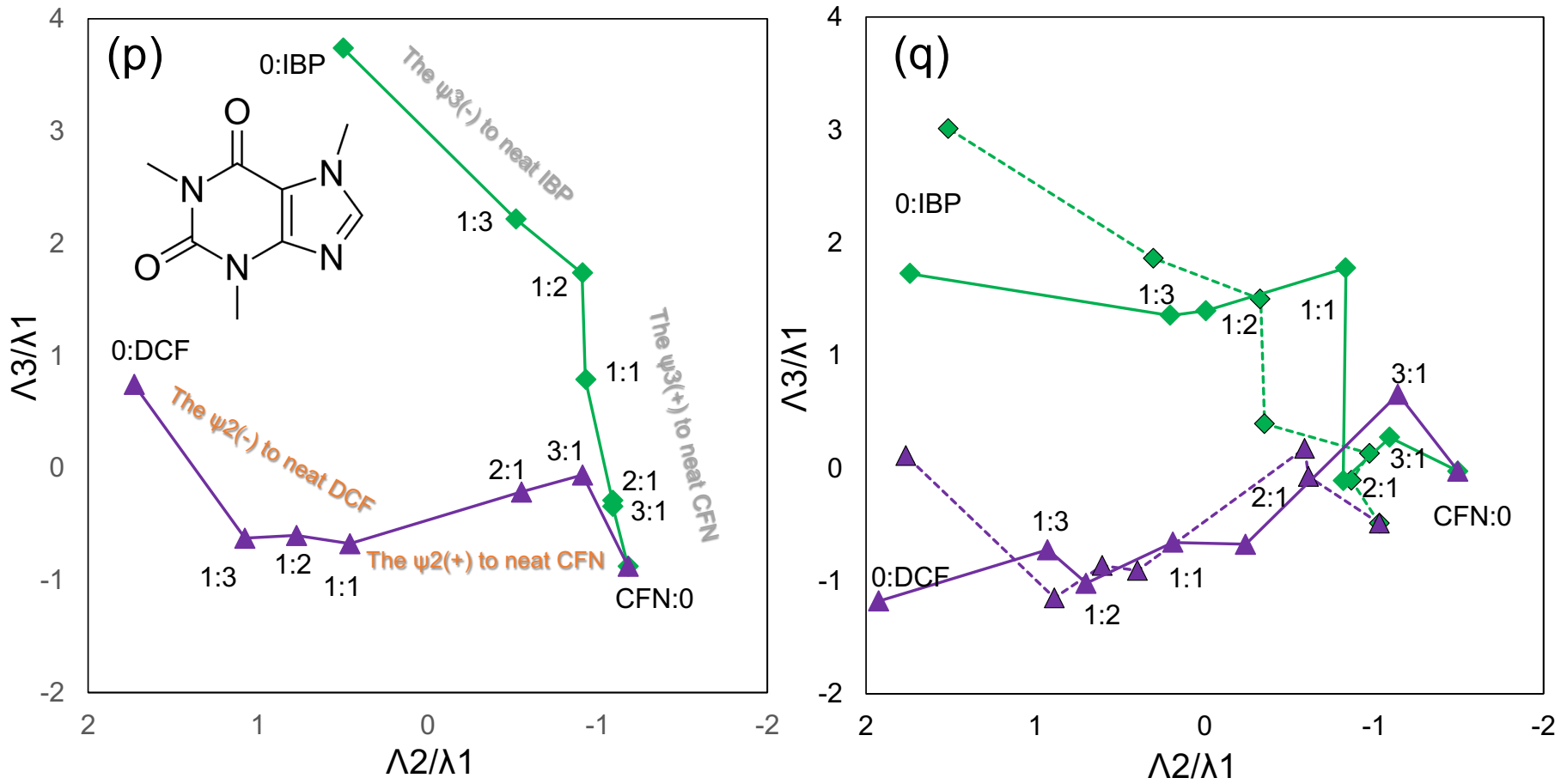

Figure S8 (p and q). The trajectories of the CFN/IBP (green diamonds) and CFN/DCF (violet triangles) mixtures. They shared the neat CFN's vector (CFN:0). The molar ratios were represented along the corresponding plots. The trajectory of the CFN/DCF mixtures traced along the verical (λ2/λ1)-axis (DCF owning dominance in the SVD analysis), whereas that of the CFN/IBP mixtures pursued along the perpendicular (λ2/λ1)-axis. The S13(r) and S13(s) show the trajectories of the average spectra and the individually measured spectra, respectively.

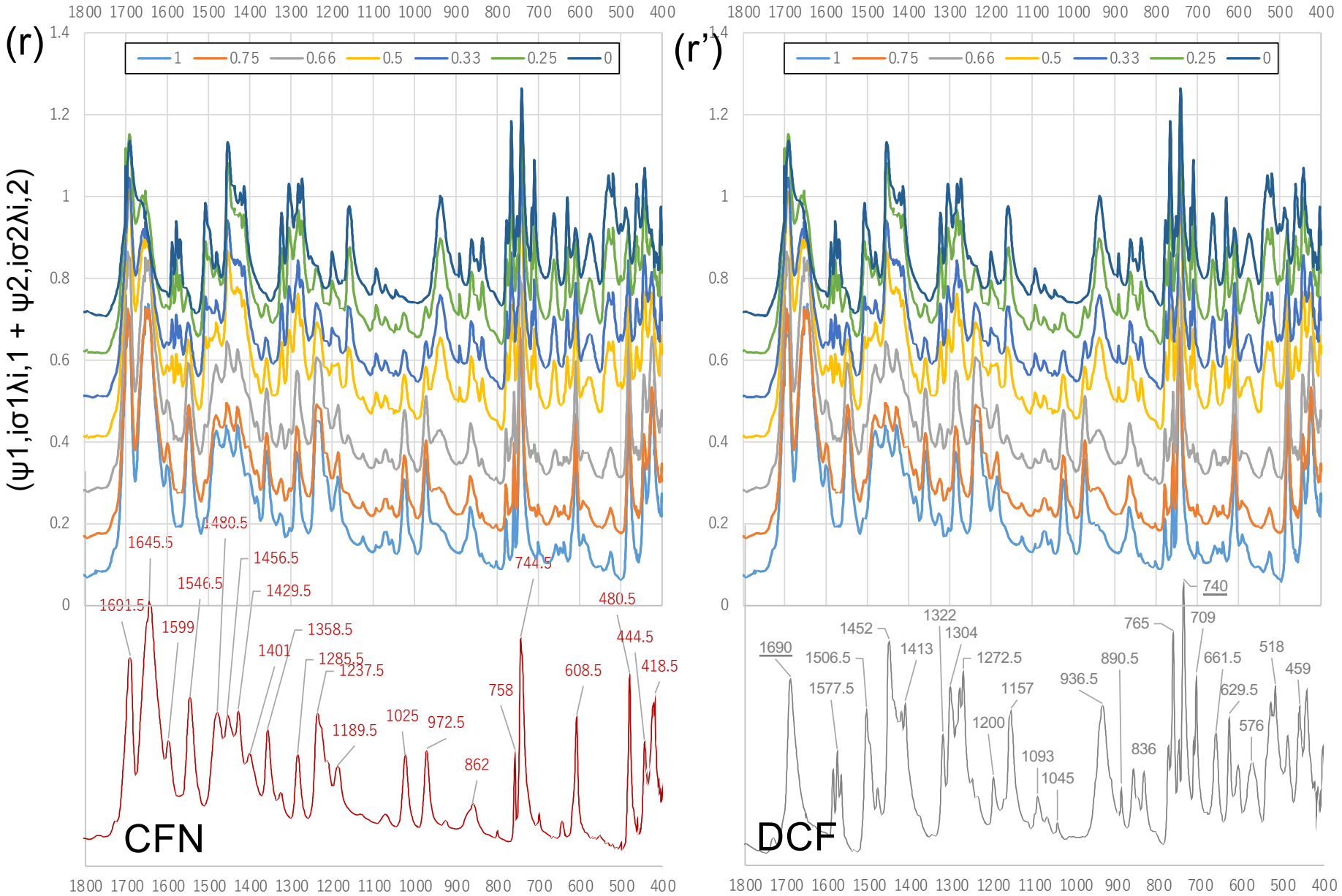
(r)
(r')
(ψ1,iσ1λi,1 + ψ2,iσ2λi,2)
1 0.75 0.66 0.5 0.33 0.25 0
1800 1700 1600 1500 1400 1300 1200 1100 1000 900 800 700 600 500 400
0 0.2 0.4 0.6 0.8 1 1.2 1.4
1691.5
1645.5
1599
1546.5
1480.5
1456.5
1429.5
1401
1358.5
1285.5
1237.5
1189.5
1025
972.5
862
758
744.5
608.5
480.5
444.5
418.5
CFN
1690
1577.5
1506.5
1452
1413
1322
1304
1272.5
1200
1157
1093
1045
936.5
890.5
836
765
740
709
661.5
629.5
576
518
459
DCF

Figure S8

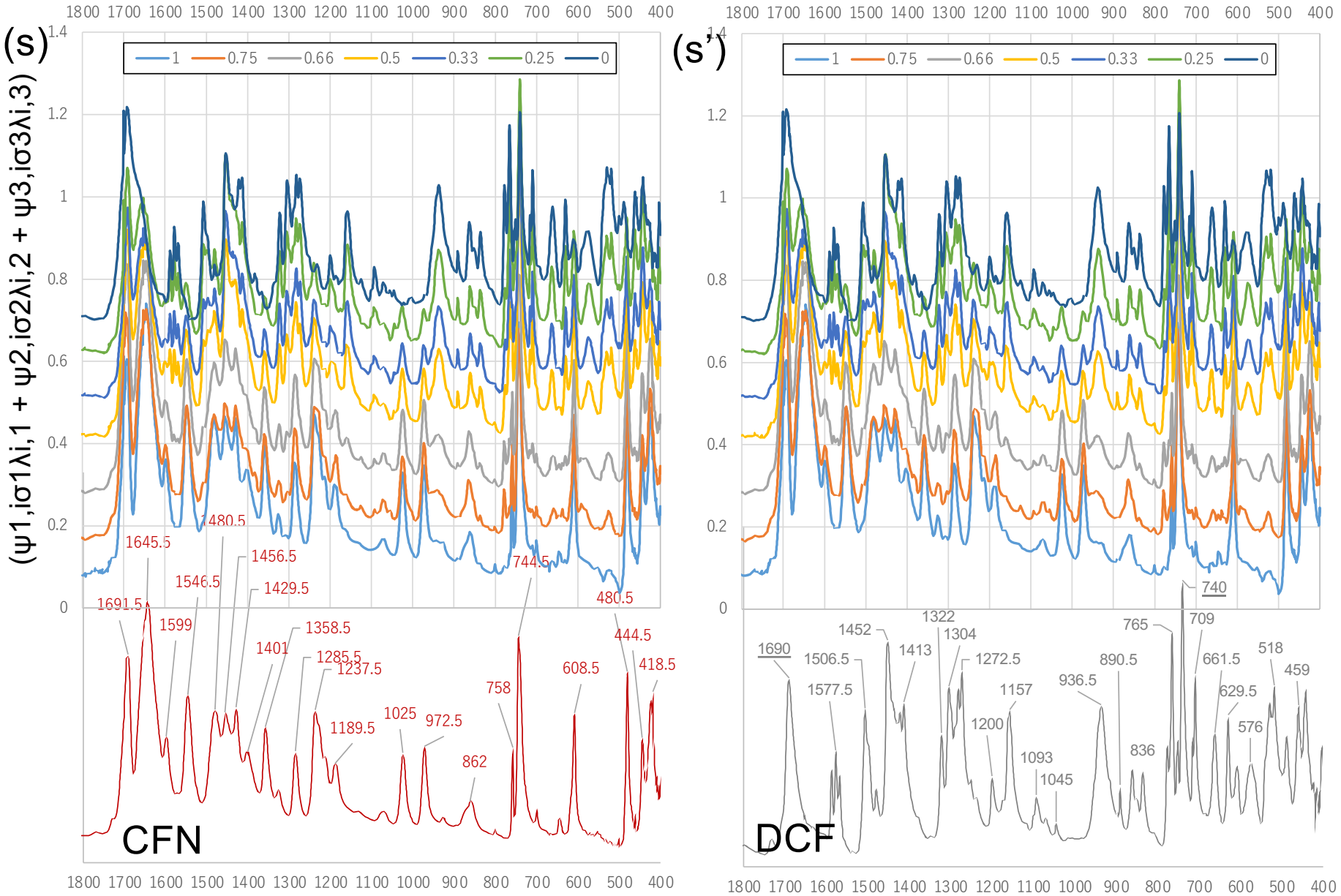
(s)
(ψ1,iσ1λi,1 + ψ2,iσ2λi,2 + ψ3,iσ3λi,3)
1 0.75 0.66 0.5 0.33 0.25 0
1691.5
1645.5
1599
1546.5
1480.5
1456.5
1429.5
1401
1358.5
1285.5
1237.5
1189.5
1025
972.5
862
758
744.5
608.5
480.5
444.5
418.5
CFN
(s')
1 0.75 0.66 0.5 0.33 0.25 0
740
1690
1577.5
1506.5
1452
1413
1322
1304
1272.5
1200
1157
1093
1045
936.5
890.5
836
765
709
661.5
629.5
576
518
459
DCF

Figure S8

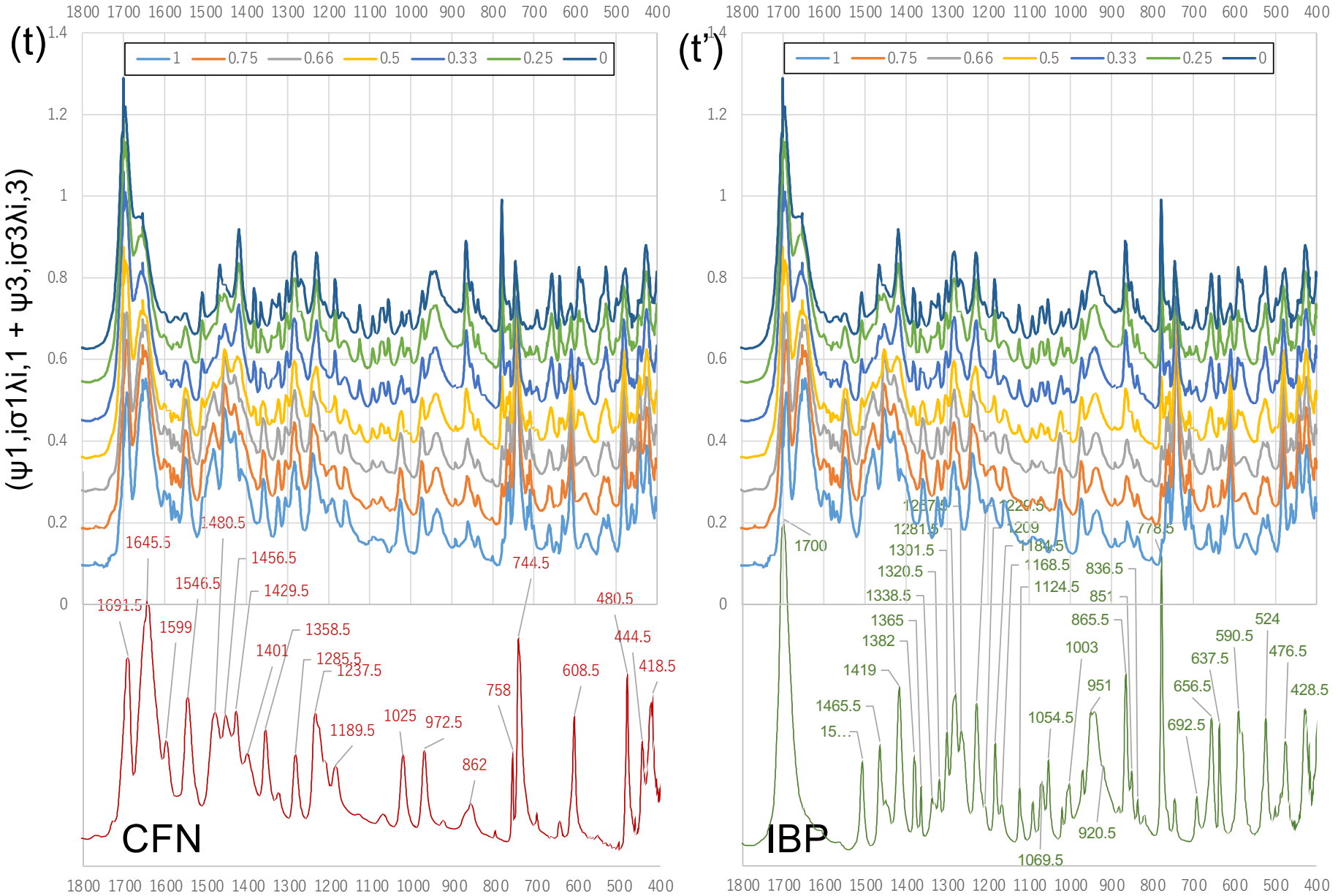
(t)
(t')
(ψ1,iσ1λi,1 + ψ3,iσ3λi,3)
1 0.75 0.66 0.5 0.33 0.25 0
1800 1700 1600 1500 1400 1300 1200 1100 1000 900 800 700 600 500 400
0 0.2 0.4 0.6 0.8 1 1.2 1.4
1691.5
1645.5
1599
1546.5
1480.5
1456.5
1429.5
1401
1358.5
1285.5
1237.5
1189.5
1025
972.5
862
758
744.5
608.5
480.5
444.5
418.5
CFN
1700
1465.5
1419
1382
1365
1338.5
1320.5
1301.5
1281.5
1209
1184.5
1168.5
1124.5
1069.5
1054.5
1003
951
920.5
865.5
851
836.5
778.5
692.5
656.5
637.5
590.5
524
476.5
428.5
IBP

Figure S8

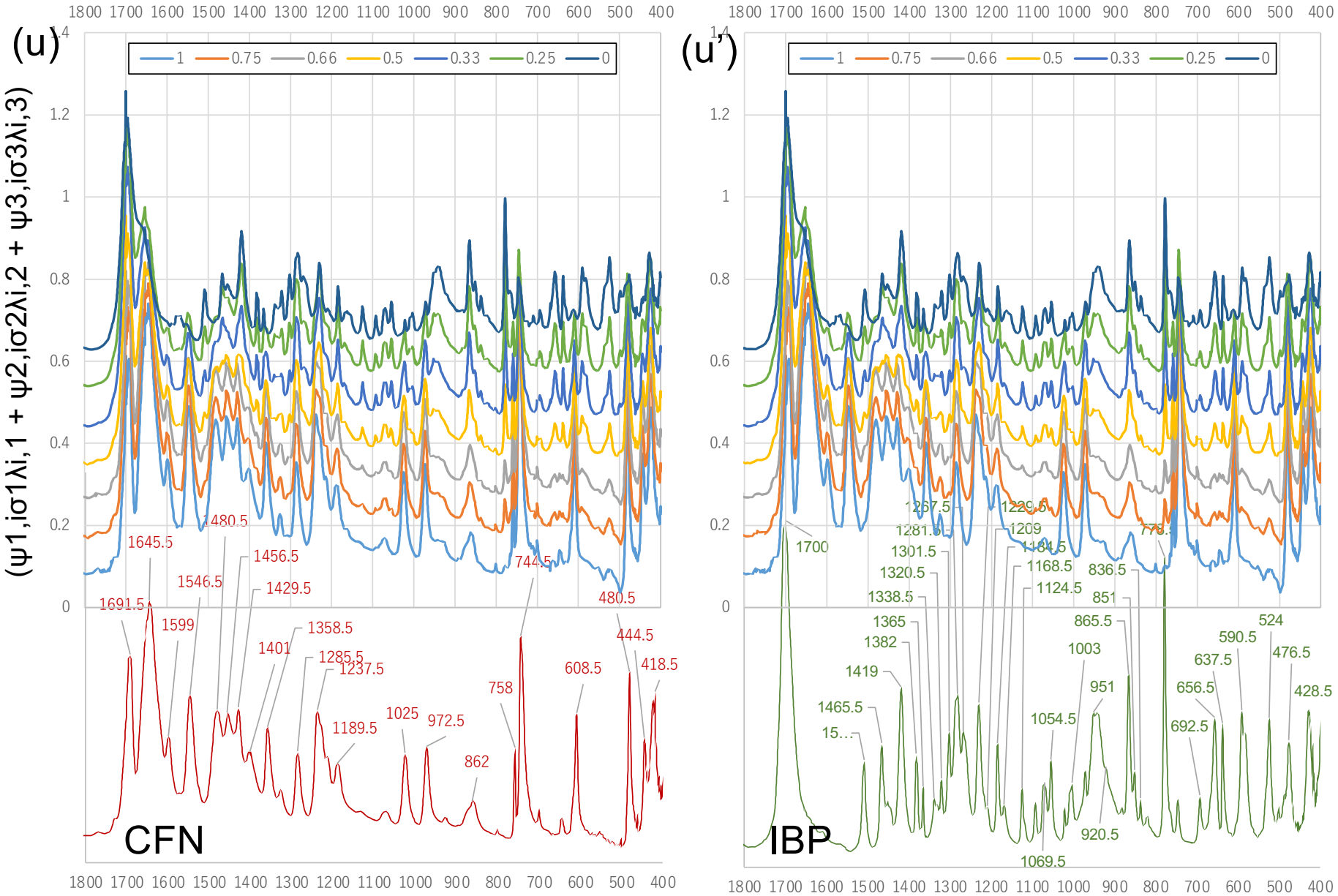
(u)
(u')
(ψ1,iσ1λi,1 + ψ2,iσ2λi,2 + ψ3,iσ3λi,3)
1 0.75 0.66 0.5 0.33 0.25 0
CFN
IBP
1691.5
1645.5
1599
1546.5
1480.5
1456.5
1429.5
1401
1358.5
1285.5
1237.5
1189.5
1025
972.5
862
758
744.5
608.5
480.5
444.5
418.5
1700
1267.5
1229.5
1209
1184.5
1168.5
1124.5
1338.5
1320.5
1301.5
1281.5
1365
1382
1419
1465.5
1054.5
1003
951
865.5
851
836.5
920.5
1069.5
692.5
656.5
637.5
590.5
524
476.5
428.5

Figure S8

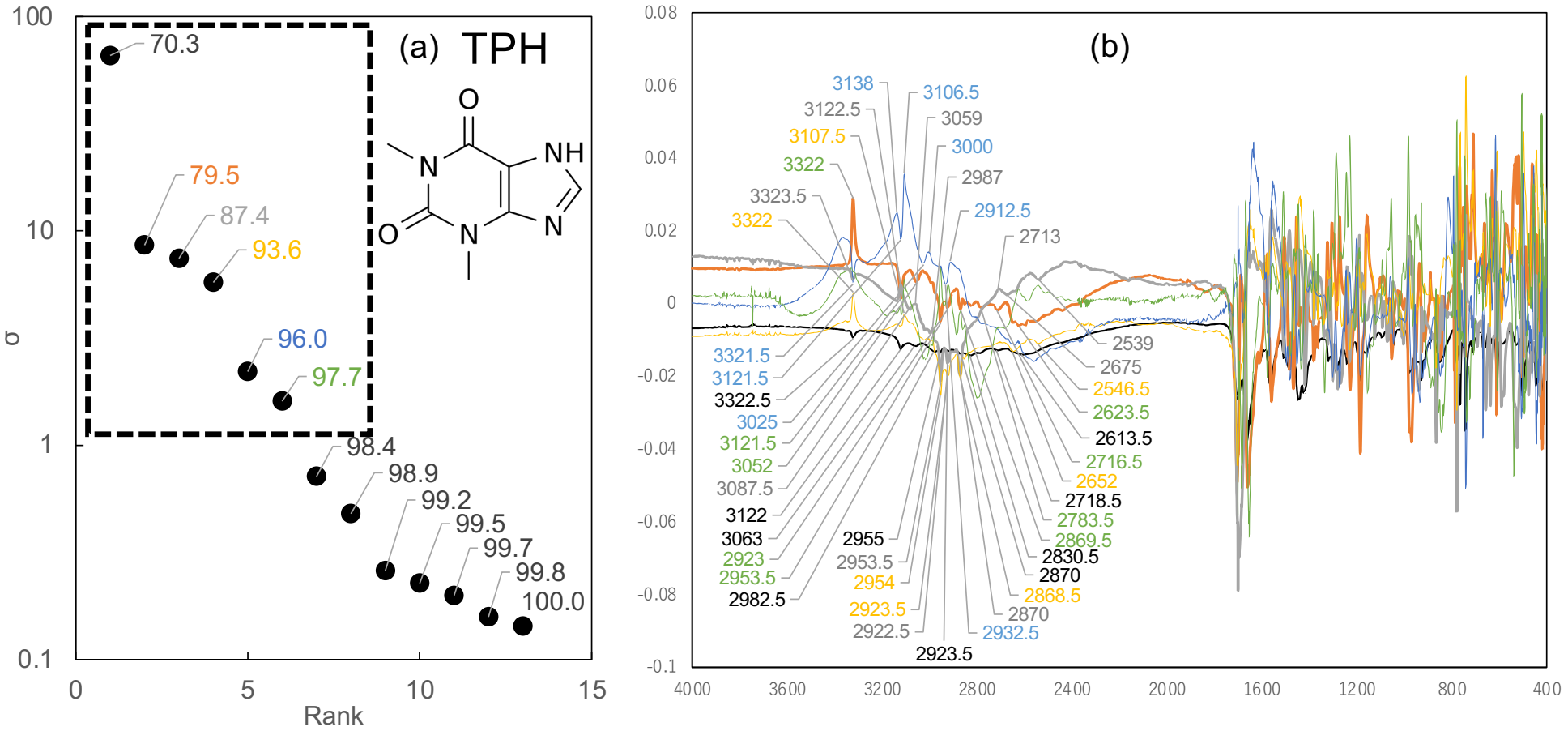

Figure S9. SVD computation for FTIR spectra of TPH/IBP and TPH/DCF mixtures provided singular values σi (a) and Basis spectra ψi (b). Cumulative proportions of σi were appended beside the σ plots, indicating that higher five σ's which were satisfied 97.7 percent of the variance. The basis spectra decomposed by the SVD computation corresponded to the components ψ1 (black), ψ2 (orange), ψ3 (gray), ψ4 (yellow), and ψ5 (blue). Details of ψ's assignments to the observed spectra in the wavenumber range 1800-400 cm^{-1} are followed (e-o).

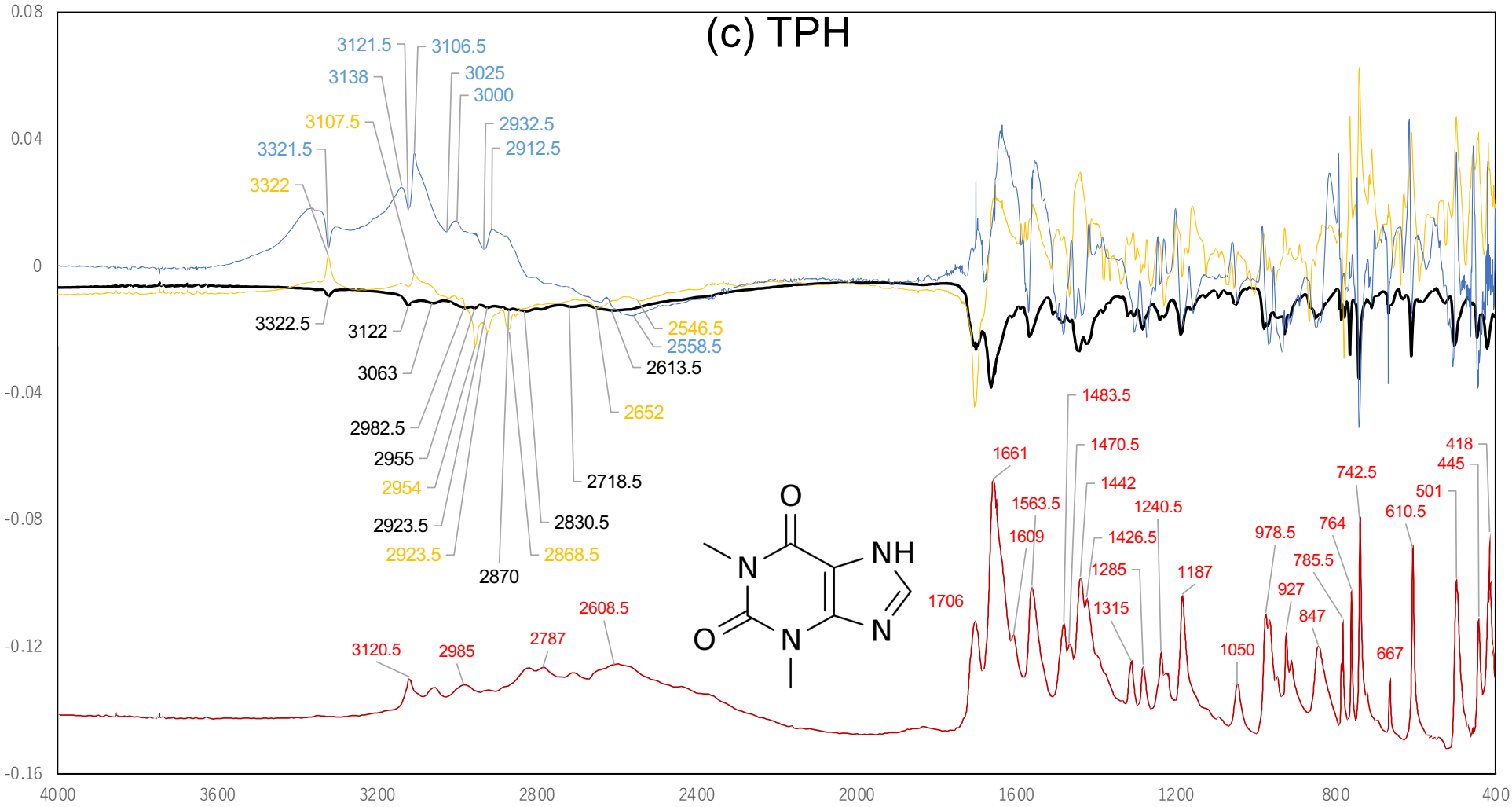

Figure S9. The basis spectra decomposed by the SVD computation corresponded to the components at the rank of 1 (black), 4 (yellow), and 5 (blue).

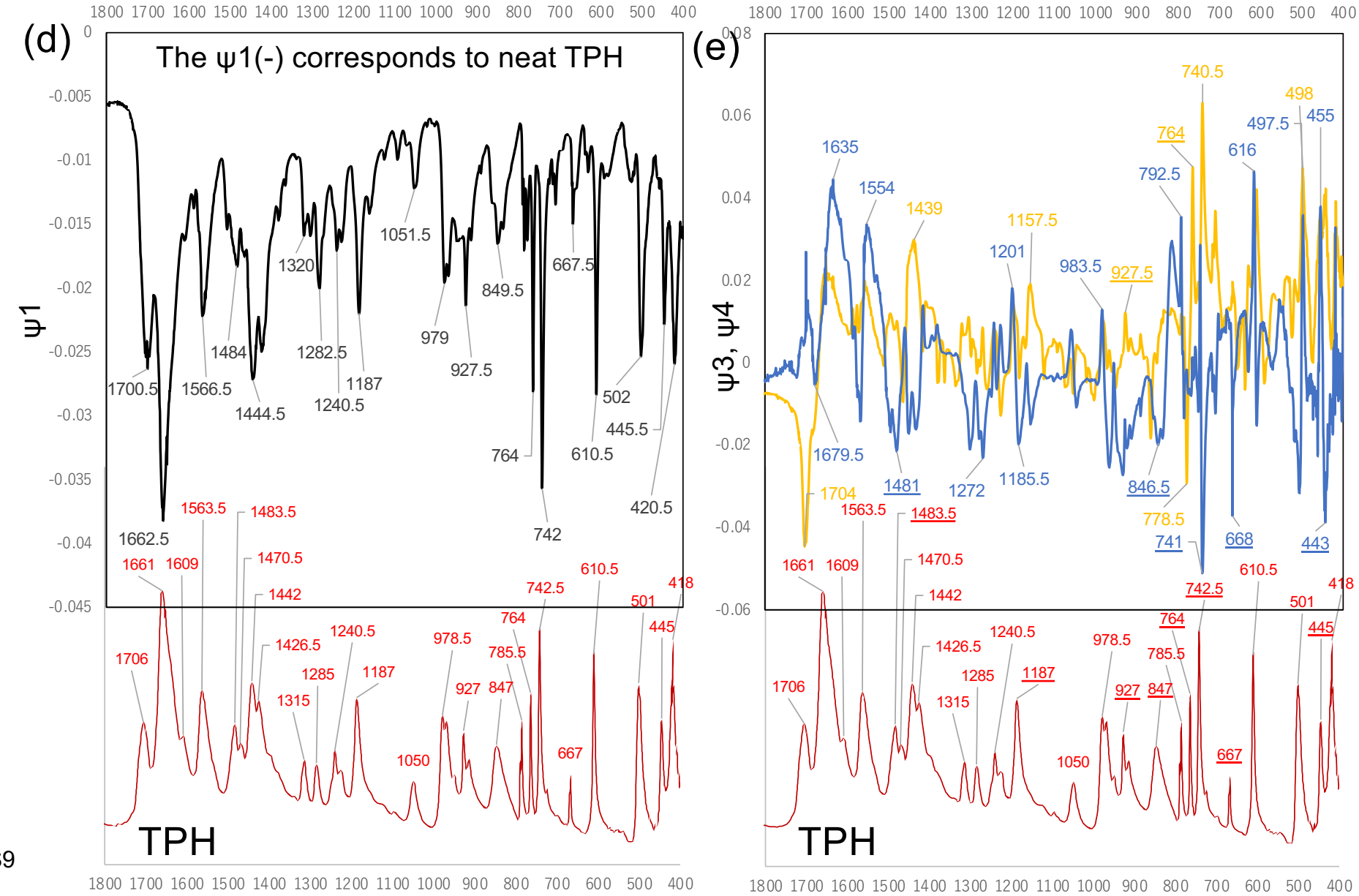
(d)
The ψ1(-) corresponds to neat TPH
ψ1
1700.5
1662.5
1566.5
1563.5
1484
1483.5
1444.5
1470.5
1442
1320
1282.5
1240.5
1187
1051.5
979
927.5
849.5
764
742
667.5
610.5
502
445.5
420.5
1706
1661
1609
1426.5
1315
1285
1240.5
1187
1050
978.5
927
847
785.5
764
742.5
667
610.5
501
445
418
TPH
(e)
ψ3, ψ4
1635
1554
1439
1679.5
1481
1272
1157.5
1201
1185.5
983.5
927.5
846.5
740.5
792.5
764
778.5
741
616
668
498
497.5
455
443
1704
1706
1661
1609
1563.5
1483.5
1470.5
1442
1426.5
1315
1285
1240.5
1187
1050
978.5
927
847
785.5
764
742.5
667
610.5
501
445
418
TPH

Figure S9

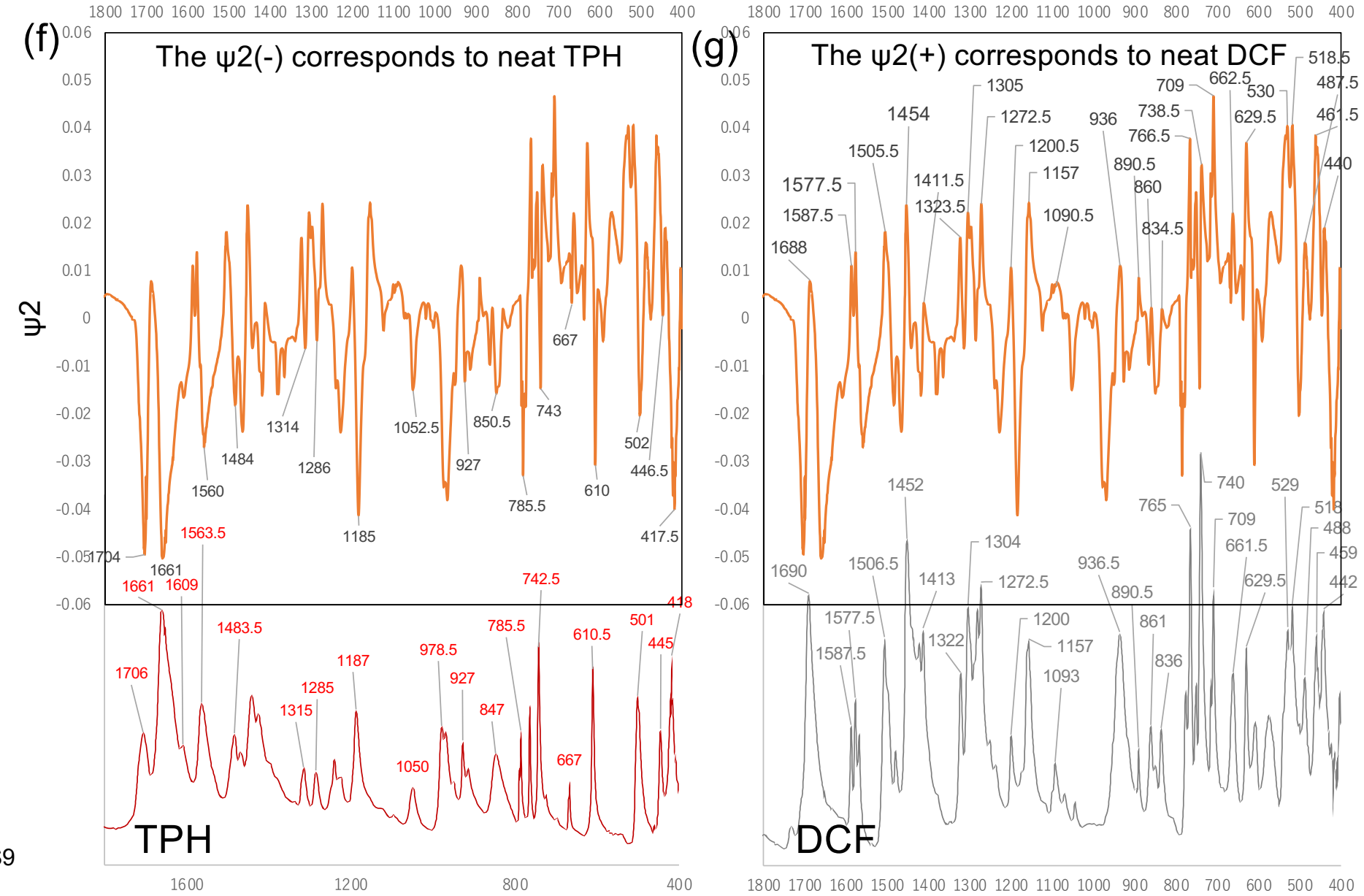
(f)
The ψ2(-) corresponds to neat TPH
ψ2
1704
1661
1661
1609
1563.5
1560
1484
1314
1286
1185
1052.5
927
850.5
785.5
743
667
610
502
446.5
417.5
TPH
1706
1483.5
1285
1315
1187
978.5
927
1050
847
785.5
742.5
667
610.5
501
445
418
(g)
The ψ2(+) corresponds to neat DCF
1688
1577.5
1587.5
1505.5
1454
1411.5
1323.5
1305
1272.5
1200.5
1157
1090.5
936
890.5
860
834.5
738.5
766.5
709
662.5
629.5
530
518.5
487.5
461.5
440
DCF
1690
1506.5
1452
1413
1322
1304
1272.5
1200
1157
1093
936.5
890.5
861
836
765
740
709
661.5
629.5
529
516
488
459
442

Figure S9

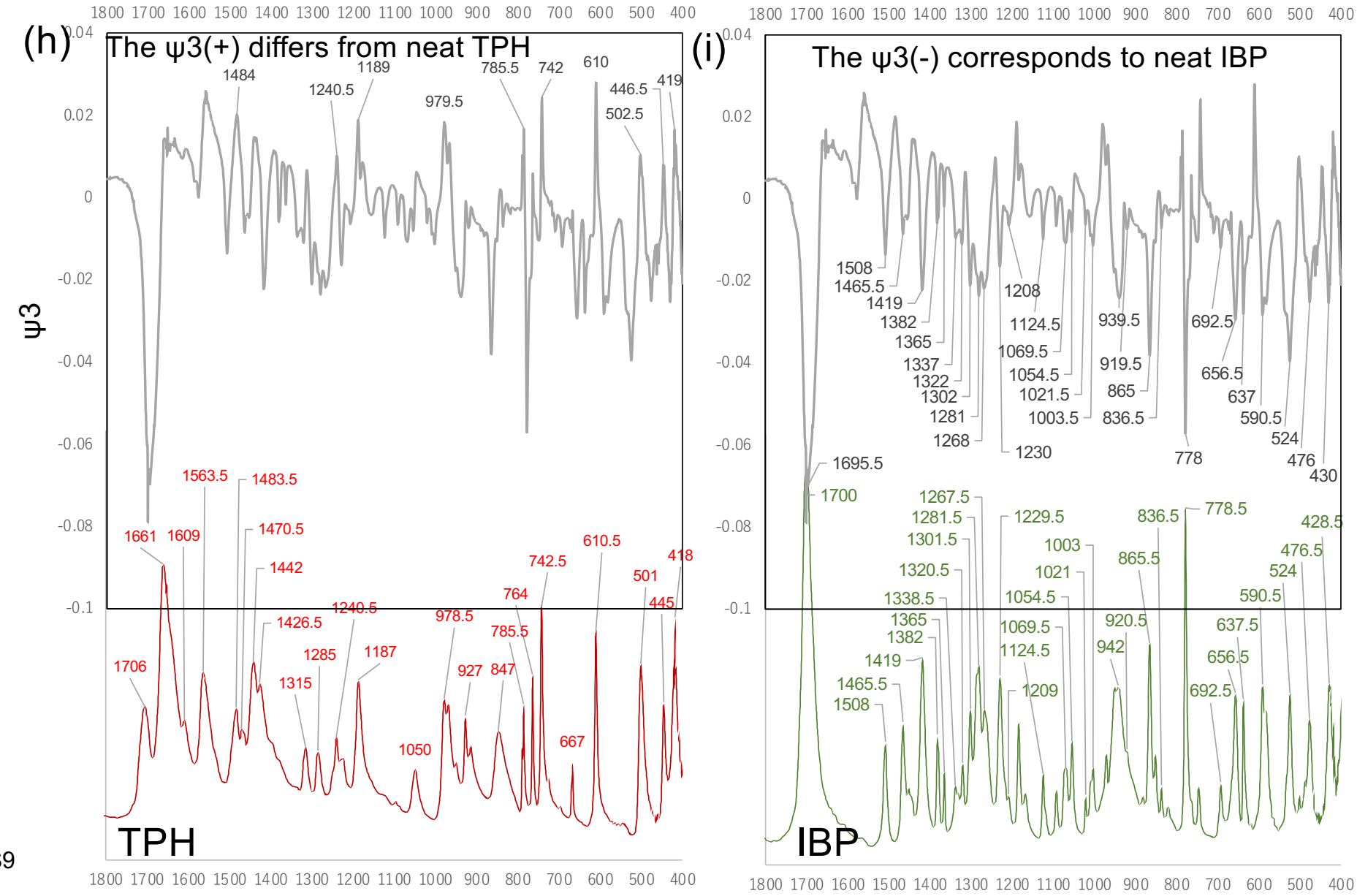
(h)
The ψ3(+) differs from neat TPH
ψ3
1800 1700 1600 1500 1400 1300 1200 1100 1000 900 800 700 600 500 400
0.04
0.02
0
-0.02
-0.04
-0.06
-0.08
-0.1
1484
1240.5
1189
979.5
785.5
742
610
446.5
419
502.5
1563.5
1483.5
1661
1609
1470.5
1442
1426.5
1240.5
1285
1187
1315
1706
978.5
927
847
785.5
764
742.5
610.5
501
418
445
1050
667
TPH
(i)
The ψ3(-) corresponds to neat IBP
1508
1465.5
1419
1382
1365
1337
1322
1302
1281
1268
1208
1124.5
1069.5
1054.5
1021.5
1003.5
1230
939.5
919.5
865
836.5
778
692.5
656.5
637
590.5
524
476
430
1695.5
1700
1267.5
1281.5
1301.5
1320.5
1338.5
1365
1382
1419
1465.5
1508
1229.5
1003
1021
1054.5
1069.5
1124.5
1209
836.5
865.5
920.5
942
778.5
428.5
476.5
524
590.5
637.5
656.5
692.5
IBP

Figure S9

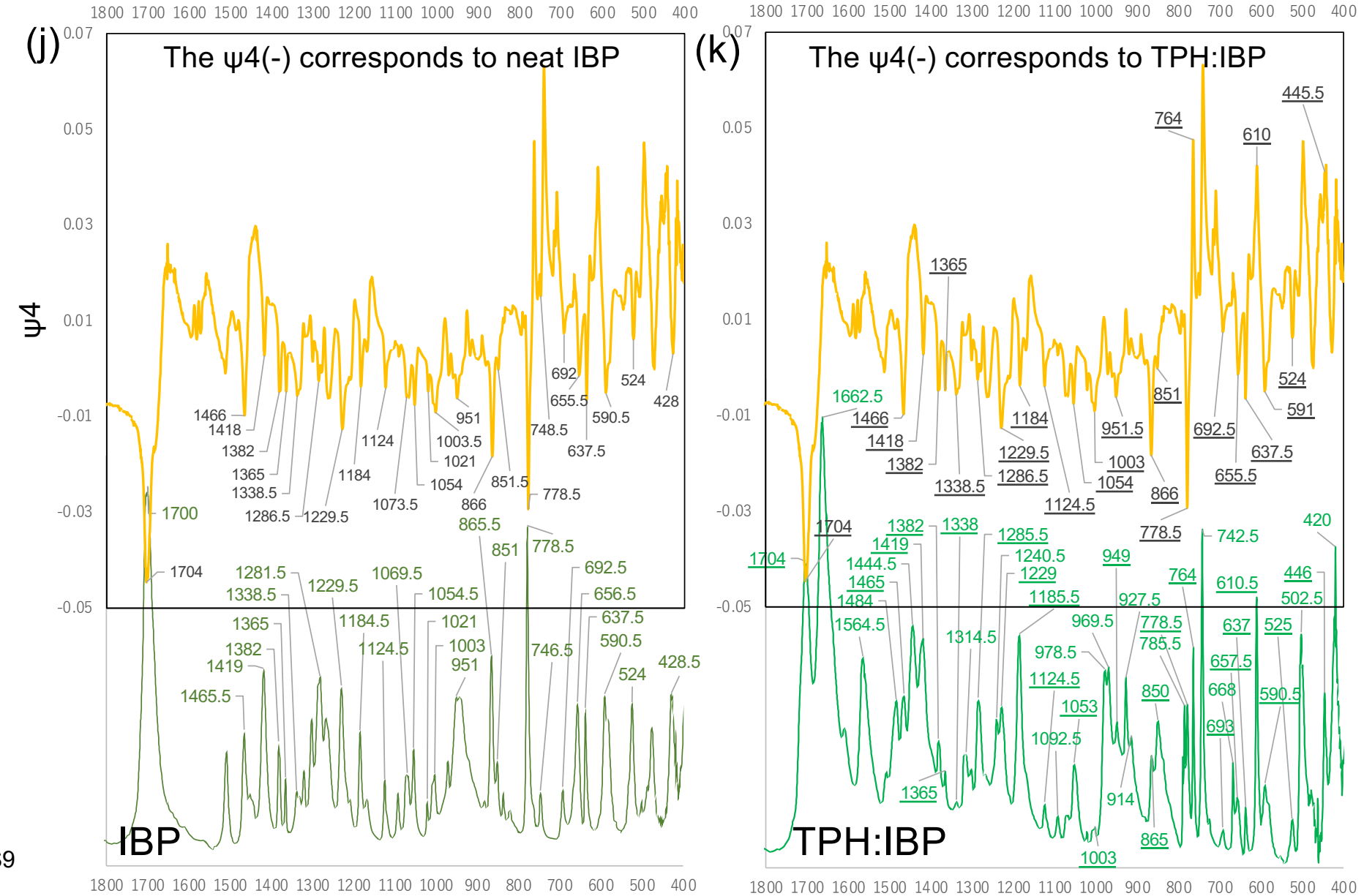
(j)
The ψ4(-) corresponds to neat IBP
ψ4
IBP
(k)
The ψ4(-) corresponds to TPH:IBP
TPH:IBP

Figure S9

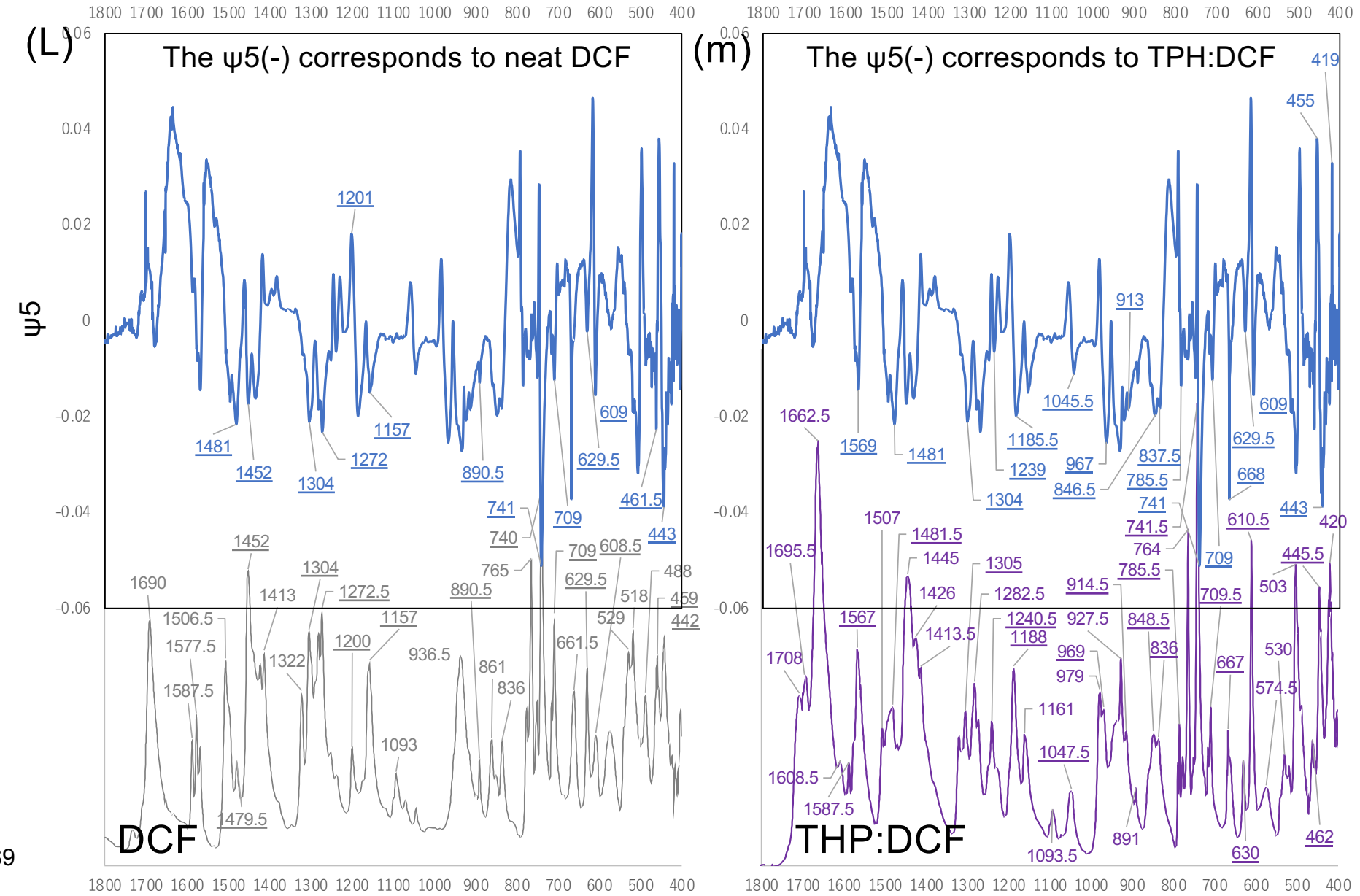
(L)
The ψ5(-) corresponds to neat DCF
ψ5
DCF
(m)
The ψ5(-) corresponds to TPH:DCF
THP:DCF

Figure S9

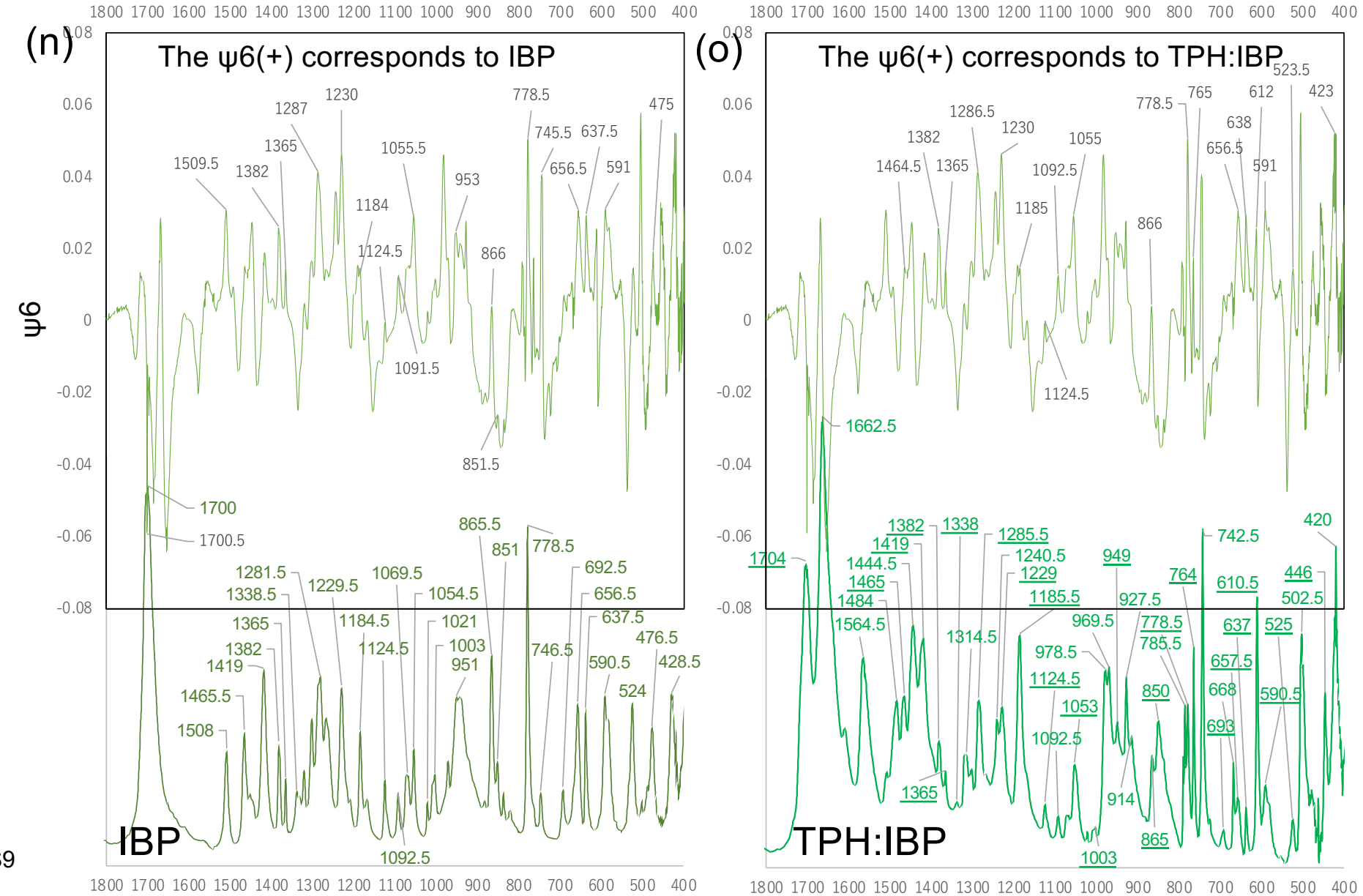
(n)
The ψ6(+) corresponds to IBP
ψ6
IBP
(o)
The ψ6(+) corresponds to TPH:IBP
TPH:IBP

Figure S9

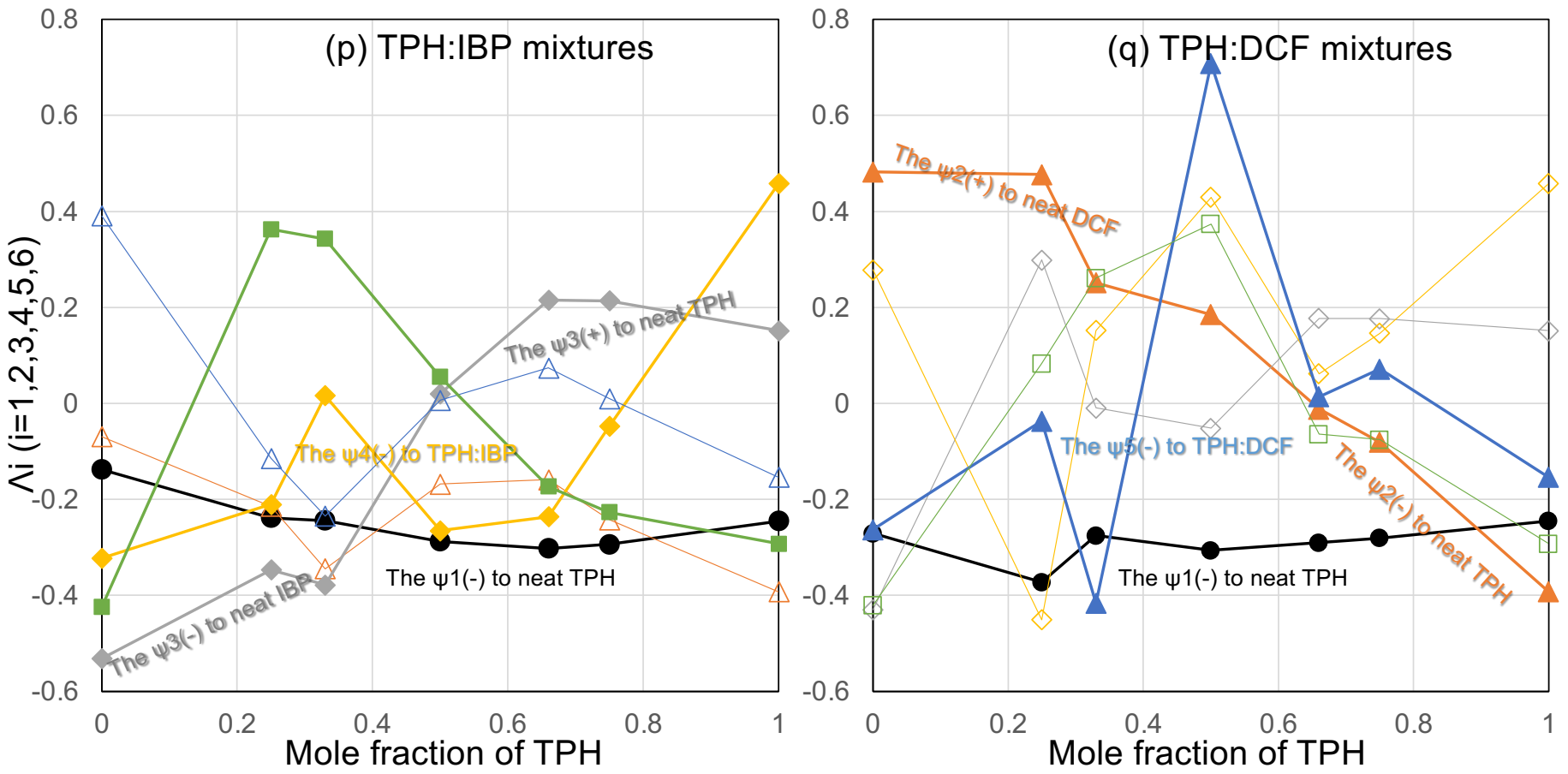

Figure S9 (p and q). The components of the first to fifth singular vectors as a function of mole fraction of TPH. The λ1, λ2, λ3, λ4, λ5, and λ6 were represented by closed black circles, orange triangles, gray diamonds, yellow diamonds, blue triangles, and green squares. For λ2, λ3, λ4, λ5, and λ6, closed and open symbols corresponded to the composition with the basis functions correlated to which the IBP or DCF mixtures, respectively.

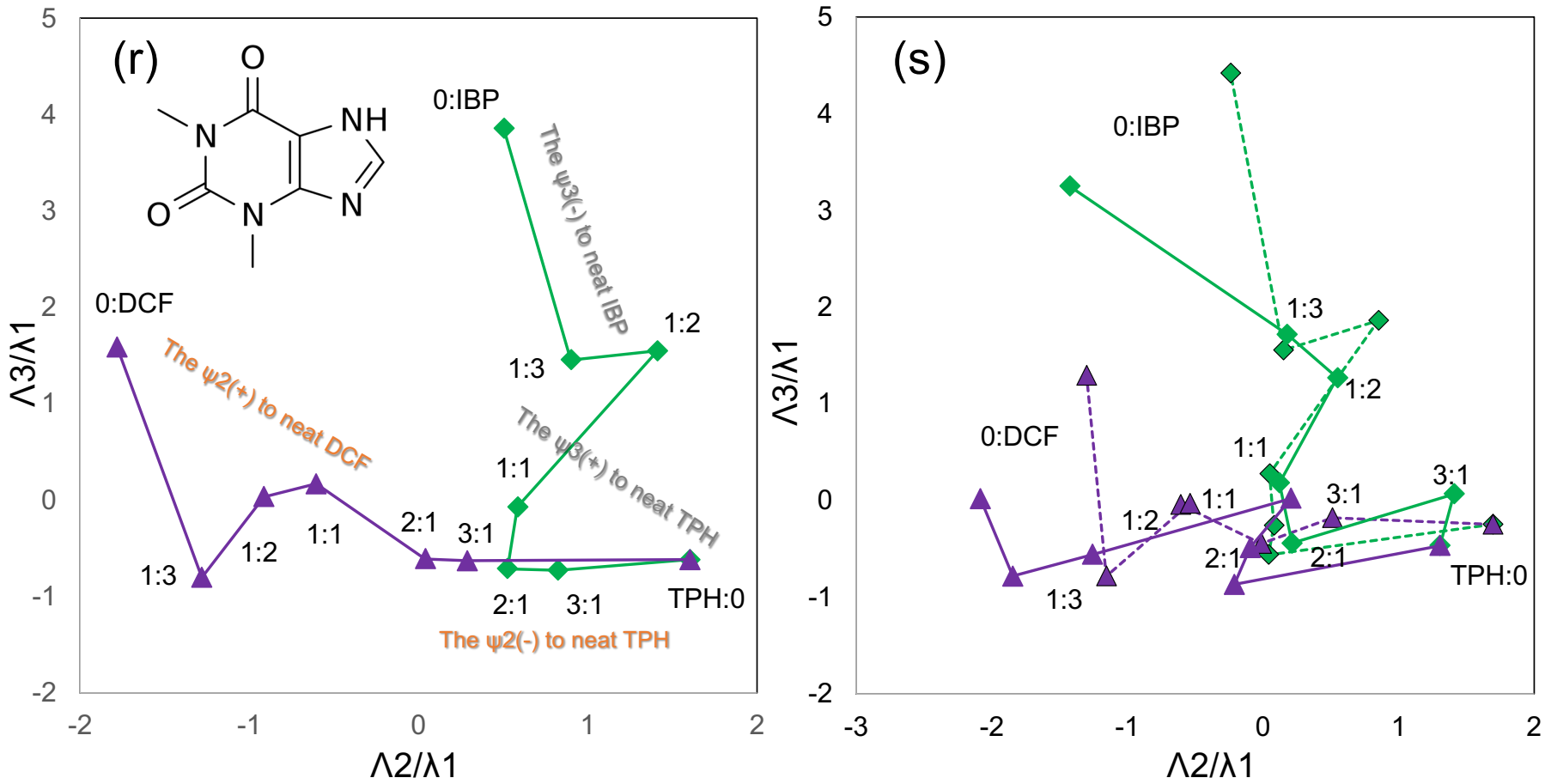

Figure S9 (r and s). The trajectories of the TPH/IBP (green diamonds) and TPH/DCF (violet triangles) mixtures. They shared the neat TPH's vector (TPH:0). The molar ratios were represented along the corresponding plots. The trajectory of the TPH/DCF mixtures traced along the verical (λ2/λ1)-axis (DCF owning dominance in the SVD analysis), whereas that of the TPH/IBP mixtures pursued along the perpendicular (λ2/λ1)-axis, indicating independence of the interactions in these TPH/IBP and TPH/DCF mixtures. The S13(r) and S13(s) show the trajectories of the average spectra and the individually measured spectra, respectively.

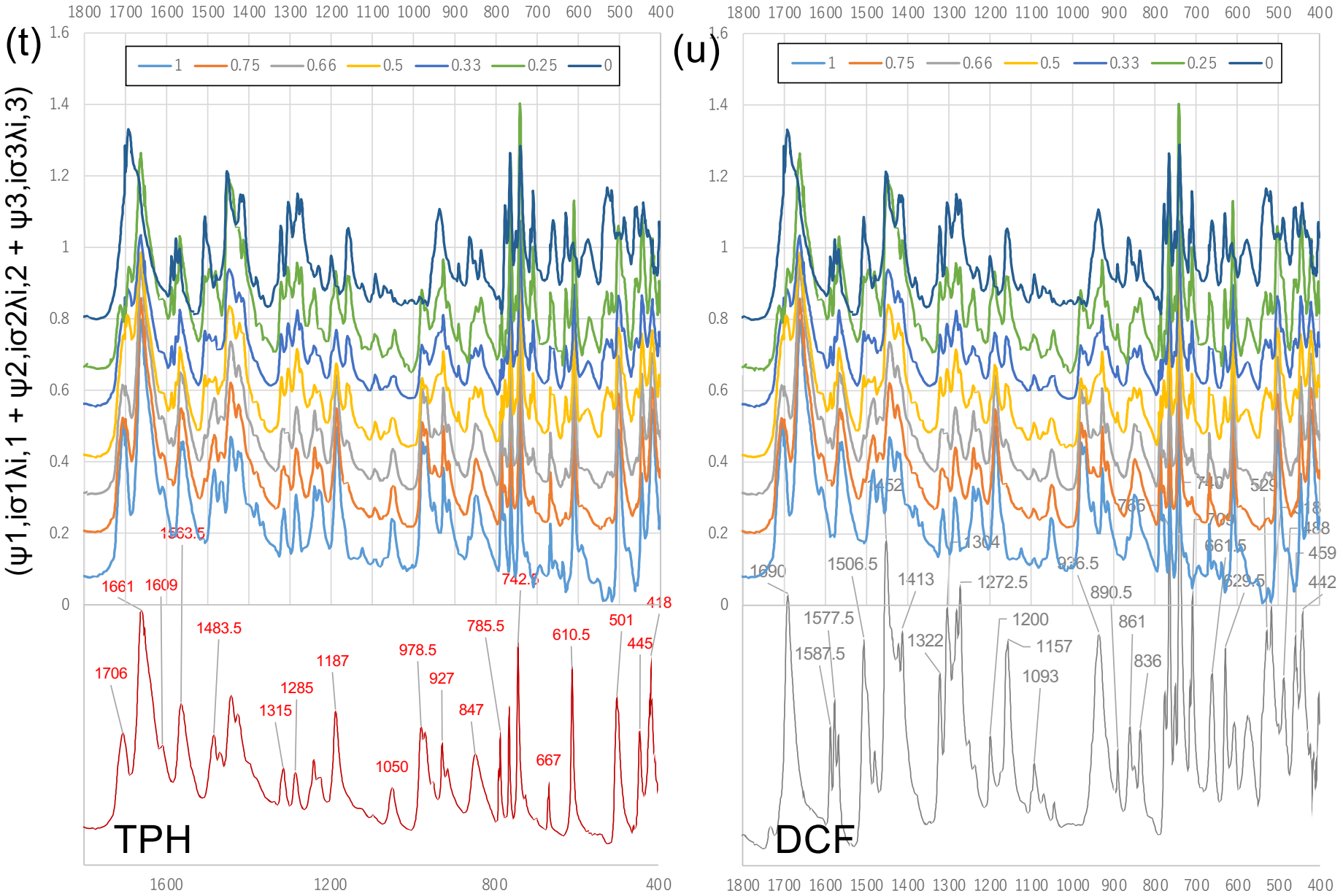
(t)
(u)
(ψ1,iσ1λi,1 + ψ2,iσ2λi,2 + ψ3,iσ3λi,3)
1 0.75 0.66 0.5 0.33 0.25 0
1800 1700 1600 1500 1400 1300 1200 1100 1000 900 800 700 600 500 400
1.6 1.4 1.2 1 0.8 0.6 0.4 0.2 0
1661 1609 1563.5 1483.5 1706 1285 1315 1187 978.5 927 1050 847 785.5 742.5 667 610.5 501 445 418
TPH
1690 1506.5 1577.5 1587.5 1413 1322 1304 1272.5 1200 1157 1093 936.5 890.5 861 836 740 709 661.5 629.5 529 488 459 442
DCF
1600 1200 800 400

Figure S9

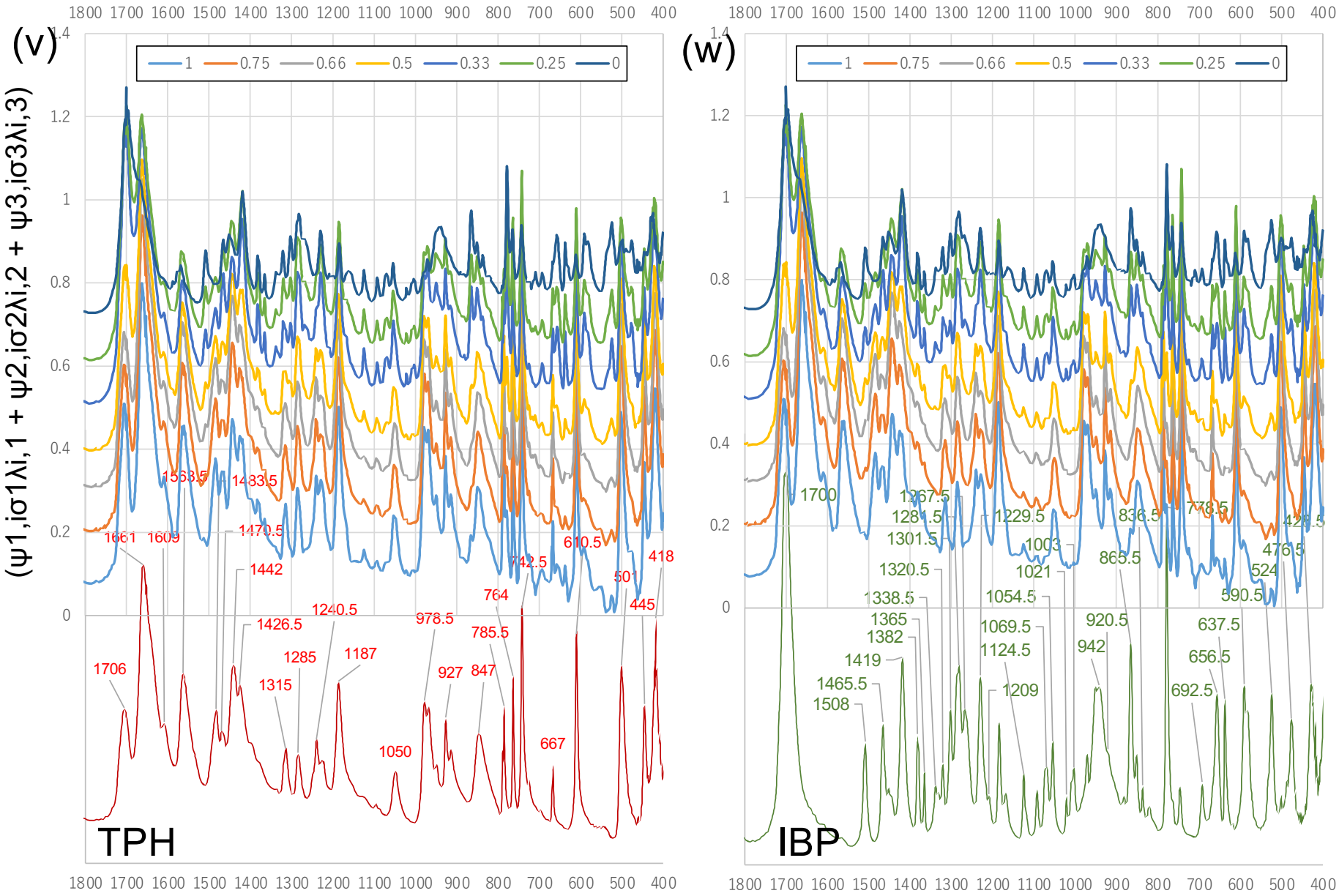
(v)
(w)
(ψ1,iσ1λi,1 + ψ2,iσ2λi,2 + ψ3,iσ3λi,3)
1 0.75 0.66 0.5 0.33 0.25 0
1800 1700 1600 1500 1400 1300 1200 1100 1000 900 800 700 600 500 400
1.4 1.2 1 0.8 0.6 0.4 0.2 0
1706 1661 1609 1563.5 1483.5 1470.5 1442 1426.5 1315 1285 1240.5 1187 1050 978.5 927 847 785.5 764 742.5 667 610.5 501 445 418
TPH
1700 1467.5 1429.5 1367.5 1281.5 1301.5 1320.5 1338.5 1365 1382 1419 1465.5 1508 1229.5 1209 1124.5 1069.5 1054.5 1021 1003 942 920.5 865.5 836.5 778.5 692.5 656.5 637.5 590.5 524 476.5 428.5
IBP

Figure S9

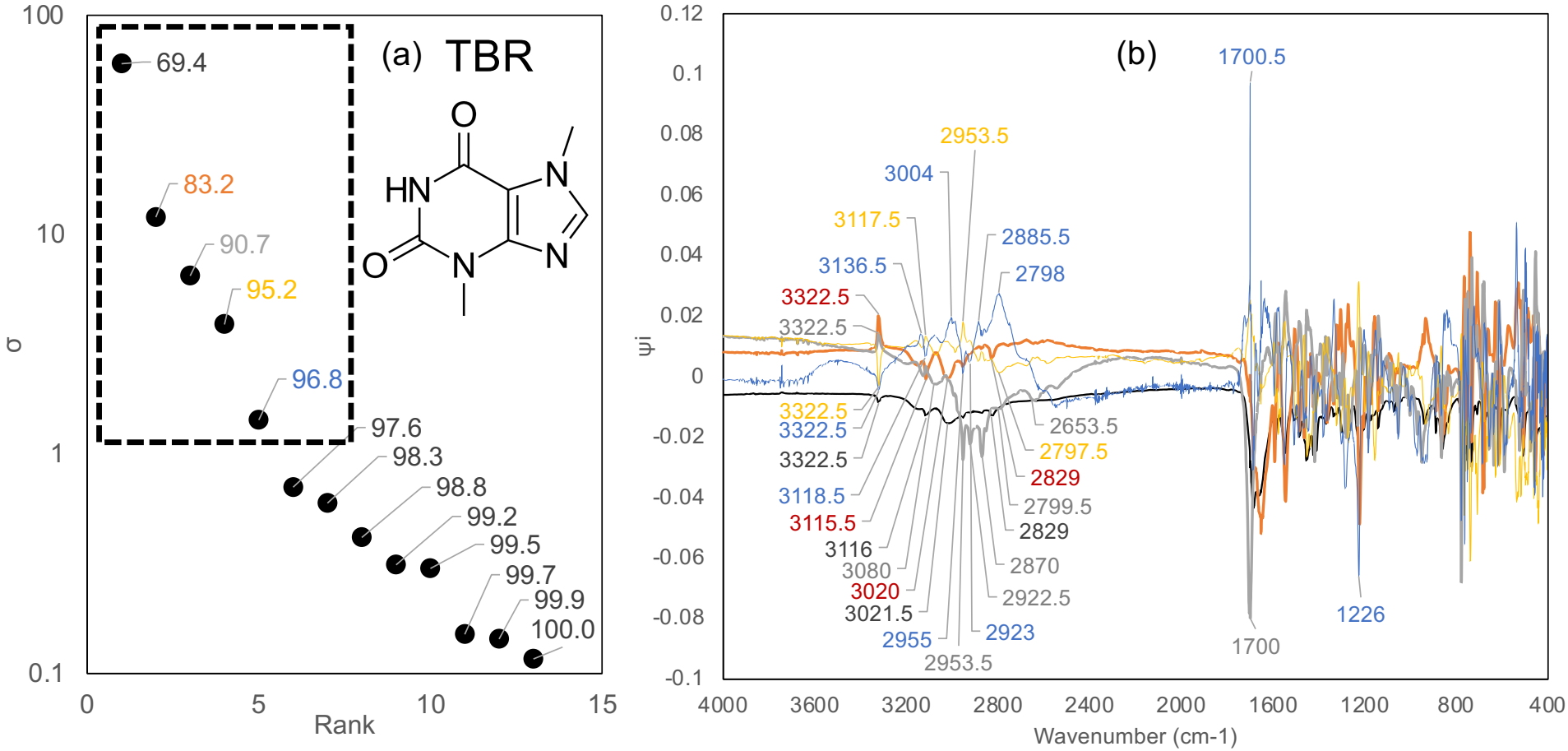

Figure S10. SVD computation for FTIR spectra of TBR/IBP and TBR/DCF mixtures provided singular values σi (a) and Basis spectra ψi(b). Cumulative proportions of σi were appended beside the σ plots, indicating that higher five σ's satisfied 97.6 percent of the variance. The basis spectra decomposed by the SVD computation corresponded to the components at the rank of 1 (black), 2 (orange), 3 (gray), 4 (yellow), and 5 (blue). Details of ψ's assignments to the observed spectra in the wavenumber range 1800-400 cm^{-1} are followed (e-o').

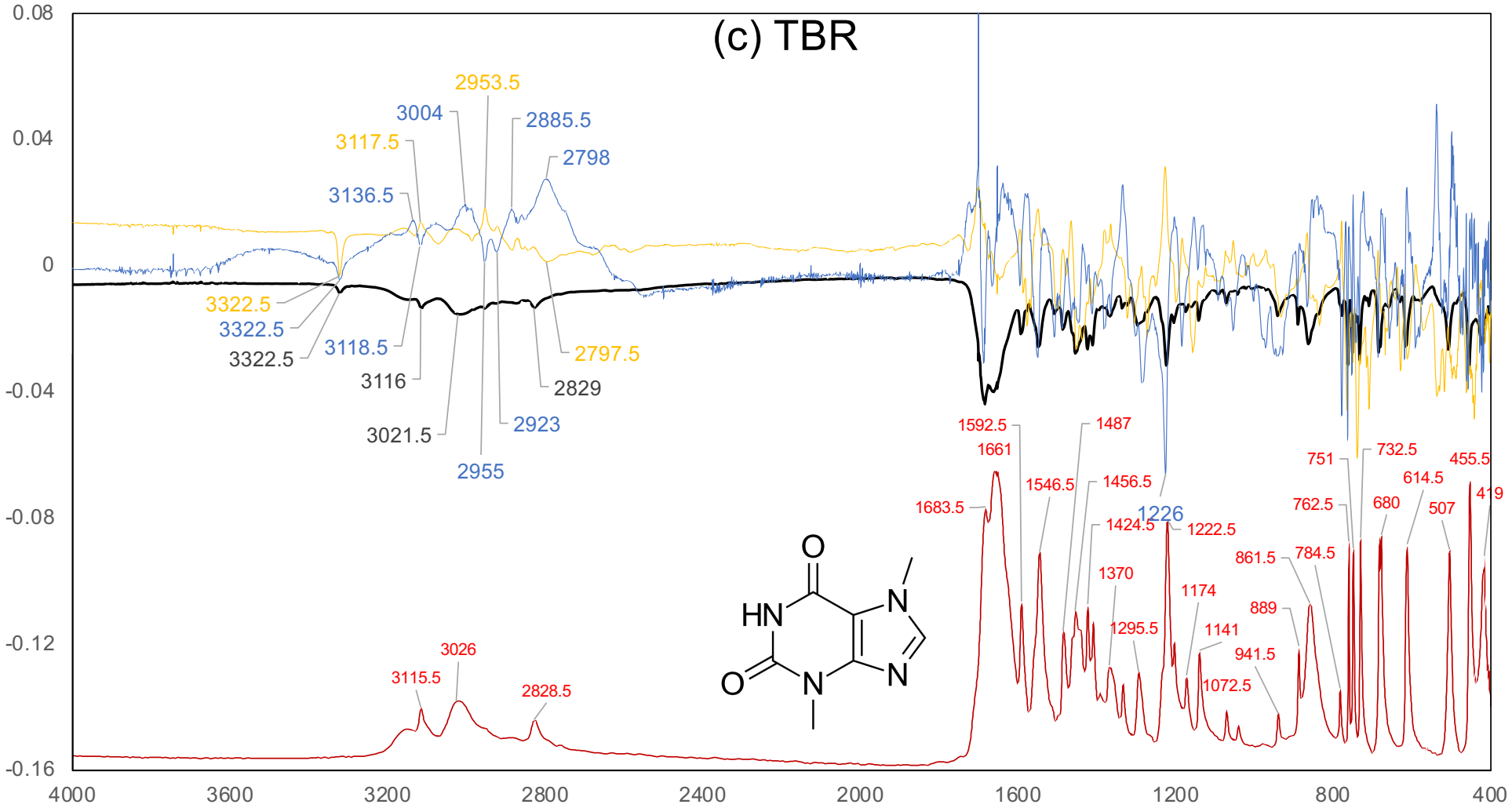

Figure S10. The basis spectra decomposed by the SVD computation corresponded to the components at the rank of 1 (black), 4 (yellow), and 5 (blue).

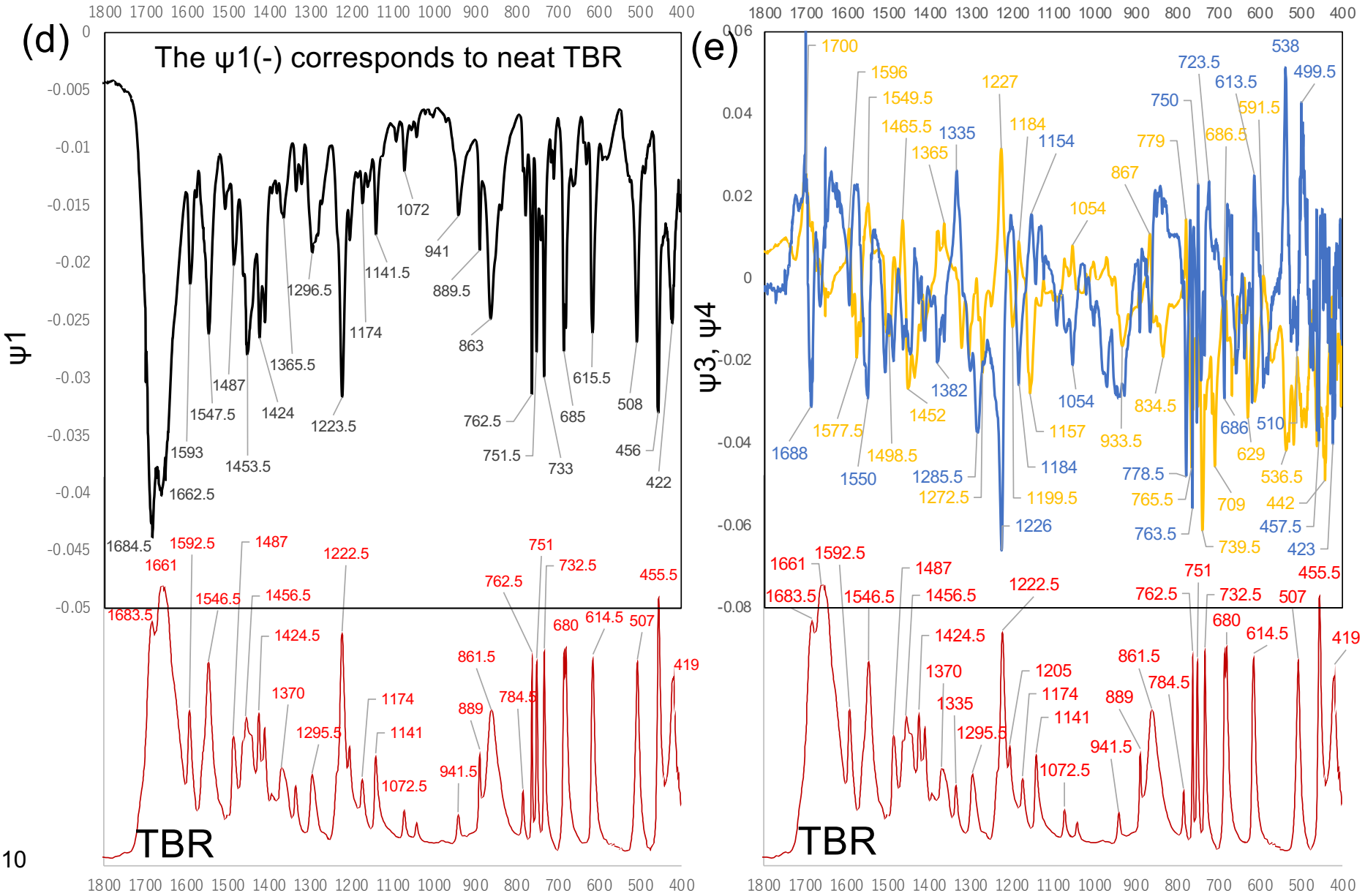
(d)
The ψ1(-) corresponds to neat TBR
ψ1
1800 1700 1600 1500 1400 1300 1200 1100 1000 900 800 700 600 500 400
0
-0.005
-0.01
-0.015
-0.02
-0.025
-0.03
-0.035
-0.04
-0.045
-0.05
1684.5
1662.5
1593
1547.5
1487
1453.5
1424
1365.5
1296.5
1223.5
1174
1141.5
1072
941
889.5
863
762.5
751.5
733
685
615.5
508
456
422
TBR
1683.5
1661
1592.5
1546.5
1487
1456.5
1424.5
1370
1295.5
1222.5
1174
1141
1072.5
941.5
889
861.5
784.5
762.5
751
732.5
680
614.5
507
455.5
419
(e)
ψ3, ψ4
0.06
0.04
0.02
0
-0.02
-0.04
-0.06
-0.08
1700
1688
1596
1577.5
1549.5
1550
1498.5
1465.5
1452
1382
1365
1335
1285.5
1272.5
1227
1226
1199.5
1184
1184
1157
1154
1054
1054
1054
1023.5
933.5
867
834.5
779
778.5
765.5
763.5
750
739.5
723.5
709
686.5
686
629
613.5
591.5
538
536.5
510
499.5
457.5
442
423
TBR
1683.5
1661
1592.5
1546.5
1487
1456.5
1424.5
1370
1335
1295.5
1222.5
1205
1174
1141
1072.5
941.5
889
861.5
784.5
762.5
751
732.5
680
614.5
507
455.5
419

Figure S10

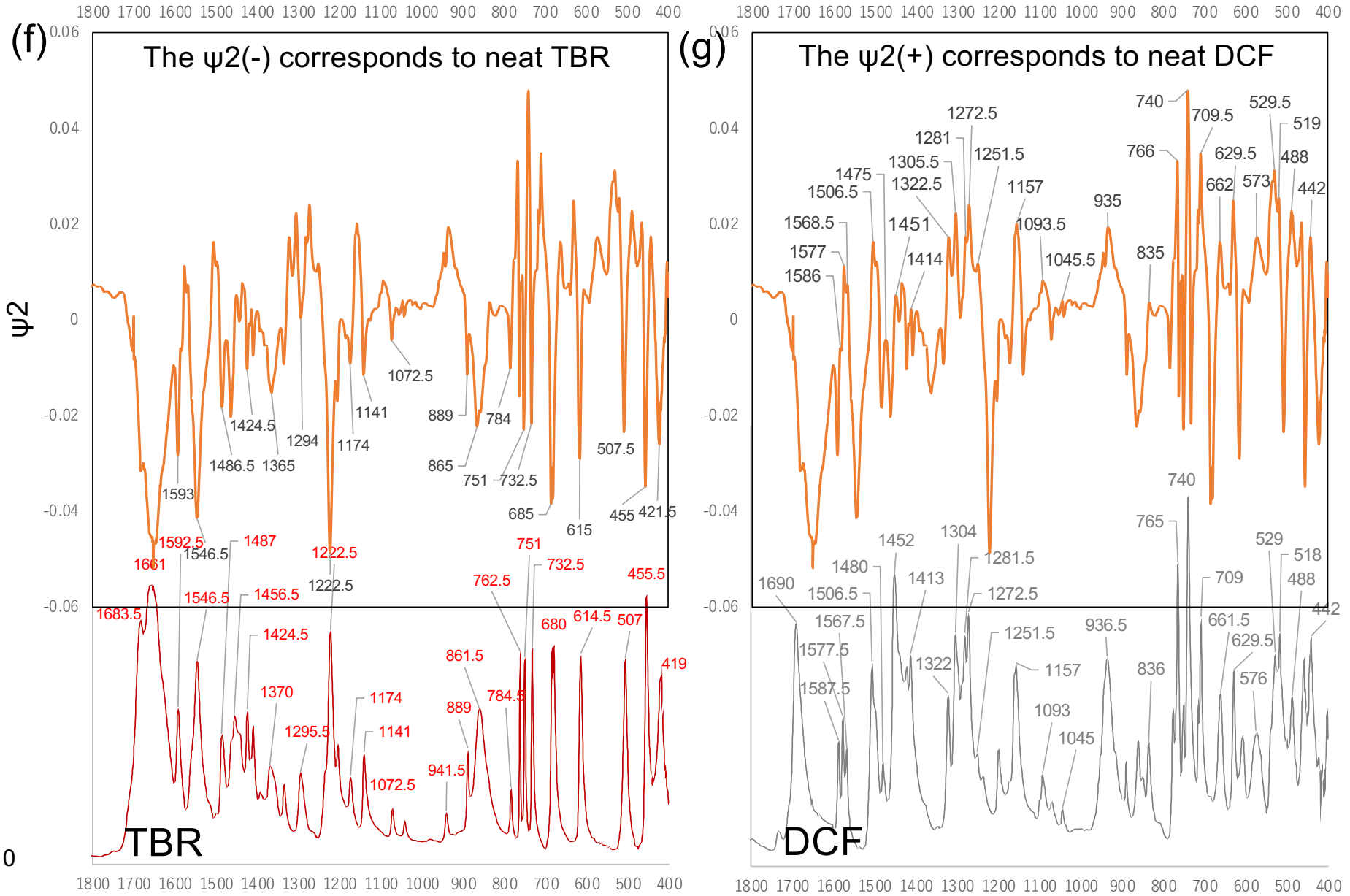
(f)
The ψ2(-) corresponds to neat TBR
ψ2
TBR
(g)
The ψ2(+) corresponds to neat DCF
DCF

Figure S10

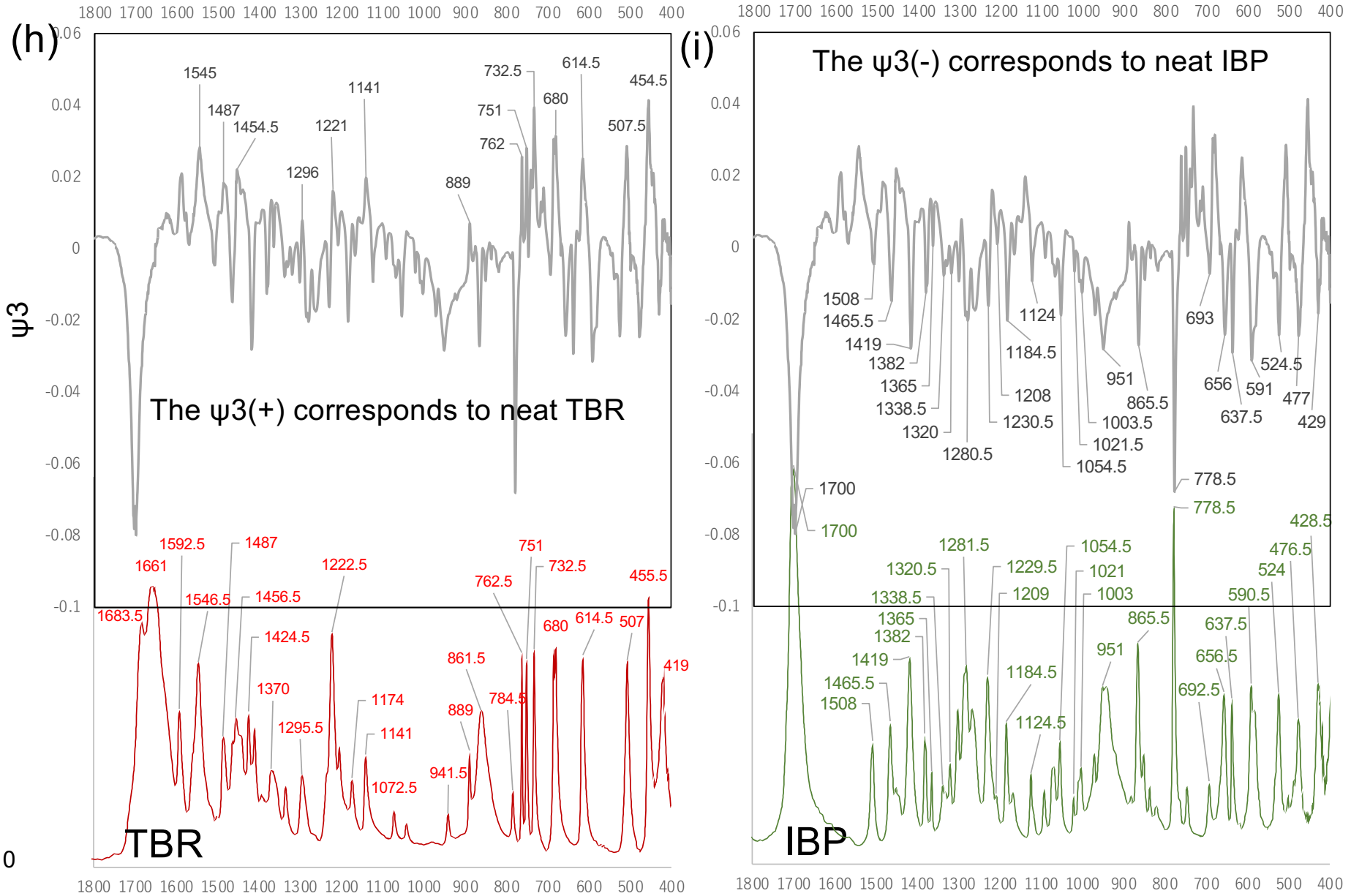
(h)
(i)
ψ3
The ψ3(+) corresponds to neat TBR
The ψ3(-) corresponds to neat IBP
TBR
IBP
1800 1700 1600 1500 1400 1300 1200 1100 1000 900 800 700 600 500 400
0.06
0.04
0.02
0
-0.02
-0.04
-0.06
-0.08
-0.1
1545
1487
1454.5
1221
1141
1296
889
732.5
751
762
680
614.5
507.5
454.5
1592.5
1661
1546.5
1487
1456.5
1683.5
1424.5
1370
1295.5
1222.5
1174
1141
1072.5
861.5
889
941.5
784.5
762.5
751
732.5
680
614.5
507
455.5
419
1508
1465.5
1419
1382
1365
1338.5
1320
1280.5
1700
1700
1281.5
1320.5
1338.5
1365
1382
1419
1465.5
1508
1229.5
1209
1184.5
1124
1208
1230.5
1124.5
1054.5
1021.5
1003.5
951
865.5
778.5
778.5
1054.5
1021
1003
951
865.5
693
656
637.5
591
524.5
477
429
428.5
476.5
524
590.5
637.5
656.5
692.5

Figure S10

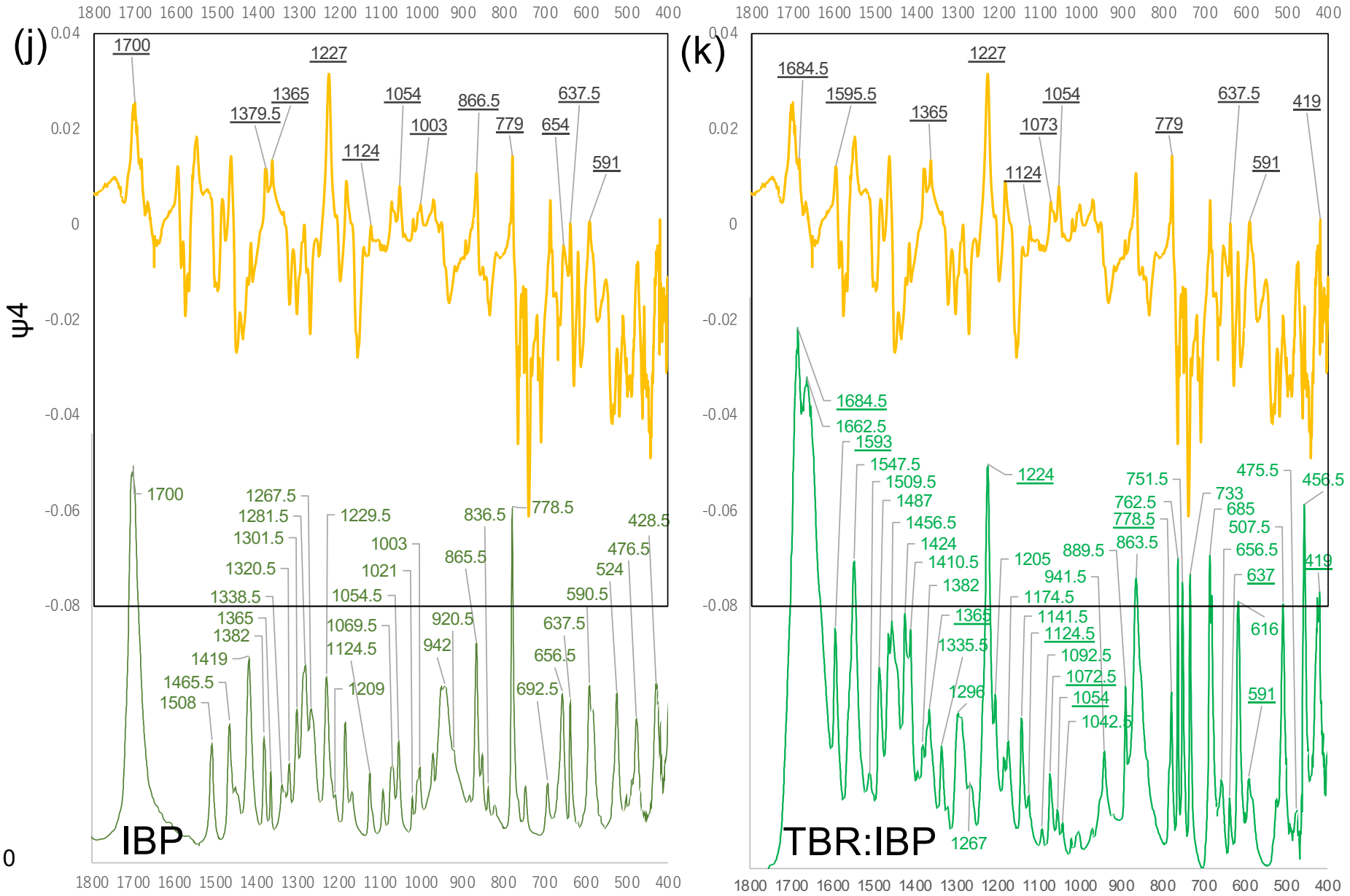
(j)
(k)
ψ4
IBP
TBR:IBP
1800 1700 1600 1500 1400 1300 1200 1100 1000 900 800 700 600 500 400
0.04
0.02
0
-0.02
-0.04
-0.06
-0.08
1700
1227
1365
1379.5
1054
1003
866.5
779
654
637.5
1124
591
1267.5
1281.5
1301.5
1320.5
1338.5
1365
1382
1419
1465.5
1508
1229.5
1003
1021
1054.5
1069.5
1124.5
1209
836.5
865.5
920.5
942
778.5
692.5
656.5
637.5
590.5
524
476.5
428.5
1684.5
1595.5
1365
1227
1124
1073
1054
779
637.5
591
419
1684.5
1662.5
1593
1547.5
1509.5
1487
1456.5
1424
1410.5
1382
1365
1335.5
1296
1267
1224
1205
1174.5
1141.5
1124.5
1092.5
1072.5
1054
1042.5
941.5
889.5
863.5
778.5
762.5
751.5
733
685
656.5
637
616
591
507.5
475.5
456.5
419

Figure S10

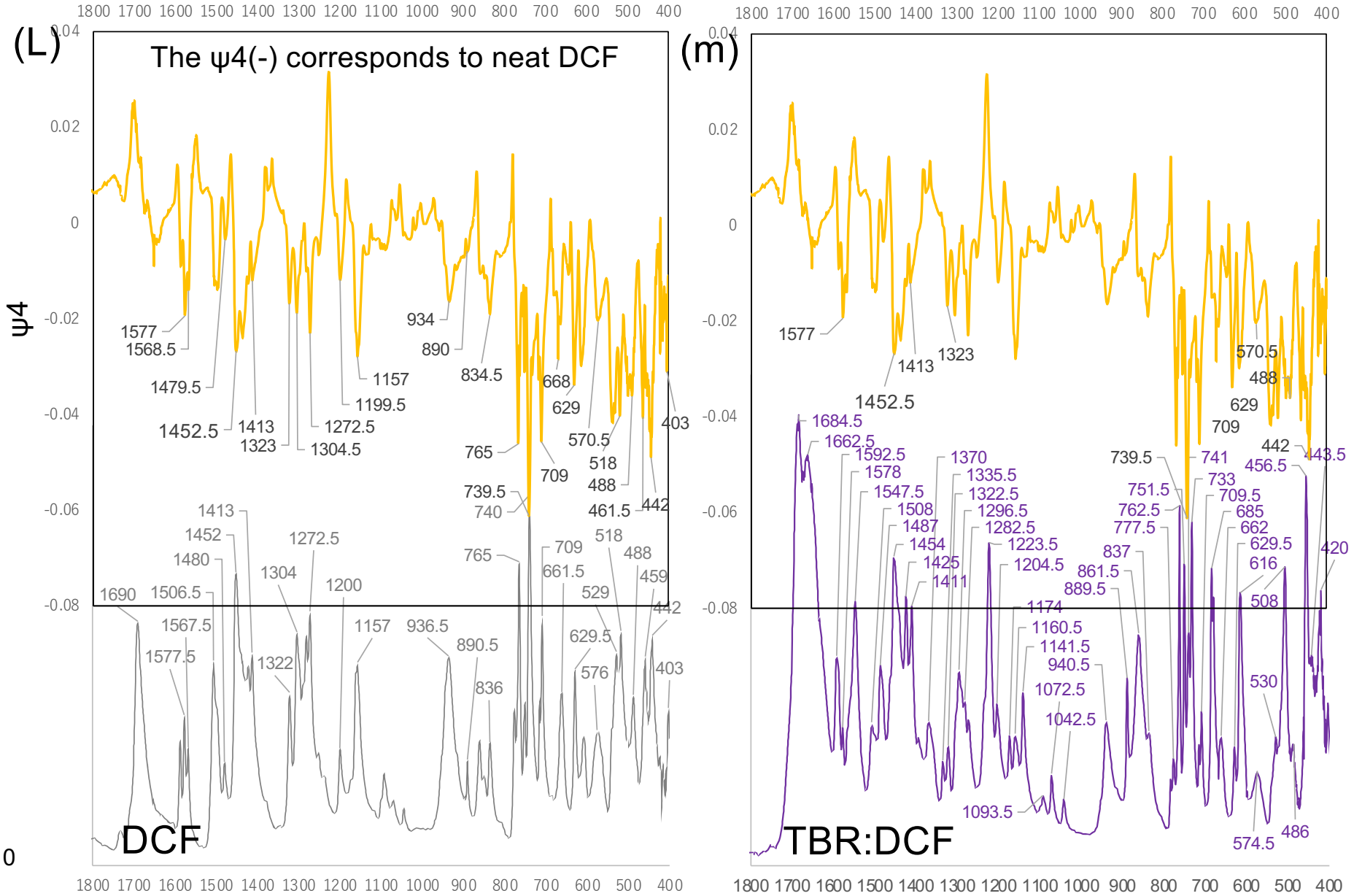
(L)
The ψ4(-) corresponds to neat DCF
ψ4
DCF
(m)
TBR:DCF
1800 1700 1600 1500 1400 1300 1200 1100 1000 900 800 700 600 500 400
0.04
0.02
0
-0.02
-0.04
-0.06
-0.08
1577
1568.5
1479.5
1452.5
1413
1323
1304.5
1272.5
1199.5
1157
934
890
834.5
765
739.5
740
709
668
629
570.5
518
488
461.5
442
403
1690
1506.5
1567.5
1577.5
1480
1452
1413
1322
1304
1272.5
1200
1157
936.5
890.5
836
765
709
661.5
629.5
576
529
518
488
459
442
403
1684.5
1662.5
1592.5
1578
1547.5
1508
1487
1454
1425
1411
1370
1335.5
1322.5
1296.5
1282.5
1223.5
1204.5
1174
1160.5
1141.5
1093.5
1072.5
1042.5
940.5
889.5
861.5
837
777.5
762.5
751.5
739.5
741
733
709.5
685
662
629.5
616
574.5
530
508
486
456.5
442
420

Figure S10

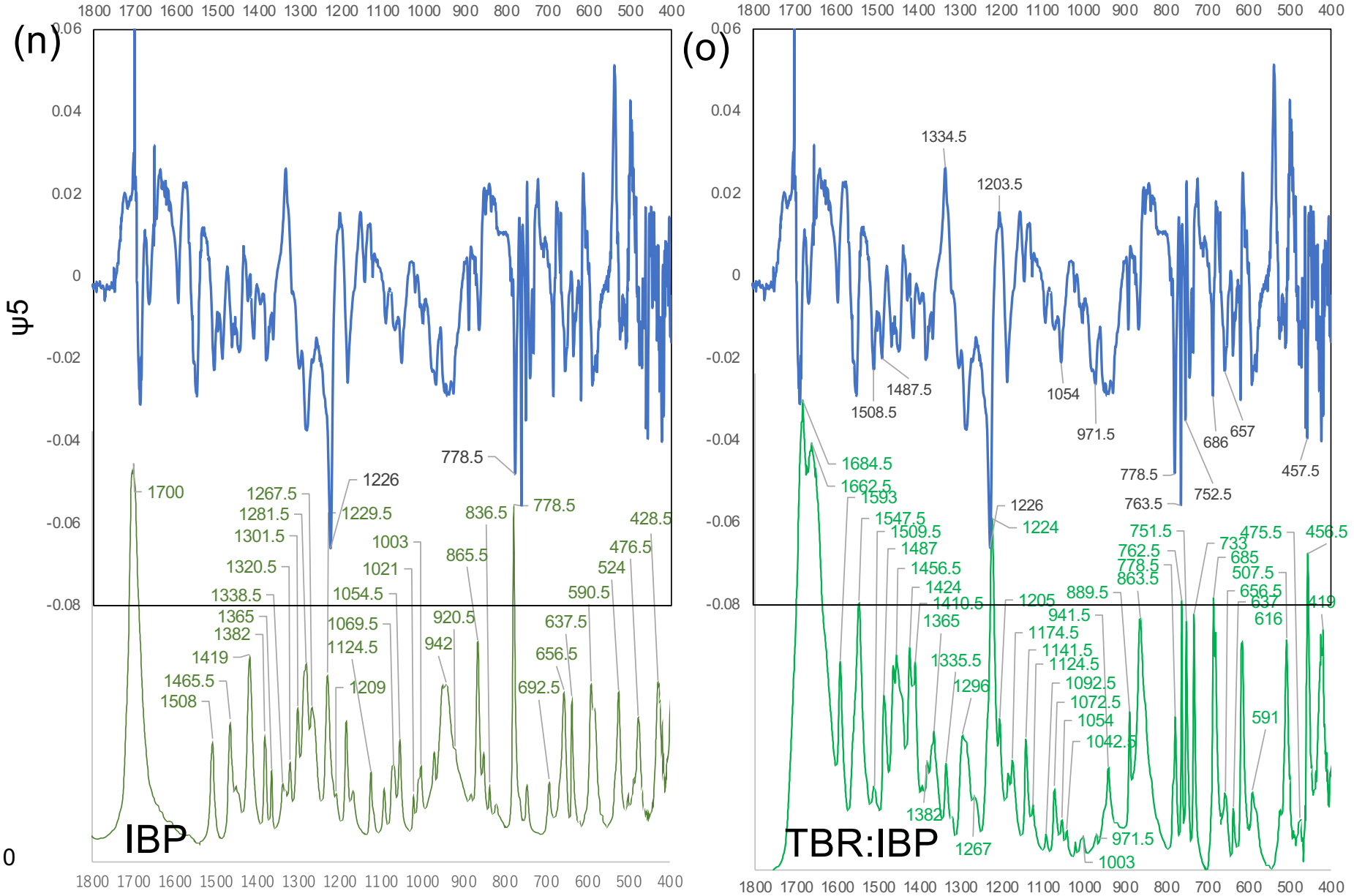
(n)
(o)
ψ5
IBP
TBR:IBP
1800 1700 1600 1500 1400 1300 1200 1100 1000 900 800 700 600 500 400
0.06
0.04
0.02
0
-0.02
-0.04
-0.06
-0.08
1700
1267.5
1281.5
1301.5
1320.5
1338.5
1365
1382
1419
1465.5
1508
1226
1229.5
1003
1021
1054.5
1069.5
1124.5
1209
778.5
836.5
865.5
920.5
942
692.5
656.5
637.5
590.5
524
476.5
428.5
1334.5
1203.5
1508.5
1487.5
1054
971.5
778.5
763.5
686
657
752.5
457.5
1684.5
1662.5
1593
1547.5
1509.5
1487
1456.5
1424
1410.5
1365
1335.5
1296
1382
1267
1226
1224
1205
889.5
941.5
1174.5
1141.5
1124.5
1092.5
1072.5
1054
1042.5
971.5
1003
751.5
762.5
778.5
863.5
733
685
507.5
656.5
637
616
475.5
456.5
419
591

Figure S10

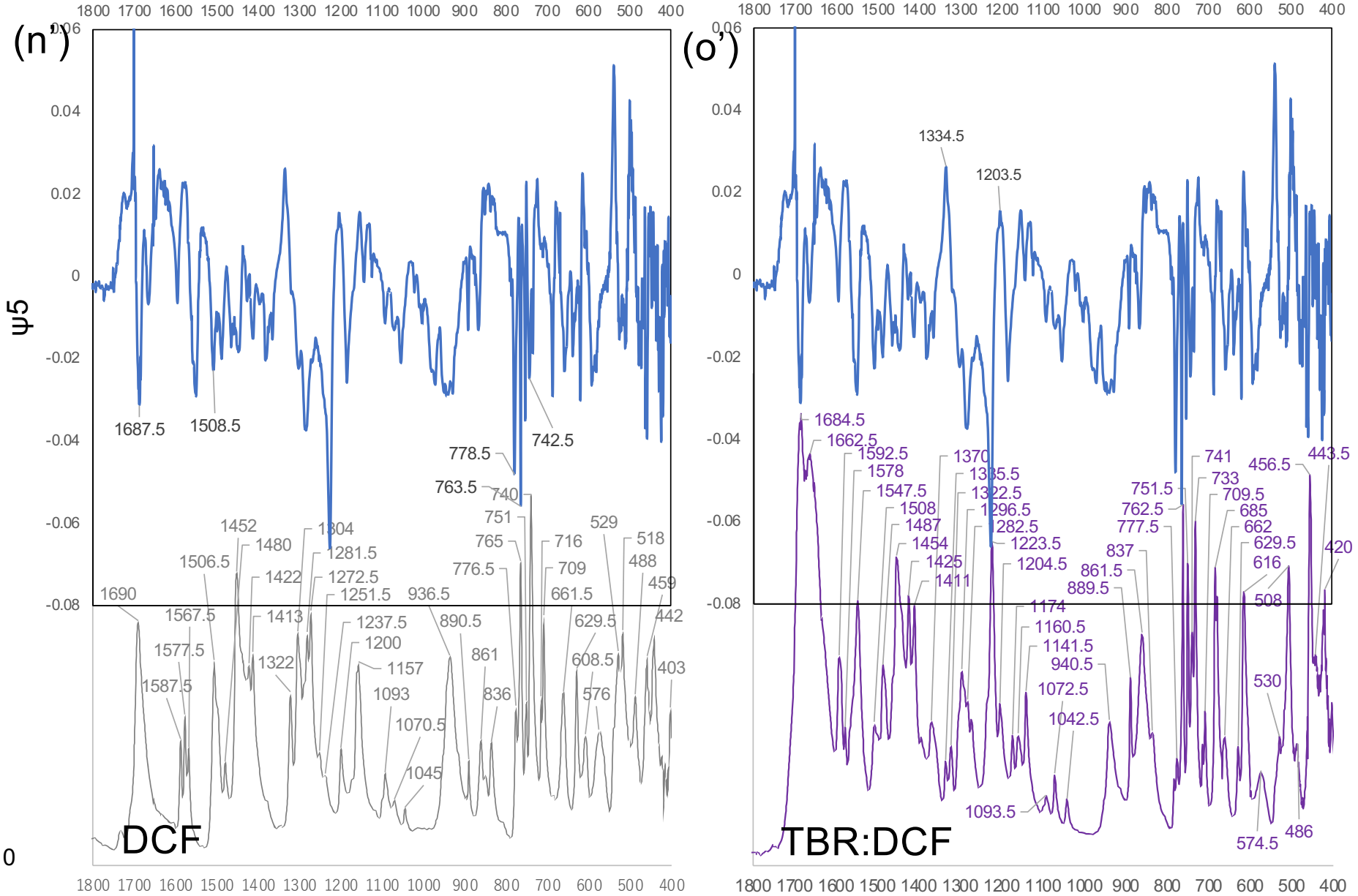
(n')
(o')
ψ5
DCF
TBR:DCF
1800 1700 1600 1500 1400 1300 1200 1100 1000 900 800 700 600 500 400
0.06
0.04
0.02
0
-0.02
-0.04
-0.06
-0.08
1687.5
1508.5
778.5
763.5
742.5
740
751
765
776.5
716
709
661.5
529
518
488
459
442
403
1690
1567.5
1577.5
1587.5
1506.5
1452
1480
1422
1413
1322
1304
1281.5
1272.5
1251.5
1237.5
1200
1157
1093
1070.5
1045
936.5
890.5
861
836
629.5
608.5
576
1334.5
1203.5
1684.5
1662.5
1592.5
1578
1547.5
1508
1487
1454
1425
1411
1370
1335.5
1322.5
1296.5
1282.5
1223.5
1204.5
1174
1160.5
1141.5
940.5
1072.5
1042.5
1093.5
889.5
861.5
837
777.5
762.5
751.5
741
733
709.5
685
662
629.5
616
508
530
574.5
486
456.5
443.5
420

Figure S10

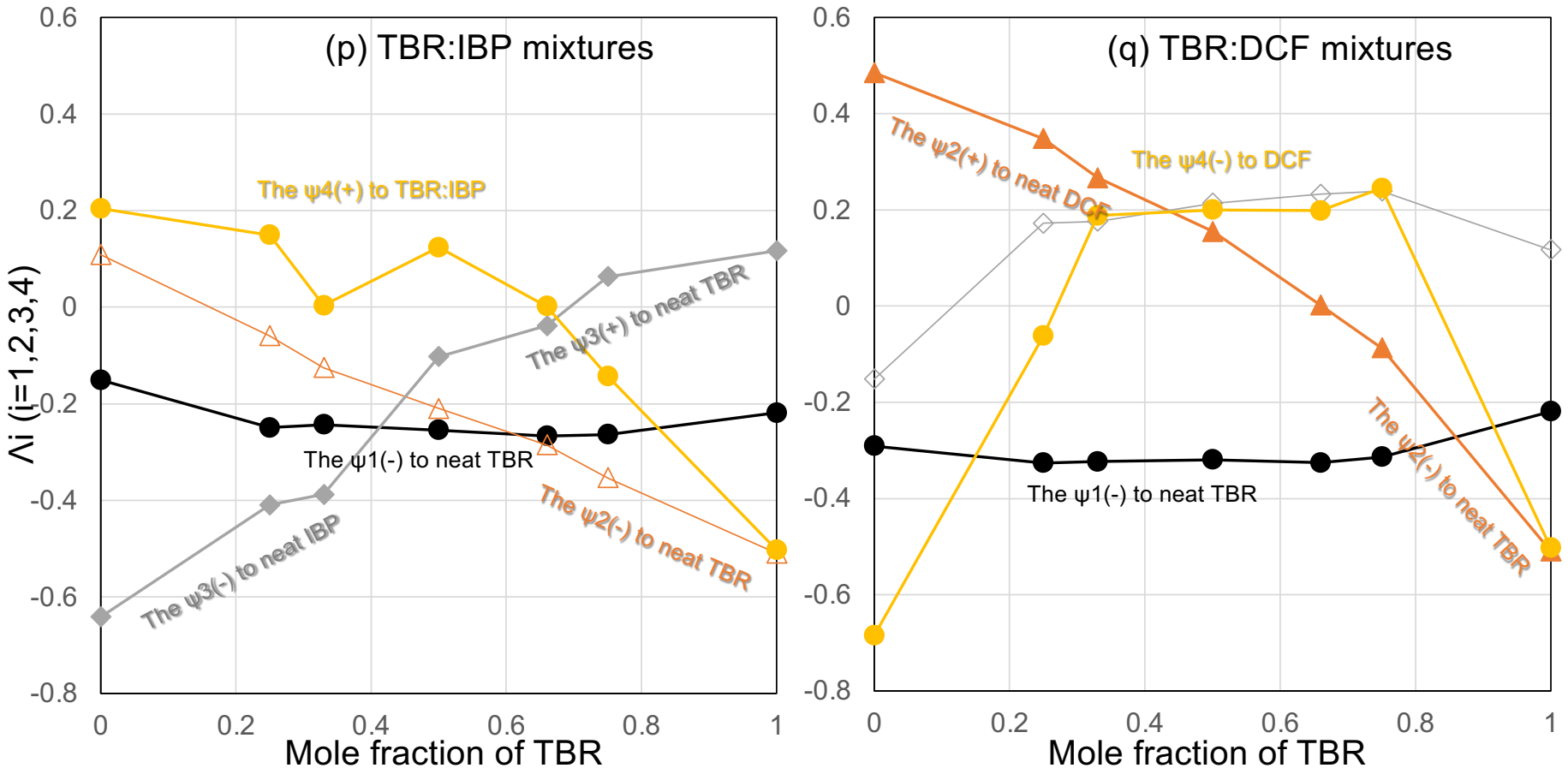

Figure S10 (p and q). The components of the first to fifth singular vectors as a function of mole fraction of TBR. The λ1, λ2, λ3, and λ4 were represented by closed black circles, orange triangles, gray diamonds, and yellow circles. The ψ5 was not assigned to any spectra, as shown in Figure S12 (n-o'). For λ2, λ3, and λ4, closed and open symbols corresponded to the composition with the basis functions correlated to which the IBP or DCF mixtures, respectively.

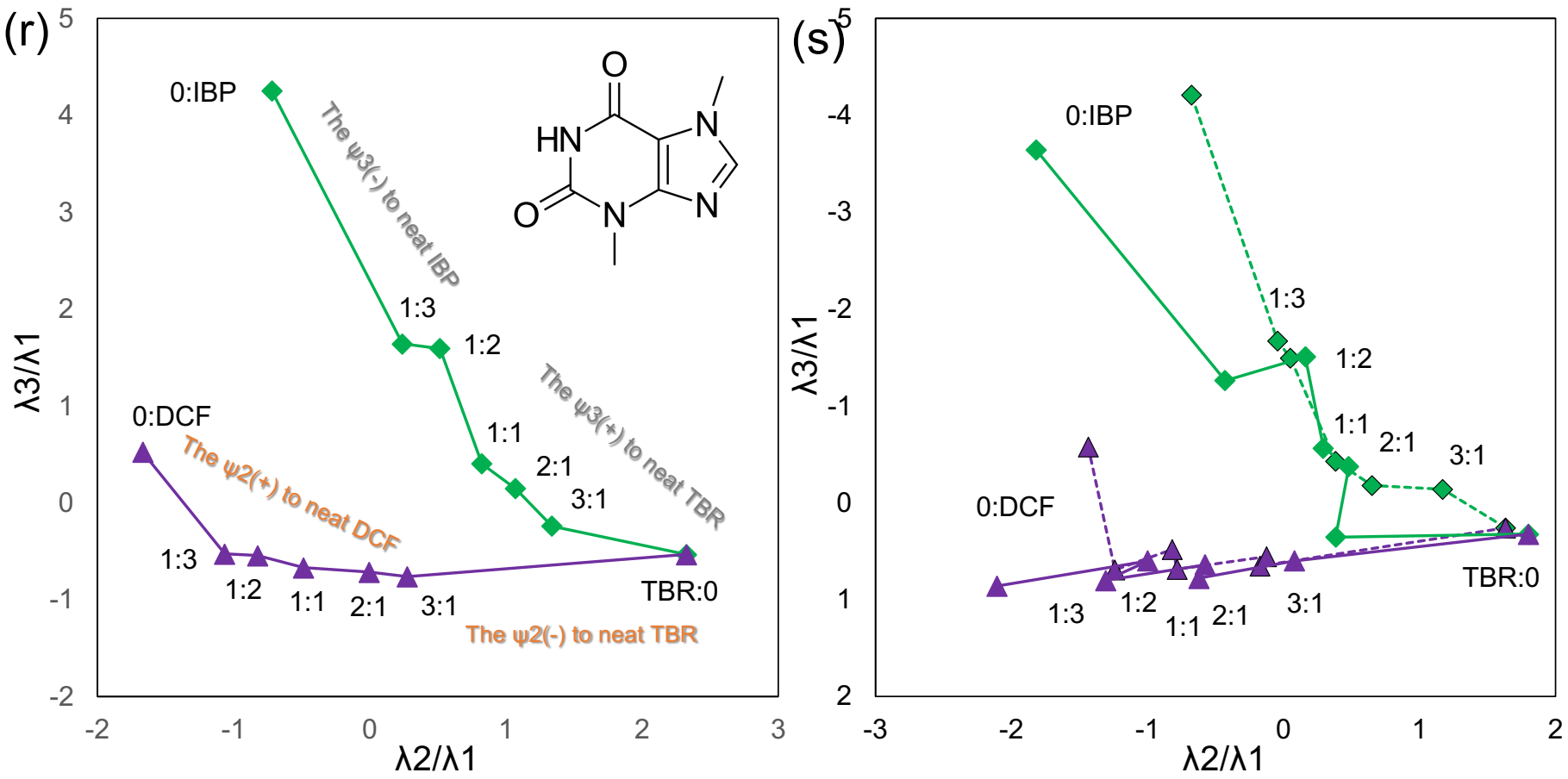

Figure S10 (r and s). The trajectories of the TBR/IBP (green diamonds) and TBR/DCF (violet triangles) mixtures. They shared the neat TBR's vector (TBR:0). The molar ratios were represented along the corresponding plots. The trajectory of the TBR/DCF mixtures traced along the (λ2/λ1)-axis (DCF owning dominance in the SVD analysis), whereas that of the TBR/IBP mixtures pursued in proportion to the diagonal line, suggesting the dependence between the trajectories of the TBR/IBP and TBR/DCF mixtures. The S13(r) and S13(s) show the trajectories of the average spectra and the individually measured spectra, respectively. For latter, the (λ2/λ1)-axis flip-flopped to adjust to the former diagram.

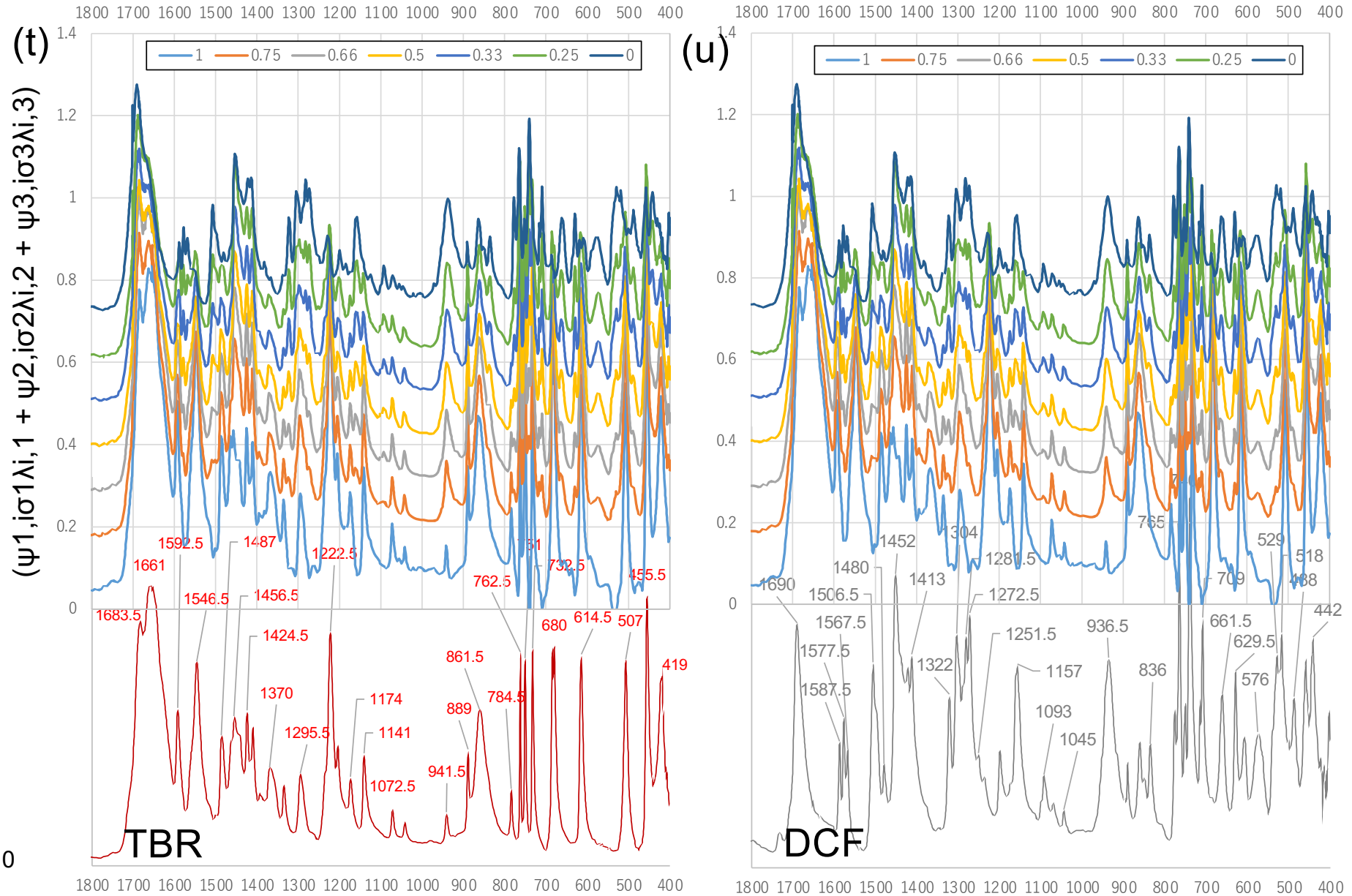
(t)
(ψ1,iσ1λi,1 + ψ2,iσ2λi,2 + ψ3,iσ3λi,3)
1 0.75 0.66 0.5 0.33 0.25 0
1683.5
1661
1592.5
1546.5
1487
1456.5
1424.5
1370
1295.5
1222.5
1174
1141
1072.5
941.5
889
861.5
784.5
762.5
680
614.5
507
455.5
419
TBR
(u)
1 0.75 0.66 0.5 0.33 0.25 0
1690
1506.5
1480
1452
1413
1322
1304
1281.5
1272.5
1251.5
1157
1093
1045
936.5
836
765
709
661.5
629.5
576
529
518
488
442
DCF

Figure S10

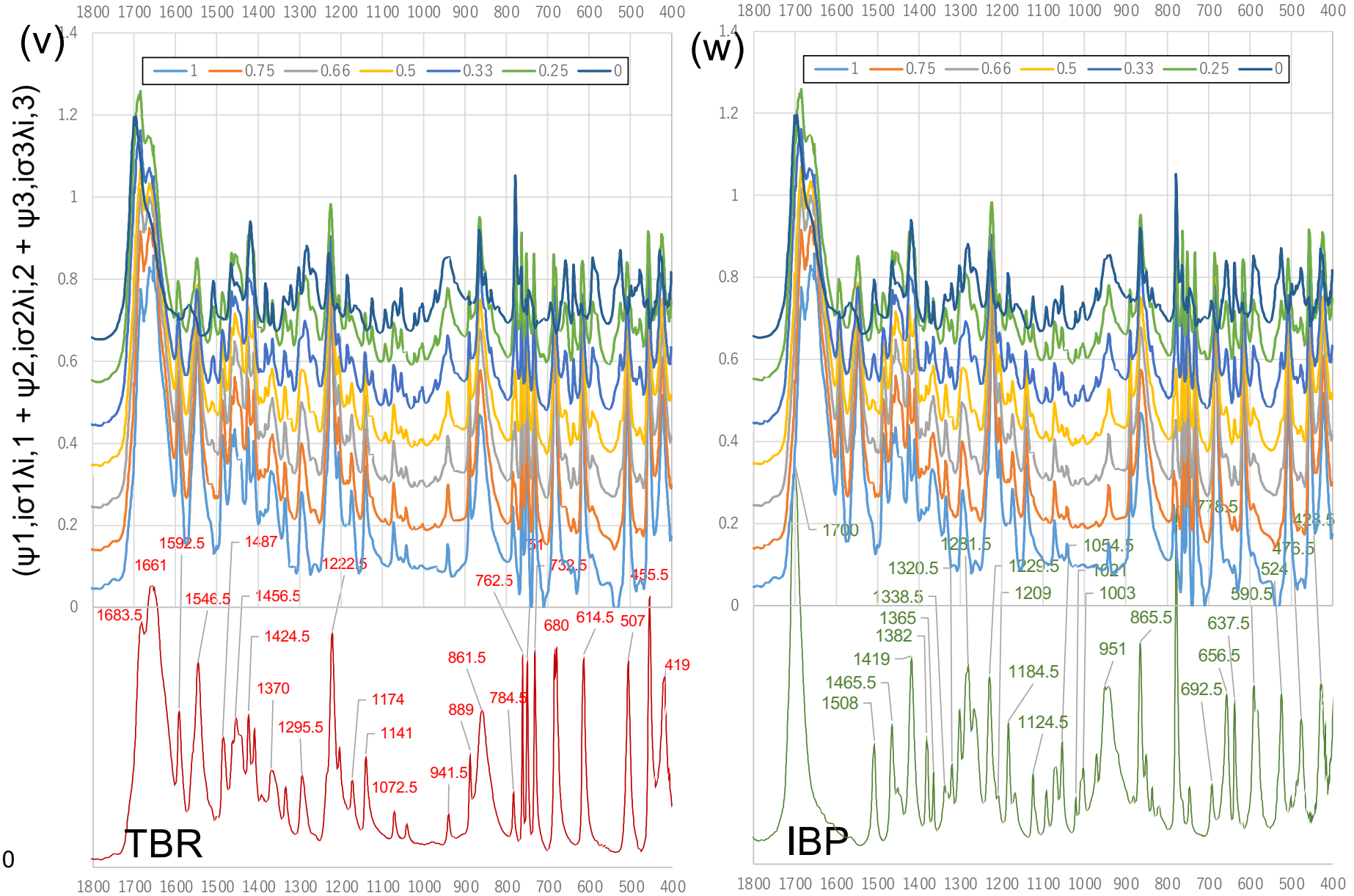
(v)
(ψ1,iσ1λi,1 + ψ2,iσ2λi,2 + ψ3,iσ3λi,3)
1 0.75 0.66 0.5 0.33 0.25 0
1683.5
1661
1592.5
1546.5
1487
1456.5
1424.5
1370
1295.5
1222.5
1174
1141
1072.5
941.5
889
861.5
784.5
762.5
732.5
680
614.5
507
455.5
419
TBR
(w)
1 0.75 0.66 0.5 0.33 0.25 0
1700
1508
1465.5
1419
1382
1365
1338.5
1320.5
1281.5
1229.5
1209
1184.5
1124.5
1054.5
1021
1003
951
865.5
778.5
692.5
656.5
637.5
590.5
524
476.5
428.5
IBP

Figure S10

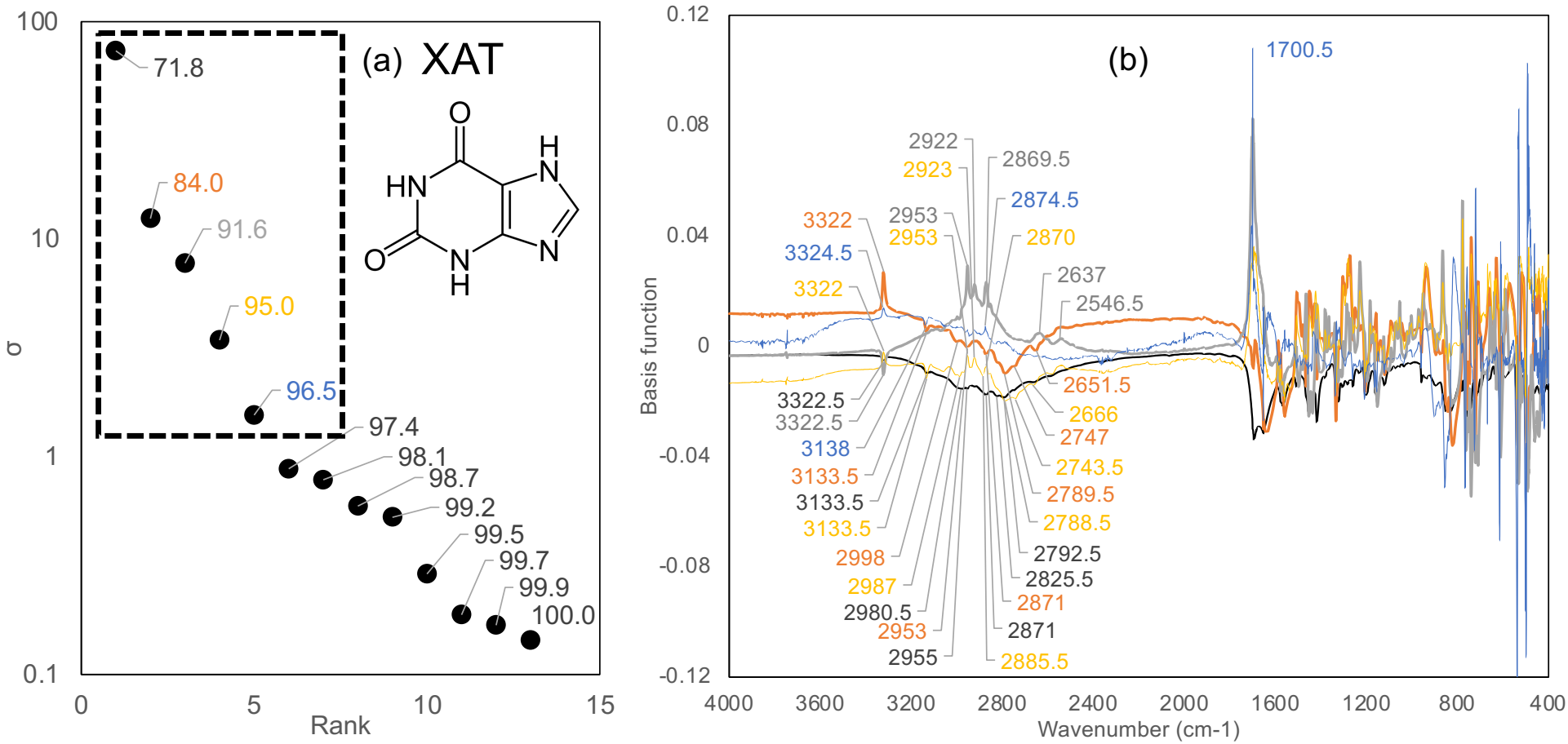

Figure S11. SVD computation for FTIR spectra of XAT/IBP and XAN/DCF mixtures provided singular values σi (a) and Basis spectra ψi(b). Cumulative proportions of σi were appended beside the σ plots, indicating that higher five σ's satisfied 97.6 percent of the variance. The basis spectra decomposed by the SVD computation corresponded to the components at the rank of 1 (black), 2 (orange), 3 (gray), 4 (yellow), and 5 (blue). Details of ψ's assignments to the observed spectra in the wavenumber range 1800-400 cm^{-1} are followed (e-o').

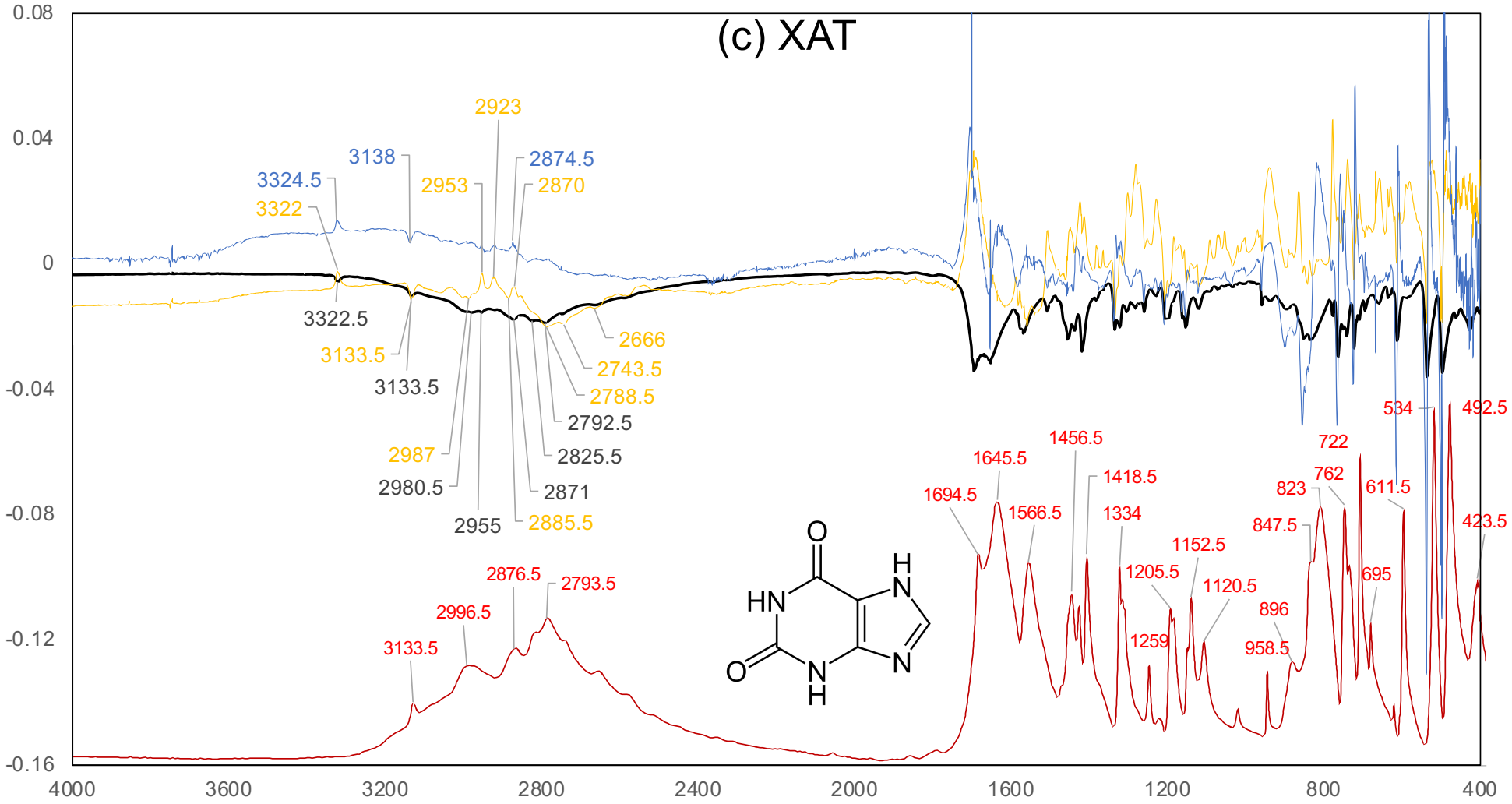

Figure S11. The basis spectra decomposed by the SVD computation corresponded to the components at the rank of 1 (black), 4 (yellow), and 5 (blue).

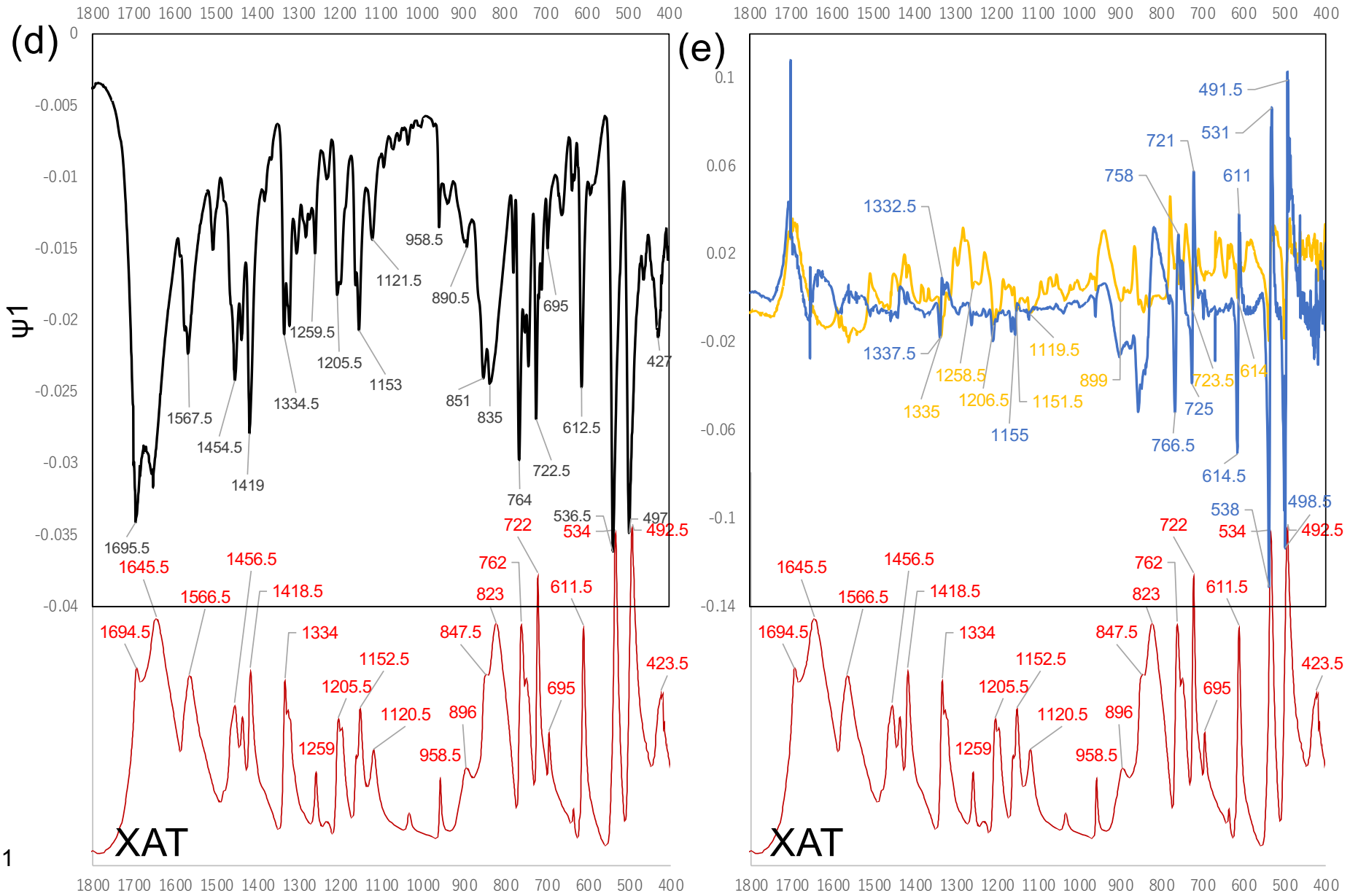
(d)
(e)
ψ1
XAT
XAT
1695.5
1645.5
1567.5
1566.5
1454.5
1456.5
1419
1418.5
1334.5
1334
1259.5
1205.5
1153
1152.5
1121.5
1120.5
958.5
1259
890.5
851
847.5
835
764
823
722
762
722.5
695
612.5
611.5
536.5
534
497
492.5
427
423.5
1694.5
1645.5
1566.5
1456.5
1418.5
1334
1152.5
1205.5
1120.5
1259
958.5
896
847.5
823
762
722
611.5
695
538
534
498.5
492.5
423.5
1332.5
1337.5
1335
1258.5
1206.5
1155
1151.5
1119.5
899
758
721
766.5
725
723.5
614.5
614
611
531
491.5

Figure S11

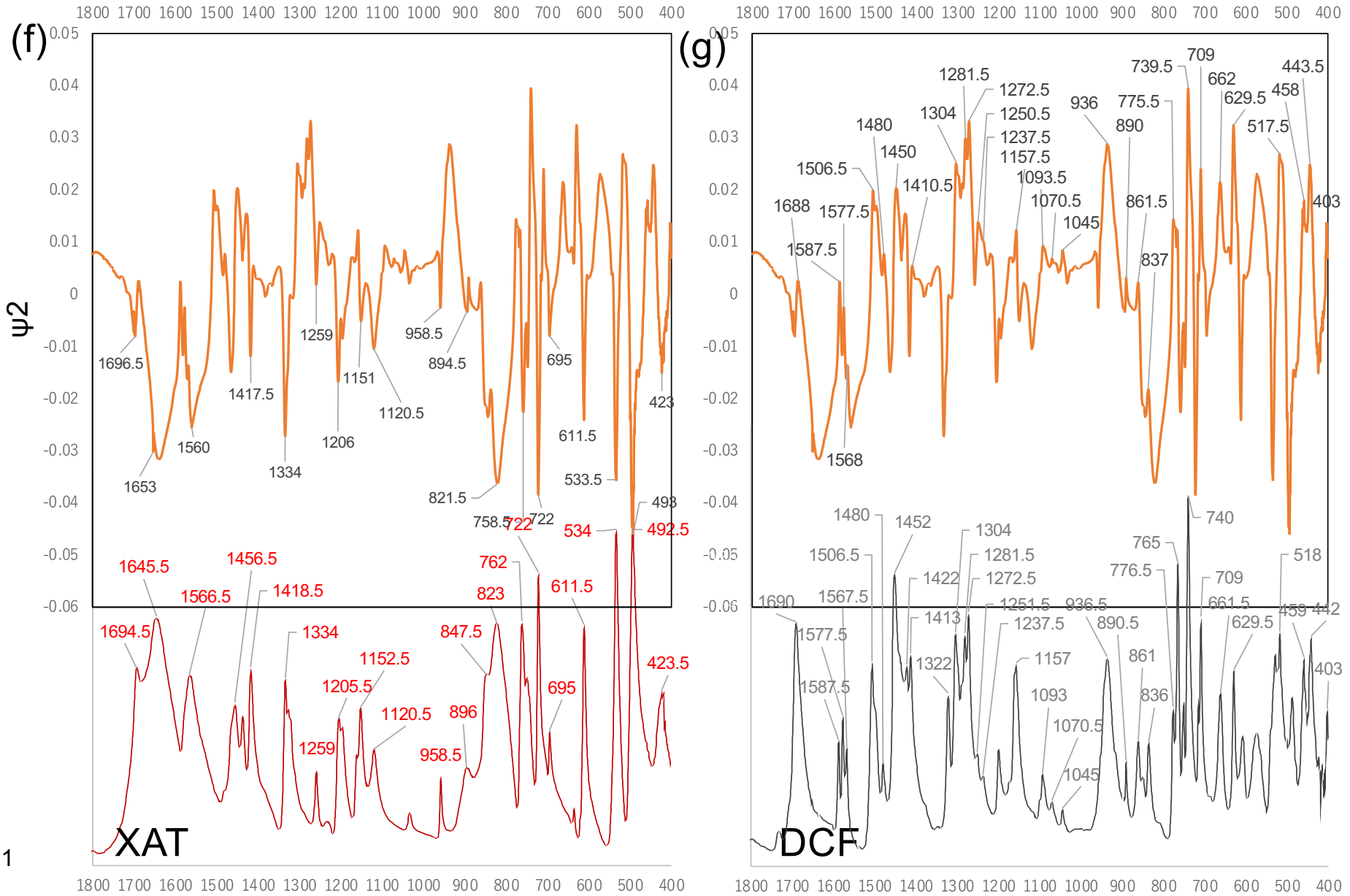
(f)
(g)
ψ2
XAT
DCF
1800 1700 1600 1500 1400 1300 1200 1100 1000 900 800 700 600 500 400
0.05 0.04 0.03 0.02 0.01 0 -0.01 -0.02 -0.03 -0.04 -0.05 -0.06
1696.5
1653
1560
1417.5
1334
1259
1206
1151
1120.5
958.5
894.5
821.5
758.5
722
695
611.5
533.5
493
492.5
534
423
1645.5
1566.5
1456.5
1418.5
1694.5
1334
1152.5
1205.5
1120.5
1259
958.5
896
847.5
823
762
611.5
695
423.5
1688
1587.5
1577.5
1568
1506.5
1480
1450
1410.5
1304
1281.5
1272.5
1250.5
1237.5
1157.5
1093.5
1070.5
1045
936
890
861.5
837
775.5
739.5
709
662
629.5
517.5
458
443.5
403
1690
1577.5
1587.5
1567.5
1506.5
1480
1452
1422
1413
1322
1304
1281.5
1272.5
1251.5
1237.5
1157
1093
1070.5
1045
936.5
890.5
861
836
765
776.5
740
709
661.5
629.5
518
459
442
403

Figure S11

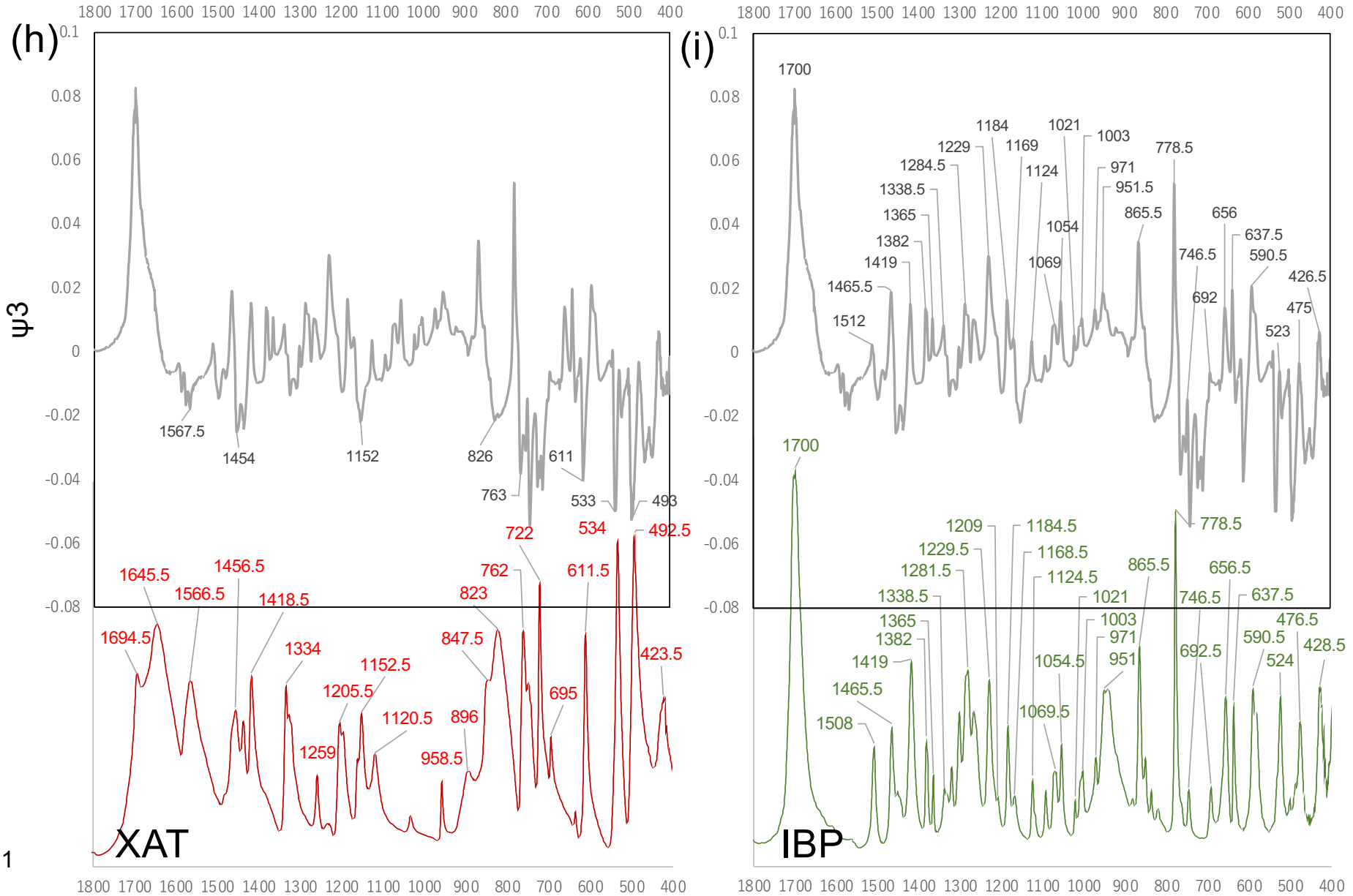
(h)
ψ3
XAT
1567.5
1454
1152
826
763
722
611
534
533
493
492.5
1645.5
1566.5
1456.5
1418.5
1694.5
1334
1152.5
1205.5
1120.5
1259
958.5
896
847.5
823
762
695
611.5
423.5
(i)
IBP
1700
1512
1465.5
1419
1382
1365
1338.5
1284.5
1229
1184
1169
1124
1069
1054
1021
1003
971
951.5
865.5
778.5
746.5
692
656
637.5
590.5
523
475
426.5
1700
1508
1465.5
1419
1382
1365
1338.5
1281.5
1229.5
1209
1184.5
1168.5
1124.5
1069.5
1054.5
1021
1003
971
951
865.5
778.5
746.5
692.5
656.5
637.5
590.5
524
476.5
428.5

Figure S11

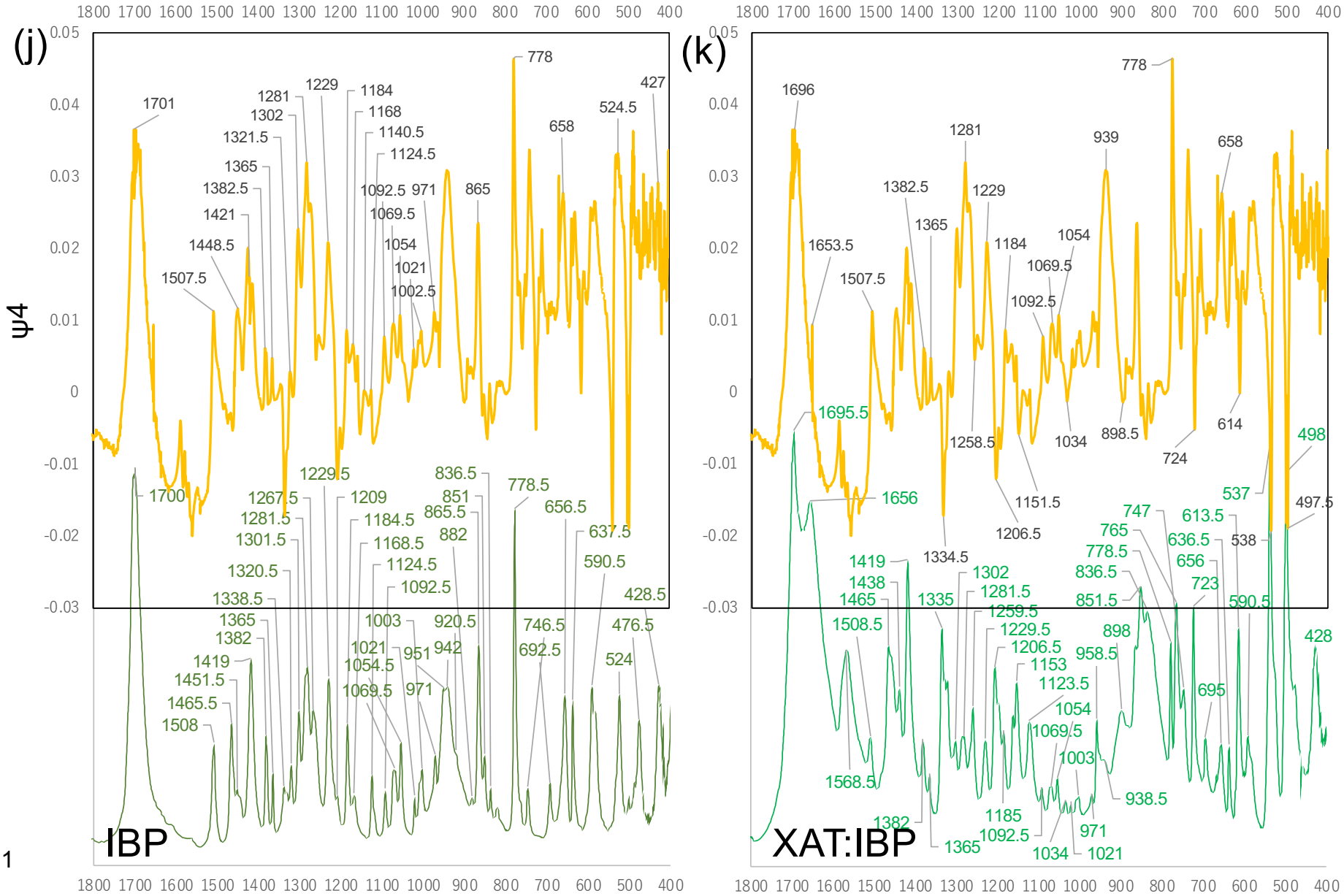
(j)
IBP
ψ4
1800 1700 1600 1500 1400 1300 1200 1100 1000 900 800 700 600 500 400
0.05
0.04
0.03
0.02
0.01
0
-0.01
-0.02
-0.03
1701
1281
1302
1321.5
1365
1382.5
1421
1448.5
1507.5
1229
1184
1168
1140.5
1124.5
1092.5
971
1069.5
1054
1021
1002.5
865
778
658
524.5
427
1700
1267.5
1281.5
1301.5
1320.5
1338.5
1365
1382
1419
1451.5
1465.5
1508
1229.5
1209
1184.5
1168.5
1124.5
1092.5
1003
1021
1054.5
1069.5
951
971
942
920.5
836.5
851
865.5
882
778.5
656.5
637.5
590.5
428.5
746.5
692.5
476.5
524
(k)
XAT:IBP
1696
1653.5
1507.5
1695.5
1656
1419
1438
1465
1508.5
1568.5
1382
1365
1334.5
1335
1302
1281
1259.5
1229.5
1206.5
1153
1123.5
1054
1069.5
1003
1034
1021
971
1185
1092.5
938.5
898
958.5
778
1281
1382.5
1229
1365
1184
1054
1069.5
1092.5
939
658
1258.5
1034
898.5
724
614
1151.5
1206.5
498
537
497.5
747
765
778.5
836.5
851.5
613.5
636.5
656
723
538
590.5
695
428

Figure S11

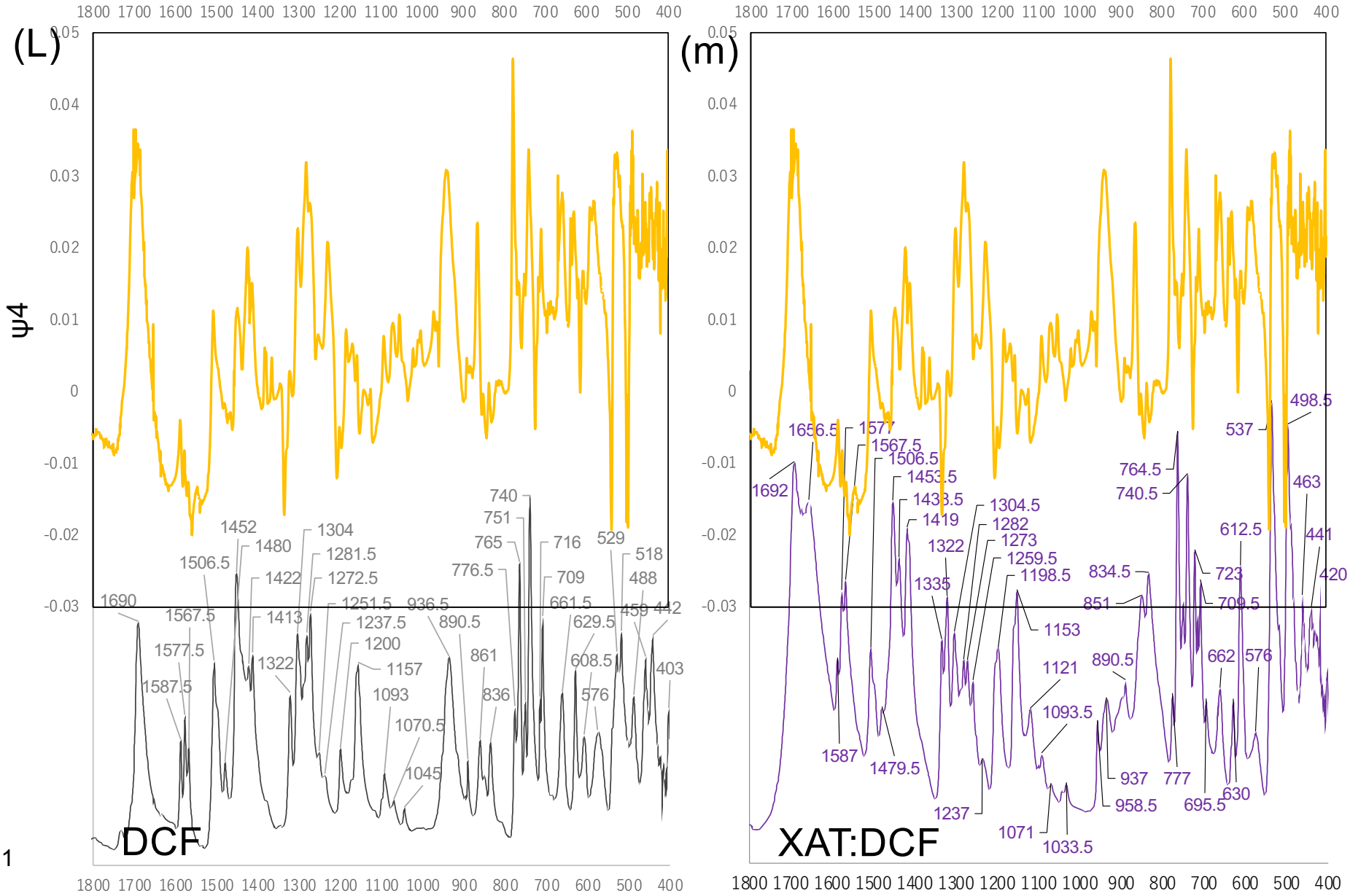
(L)
(m)
ψ4
DCF
XAT:DCF
1800 1700 1600 1500 1400 1300 1200 1100 1000 900 800 700 600 500 400
0.05
0.04
0.03
0.02
0.01
0
-0.01
-0.02
-0.03
1690
1567.5
1577.5
1587.5
1506.5
1452
1480
1422
1413
1322
1304
1281.5
1272.5
1251.5
1237.5
1200
1157
1093
1070.5
1045
936.5
890.5
861
836
740
751
765
776.5
716
709
661.5
629.5
608.5
576
529
518
488
459
442
403
1692
1656.5
1577
1567.5
1506.5
1453.5
1438.5
1419
1322
1335
1304.5
1282
1273
1259.5
1198.5
1153
1121
1093.5
1071
1033.5
1587
1479.5
1237
937
958.5
890.5
834.5
851
764.5
740.5
777
695.5
662
630
612.5
576
537
498.5
463
441
420
723
709.5

Figure S11

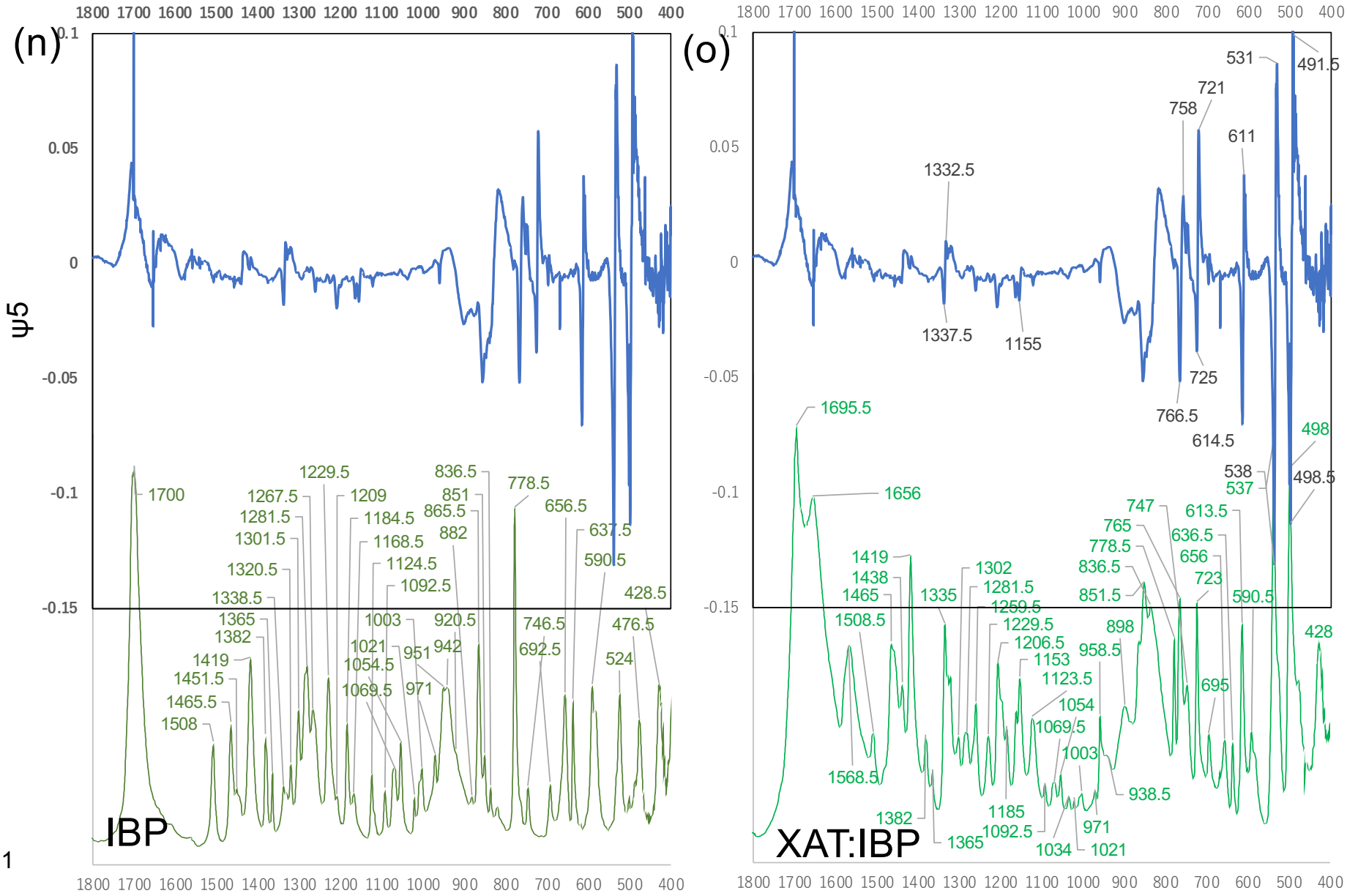
(n)
(o)
ψ5
IBP
XAT:IBP
1800 1700 1600 1500 1400 1300 1200 1100 1000 900 800 700 600 500 400
0.1
0.05
0
-0.05
-0.1
-0.15
1700
1695.5
1656
1568.5
1508.5
1508
1465.5
1465
1451.5
1438
1419
1382
1365
1338.5
1335
1320.5
1302
1301.5
1281.5
1281.5
1267.5
1259.5
1229.5
1229.5
1209
1206.5
1184.5
1168.5
1153
1124.5
1123.5
1092.5
1069.5
1054.5
1054
1034
1021
1003
1003
971
971
958.5
951
942
938.5
920.5
898
882
865.5
851.5
851
836.5
836.5
778.5
778.5
765
758
747
746.5
723
721
725
766.5
692.5
695
656.5
656
637.5
636.5
614.5
613.5
611
590.5
590.5
590.5
537
538
531
524
498.5
498
491.5
476.5
428.5
428
1332.5
1337.5
1155
1185
1092.5
1382
1365

Figure S11

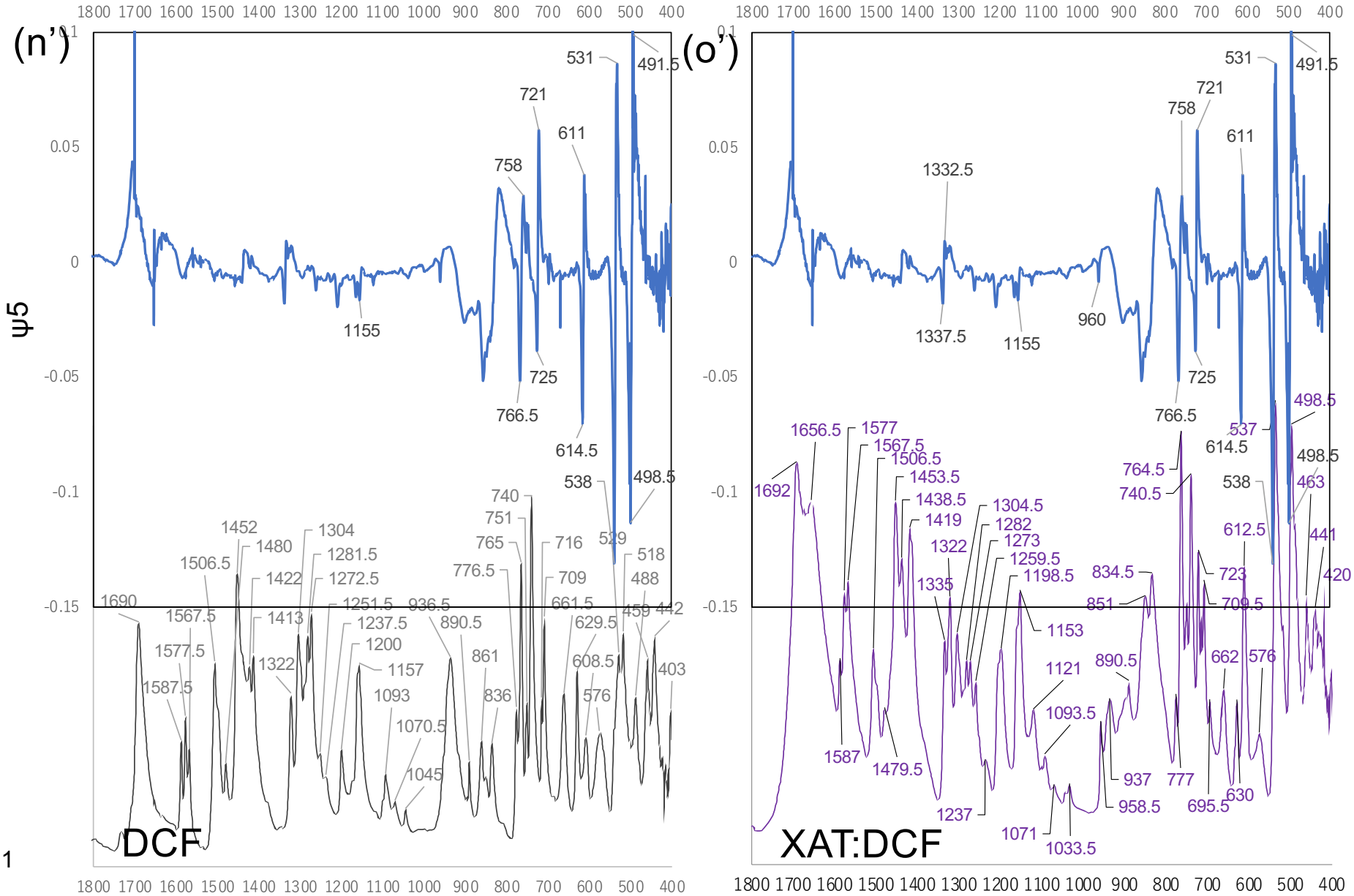
(n')
(o')
ψ5
DCF
XAT:DCF
1800 1700 1600 1500 1400 1300 1200 1100 1000 900 800 700 600 500 400
0.1
0.05
0
-0.05
-0.1
-0.15
531
491.5
721
611
758
1155
725
766.5
614.5
538
498.5
740
751
765
716
529
776.5
709
518
488
661.5
459
442
1452
1480
1304
1506.5
1281.5
1422
1272.5
1690
1567.5
1413
1251.5
936.5
1237.5
890.5
1200
1577.5
1322
1157
861
629.5
608.5
403
1587.5
1093
836
576
1070.5
1045
1332.5
1337.5
960
1656.5
1577
1567.5
1506.5
1453.5
1692
1438.5
1304.5
1419
1282
1322
1273
1259.5
1335
1198.5
834.5
723
851
709.5
1153
1121
890.5
662
576
1093.5
1587
1479.5
937
777
1237
958.5
695.5
630
1071
1033.5
764.5
740.5
537
498.5
463
612.5
441
420

Figure S11

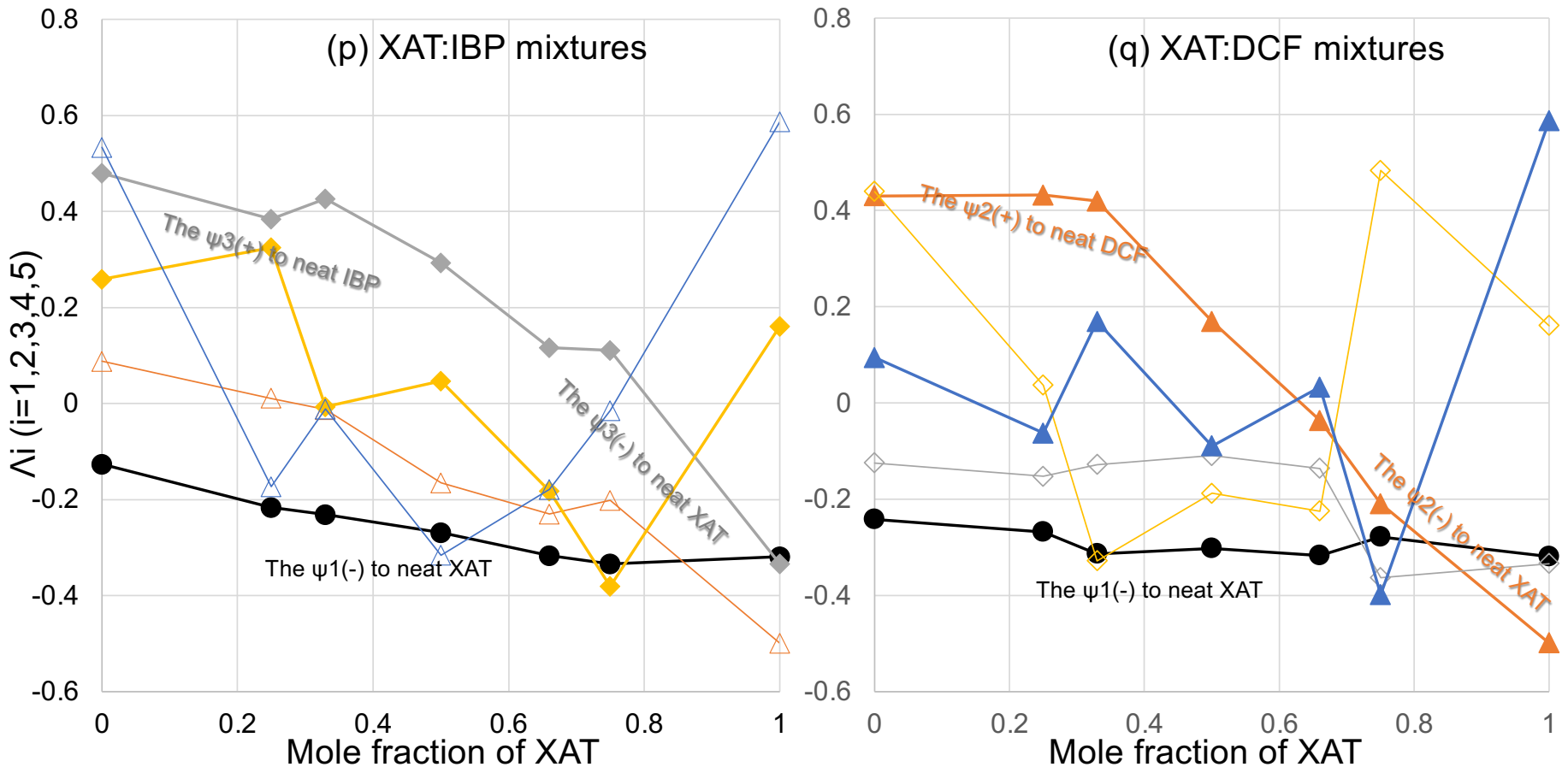

Figure S11 (p and q). The components of the first to fifth singular vectors as a function of mole fraction of XAT. The λ1, λ2, λ3, λ4, and λ5 were represented by closed black circles, orange triangles, gray diamonds, yellow diamonds, and blue triangles. For λ2, λ3, λ4, and λ5, closed and open symbols corresponded to the composition with the basis functions correlated to which the IBP or DCF mixtures, respectively.

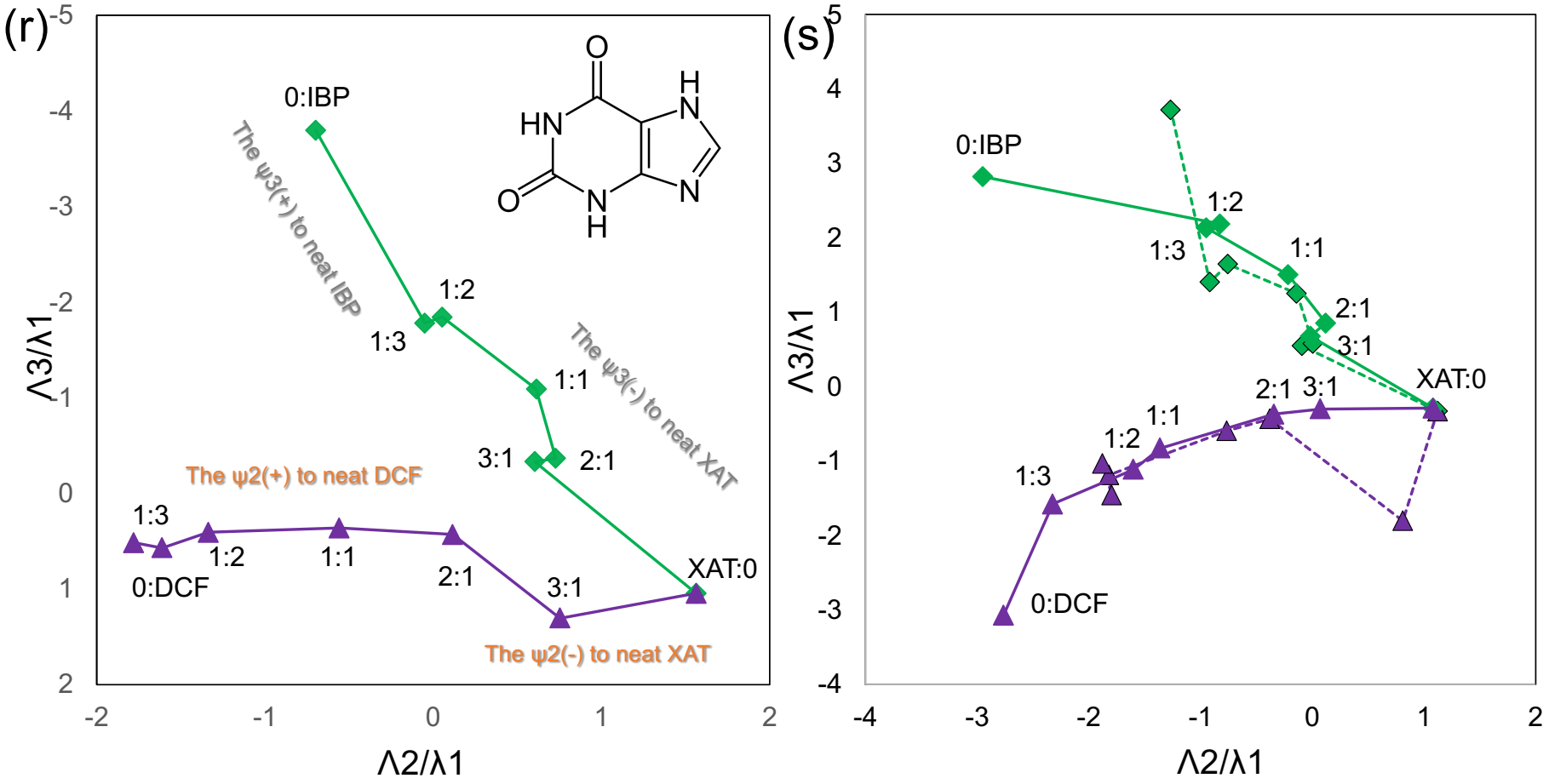

Figure S11 (r and s). The trajectories of the XAT/IBP (green diamonds) and XAT/DCF (violet triangles) mixtures, in which the (λ2/λ1)-axis flip-flopped. They shared the neat XAT's vector (XAT:0). The molar ratios were represented along the corresponding plots. The trajectory of the XAT/DCF mixtures traced along the (λ2/λ1)-axis (DCF owning dominance in the SVD analysis), whereas that of the XAT/IBP mixtures pursued in proportion to the diagonal line, suggesting the dependence between the trajectories of the XAT/IBP and XAT/DCF mixtures. The S13(r) and S13(s) show the trajectories of the average spectra and the individually measured spectra, respectively.

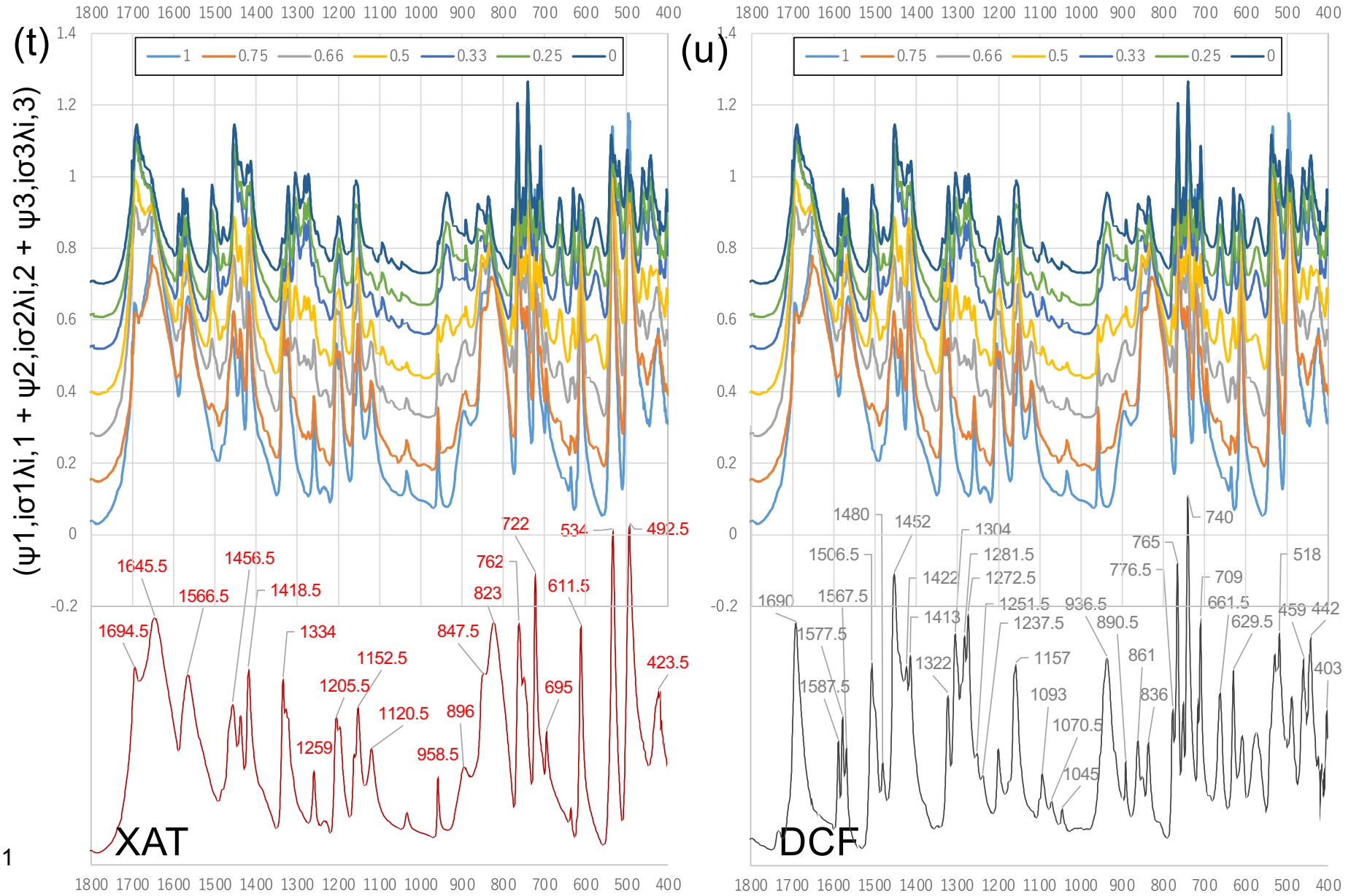
(t)
(u)
(ψ1,iσ1λi,1 + ψ2,iσ2λi,2 + ψ3,iσ3λi,3)
1 0.75 0.66 0.5 0.33 0.25 0
1800 1700 1600 1500 1400 1300 1200 1100 1000 900 800 700 600 500 400
1.4 1.2 1 0.8 0.6 0.4 0.2 0 -0.2
1645.5 1566.5 1456.5 1418.5 1694.5 1334 1152.5 1205.5 1120.5 1259 896 958.5 847.5 823 722 762 534 611.5 695 492.5 423.5
XAT
1480 1452 1304 1506.5 1281.5 1422 1272.5 1690 1567.5 1251.5 936.5 1413 1237.5 890.5 1577.5 1322 1157 861 1587.5 1093 836 1070.5 1045 740 765 776.5 709 518 661.5 629.5 459 442 403
DCF

Figure S11

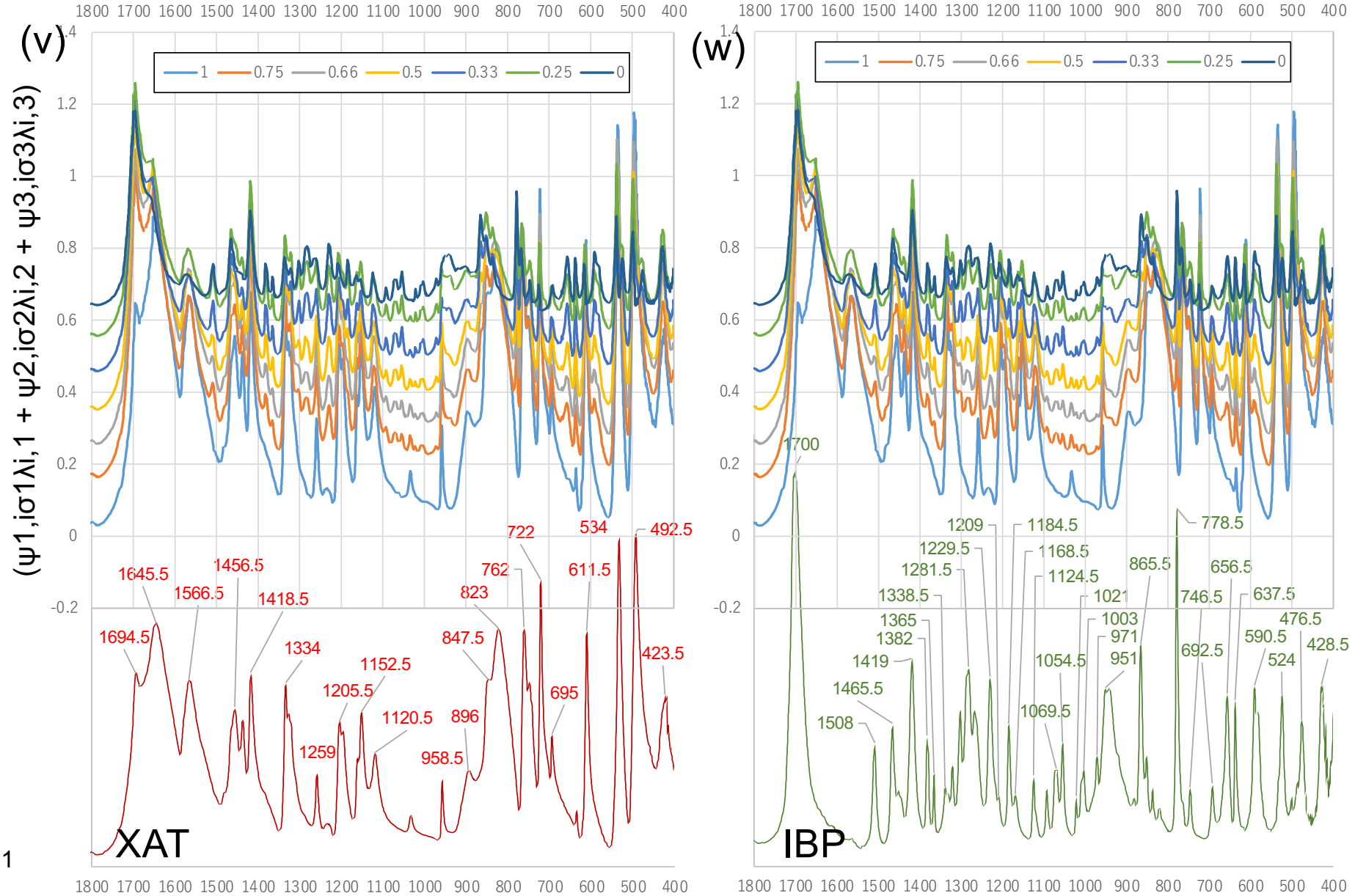
(v)
(w)
(ψ1,iσ1λi,1 + ψ2,iσ2λi,2 + ψ3,iσ3λi,3)
1 0.75 0.66 0.5 0.33 0.25 0
1800 1700 1600 1500 1400 1300 1200 1100 1000 900 800 700 600 500 400
1.4 1.2 1 0.8 0.6 0.4 0.2 0 -0.2
1645.5 1566.5 1456.5 1418.5 1694.5 1334 1152.5 1205.5 1120.5 1259 958.5 896 847.5 823 762 722 695 611.5 534 492.5 423.5
XAT
1700 1209 1229.5 1281.5 1338.5 1365 1382 1419 1465.5 1508 1184.5 1168.5 1124.5 1069.5 1054.5 1021 1003 971 951 865.5 778.5 746.5 692.5 656.5 637.5 590.5 524 476.5 428.5
IBP

Figure S11

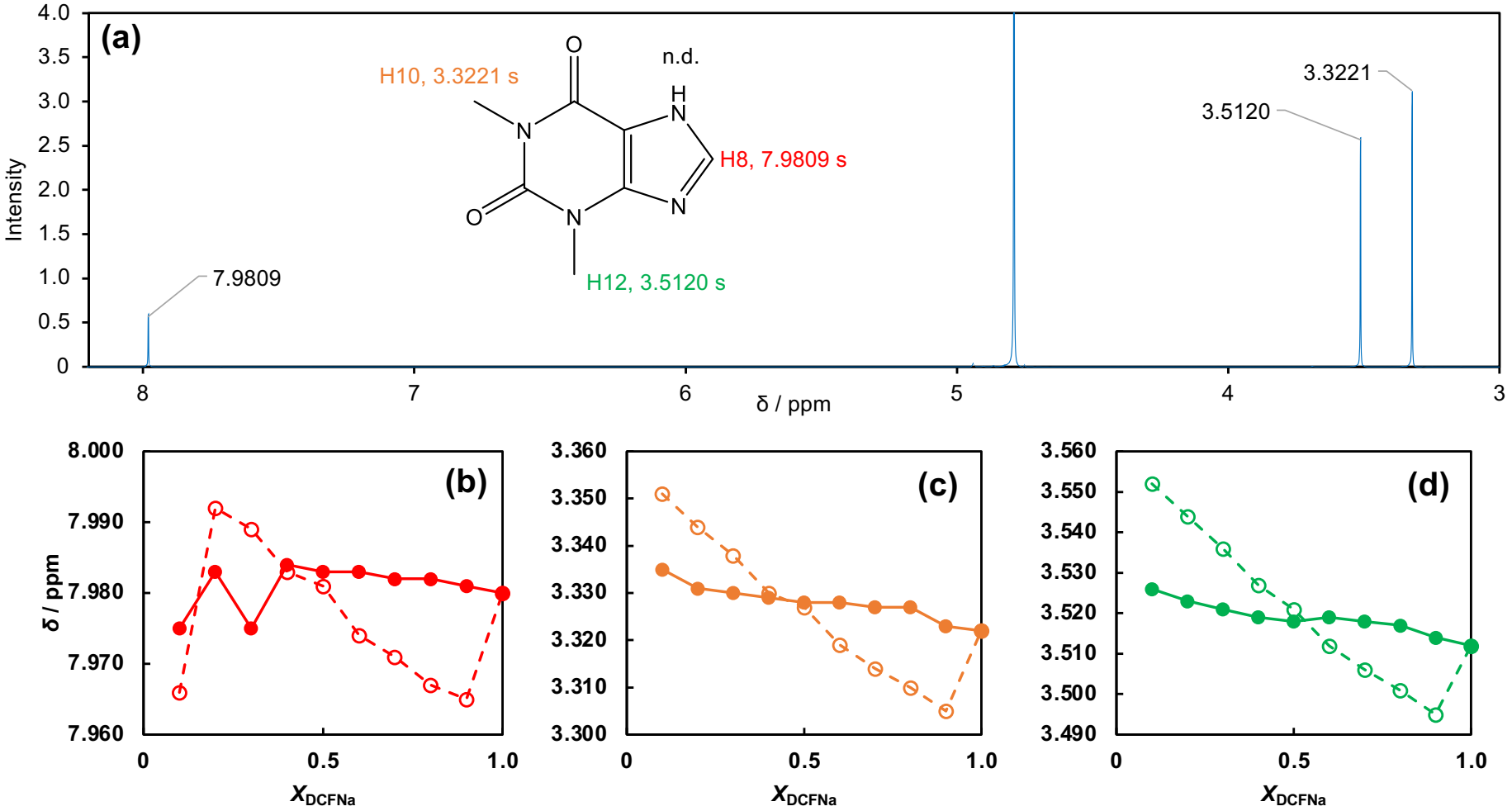

Figure S12. (a) Signal assignment for TPH on 400 MHz ^{1}H-NMR spectrum of 20 mM TPH in D_2O. The obtained chemical shifts in the various mole fractions of DCF sodium salt in the THP/DCF mixtures, for H8 (b), H10 (c), and H12 (d). The closed plots show the chemical shifts in the TPH/DCF mixtures, where the total amount of TPH and DCF sodium salt was adjusted to 20 mM. The open plots demonstrate those obtained by the measurement of TPH alone at the concentration corresponding to each mole fraction.

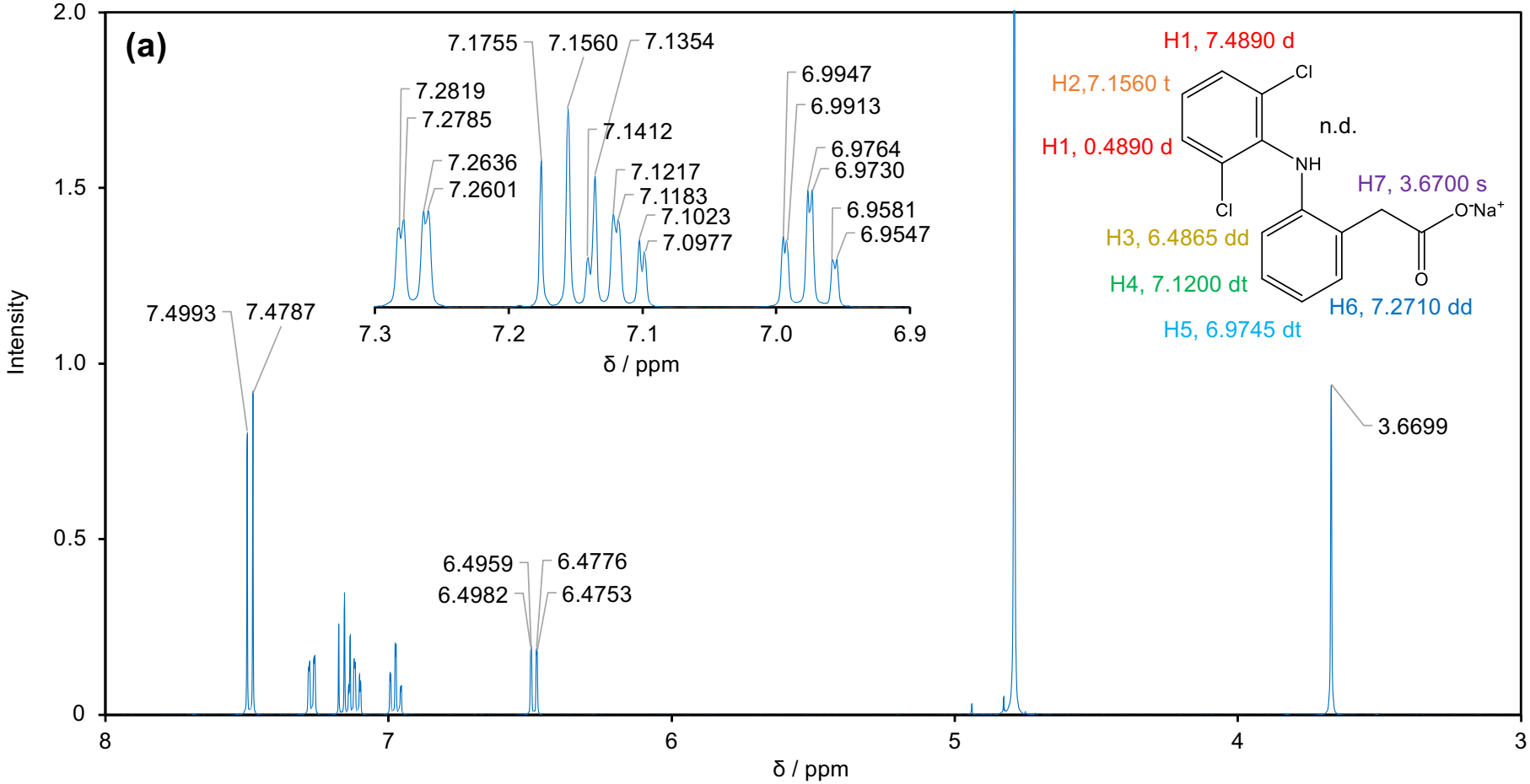

Figure S13. (a) Signal assignments for DCF sodium salt on 400 MHz ^{1}H-NMR spectrum of 20 mM DCF sodium salt in D_2O, assisted with the cross peaks in ^{1}H,^{1}H-COSY and NOESY experiments. As the 7.1560 ppm triplet signal (H1) partially overlapped with the 7.1200 double triplet signal (H4), signal details were deformed. The 7.4890 ppm doublet signal (H2) was coupled to the 7.1560 ppm triplet signal (H1) with the vicinal *J* value of 8.24 Hz. The vicinal *J* value between H3 and H4 was 8.24 Hz and that between H5 and H6 was observed as 7.32 Hz. The long-range *J* values between H3 and H5 and between H4 and H6 would be determined as 0.92 and 1.32 Hz, respectively.

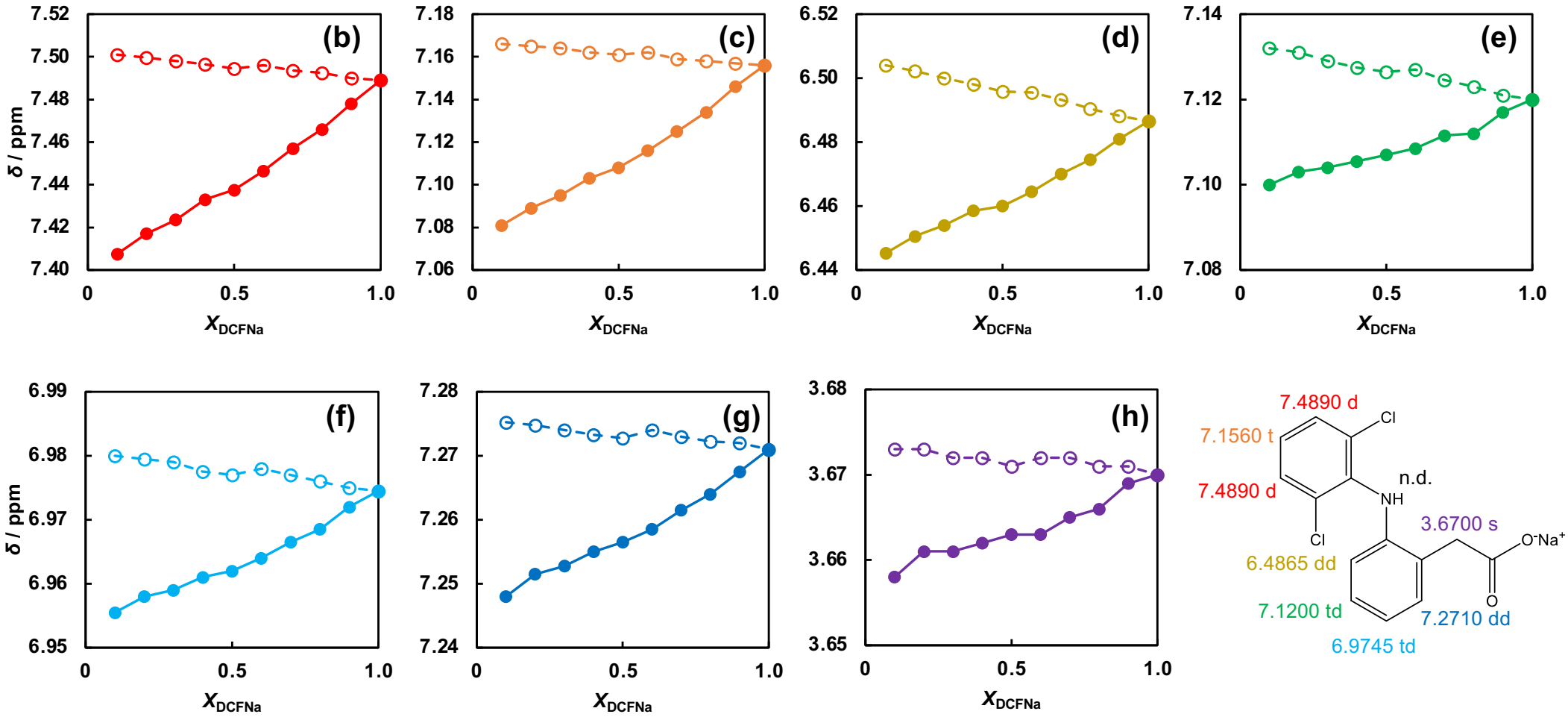

Figure S13. The obtained chemical shifts in the various mole fractions of DCF sodium salt in the THP/DCF mixtures, for H1 (b), H2 (c), H3 (d), H4 (e), H5 (f) H6 (g), and H7 (h). The closed plots show the chemical shifts in the TPH/DCF mixtures, where the total amount of TPH and DCF sodium salt was adjusted to 20 mM. The open plots demonstrate those obtained by the measurement of DCF sodium salt alone at the concentration corresponding to each mole fraction.

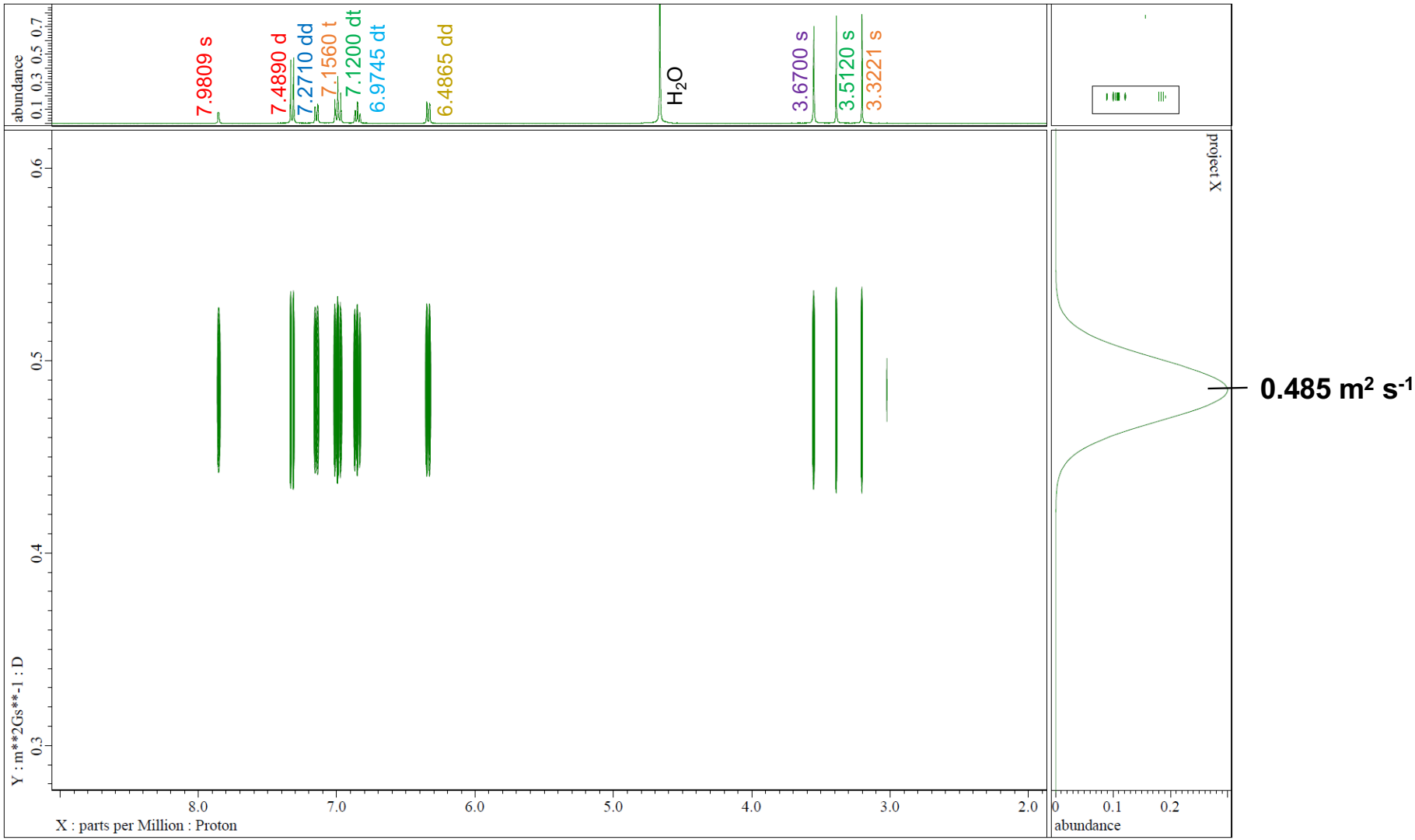

Figure S14. DOSY spectrum of the mixture containing 20 mM DCF sodium salt and 10 mM TPH in D_2O. The signals at 7.9809, 3.5120, and 3.3221 ppm were H8 and the N-Me hydrogens of TPH. The others were assigned to DCF, described in Figure S12(a). The D_{DOSY} value of 0.485 m^2 s^{-1} was observed as the property of the TPH/DCF complex formed in D_2O.

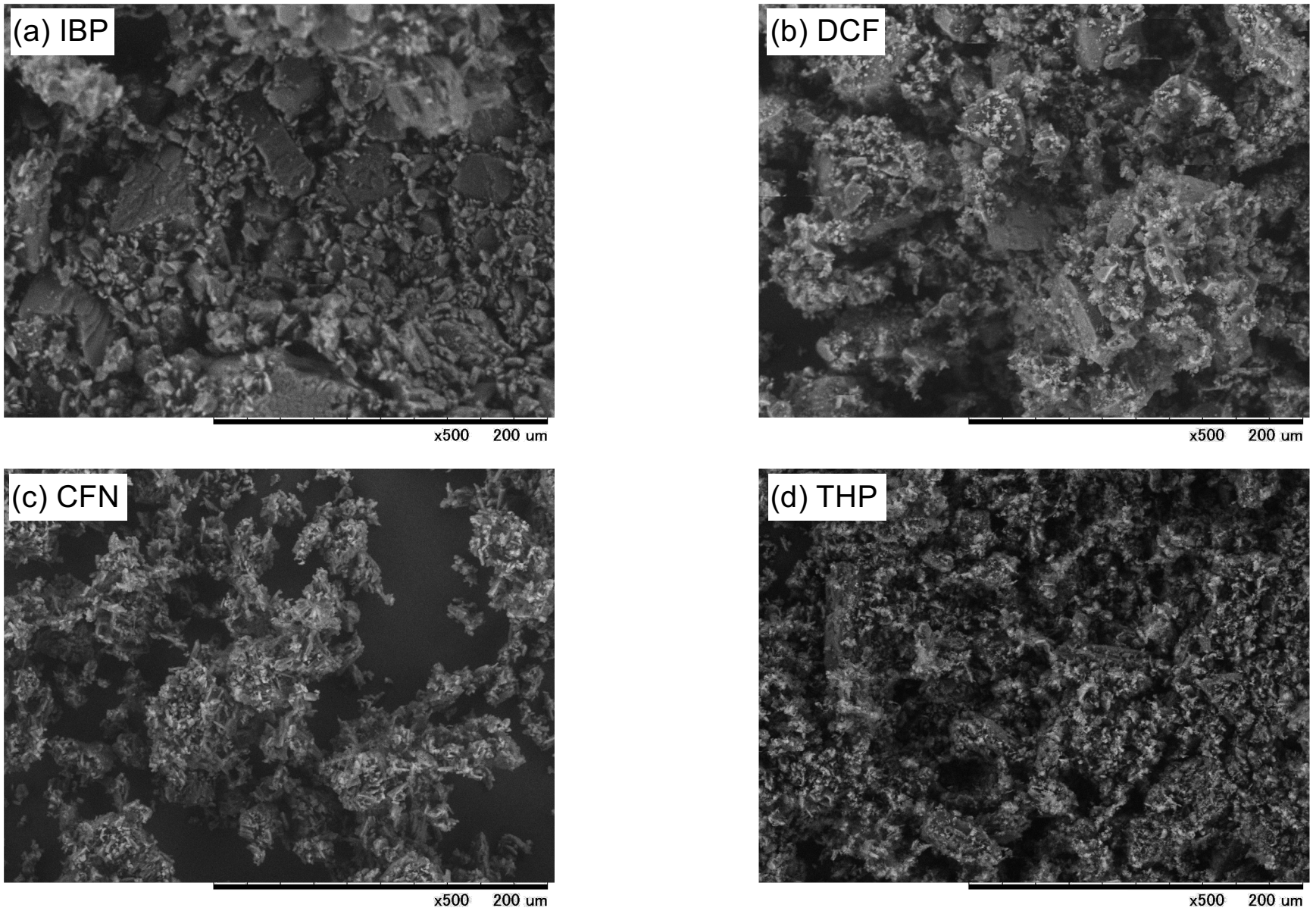
(a) IBP
x500 200 um
(b) DCF
x500 200 um
(c) CFN
x500 200 um
(d) THP
x500 200 um

Figure S15

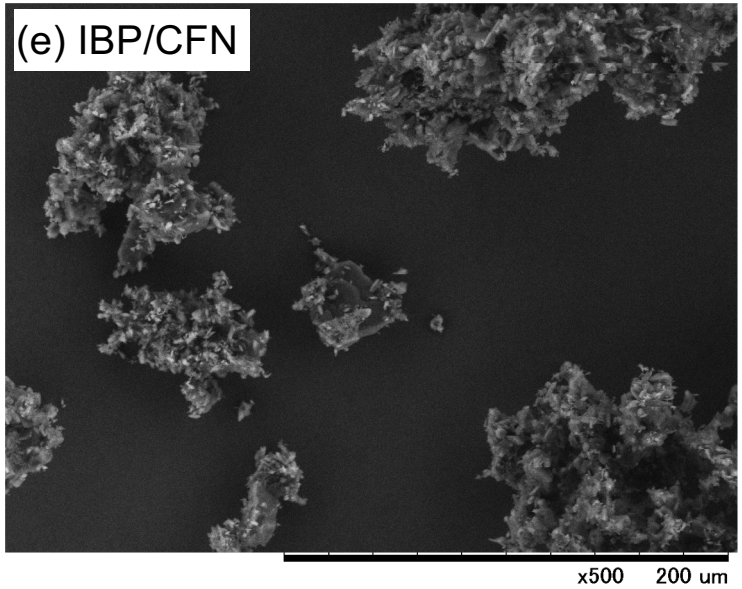
(e) IBP/CFN
x500 200 um

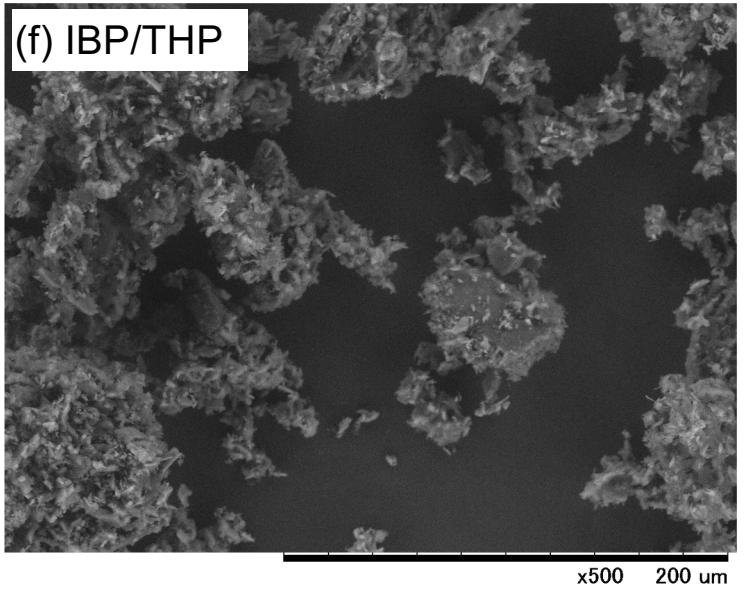
(f) IBP/THP
x500 200 um

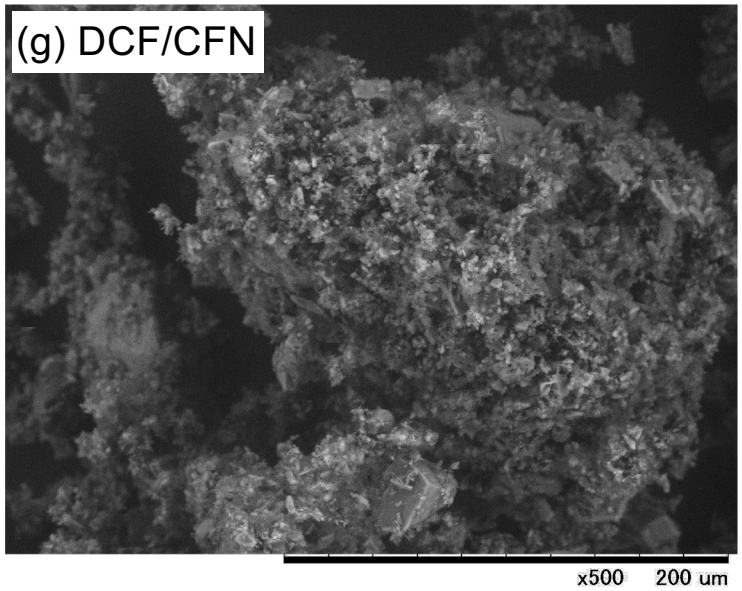
(g) DCF/CFN
x500 200 um

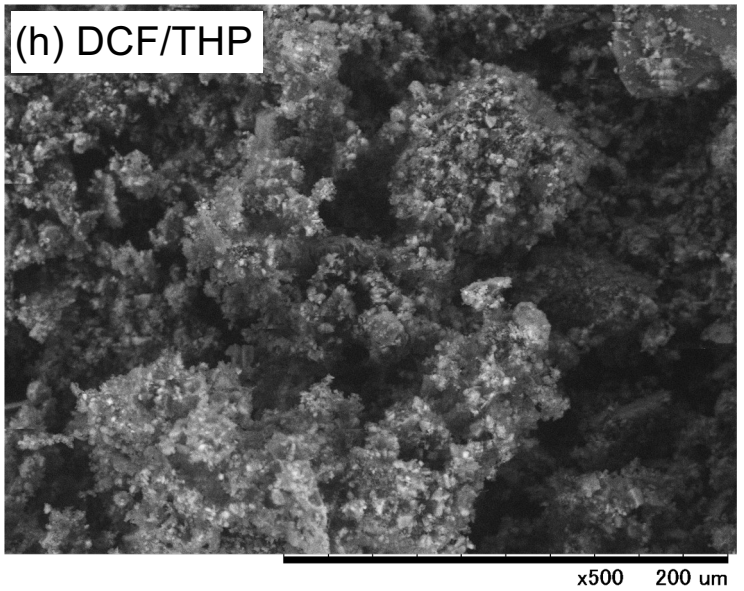
(h) DCF/THP
x500 200 um

Figure S15

Figure S15. The SEM images of IBP (a), DCF (b), CFN (c), and THP (d) after the grind. Additionally, images of equimolar mixtures IBP/CFN (e), IBP/THP (f), DCF/CFN (g), and DCF/THP (h) after 7 days from preparation (physical mixture and grind). While the crystals of IBP and DCF were observed clearly despite the grind, those of CFN and THP were observed only in powder. From this, it is shown that CFN and THP crystals were easily crushed to fine crystalline powder. The powder adsorption around the crystals is observed in the SEM image of the mixture. These SEM images will become evidence of a solid-state interaction between IBP and DCF crystals and CFN and THP powders.